CLEAVAGE FRACTURE OF GLASS

Being a thesis on

"An experimental study of the phenomenon of cleavage crack propagation in glass".

by

K.R. Linger, B.A.

Presented to the University of Keele for the Degree of Doctor of Philosophy

---

Department of Physics,
University of Keele,
Keele,
Staffordshire.

September, 1967.

ACKNOWLEDGEMENTS

I should like to thank:

Professor D.J.E. Ingram	for the use of laboratory and research facilities
Dr. D.G. Holloway	for numerous helpful discussions, competent criticisms and his careful supervision.
Mr. W. Brearley	for his lively interest and technical assistance
Mr. F. Rowerth, and Messrs. Dudley, Greasley and Marsh	for the use of technical and workshop facilities
D.S.I.R. (S.R.C.)	for their financial support
Miss K.B. Davies	for her particular care in typing this thesis.

SYNOPSIS

The strength of many bulk materials measured in tension or bending is subject to a certain amount of ambiguity. Such measurements frequently reflect the properties of the surface rather than an intrinsic property of the material. It is suggested that the measurement of a 'fracture energy' or 'work to fracture' would be free from this ambiguity and would provide a useful parameter for the comparison of inherent strengths of materials.

Detailed cleavage fracture energy measurements have been carried out on 'Float' glass, in a number of environments and at several different temperatures. The 'instantaneous' values of fracture energy ranged between ~5000 ergs cm^{-2} in vacuum and ~2500 ergs cm^{-2} in water. Chapters I and II provide an introduction to, and the theoretical basis of, the cleavage technique. In Chapter III the apparatus and experimental techniques devised and used by the author in this work are described. The results of the fracture energy measurements are recorded and analysed in Chapter IV.

During the course of the fracture energy measurements it was observed that a true equilibrium crack position was never attained. After each increment of strain the crack length increased continuously with time, and cleavage data for the fracture energy determinations was collected at pseudo-equilibrium positions, when the cracks had small but finite velocities. In retrospect it is perhaps not surprising that this crack growth was observed: delayed fracture is a well established property of glass.

The empirical study of this crack growth and the specific experiments to determine particular characteristics of the phenomenon form a major part of the thesis. Crack growth was followed for periods greater than one year when the "fracture energy" had fallen to ~200 ergs cm^{-2} and the crack velocity to ~10^{-6} cm min^{-1}. Chapter V contains the results and preliminary examination of the experiments to determine the general nature of the crack growth.

The final chapter comprises a development and discussion of a possible plastic flow criterion of fracture. A tentative quantitative examination of the predictions of this theory is attempted, and it is encouraging to find a reasonable agreement with experiment. Finally, further discussion is given to the interpretation of the high values of fracture energy and the extended crack growth. The high values of fracture energies and the crack growth are attributed to a plastic flow process which involves a time dependent yield stress and an environment dependent critical plastic zone size.

CONTENTS

LIST OF FIGURES

CHAPTER I

THE CONCEPT OF 'STRENGTH'

1.1 Introduction

As early as 1638 Galileo had noted that solids resisted loads by virtue of their cohesion. The factor controlling the cohesion of a solid is the bonding which holds the atoms together, and the nature of the structure which results from these bonds. In this introductory chapter the effects of the cohesion of solids from the atomic bond to the bulk material will be outlined. The factors which influence the bonding and the structure, and which result in changes in the cohesion will be examined. 'Strength' when discussed with respect to solids may be considered to be the resistance the material exhibits to fracture. Fracture is the destruction of the continuity of a body. For ductile materials the onset of permanent deformation may be the point of most interest to engineers, but many ductile materials exhibit a considerable resistance to fracture after this point. The task of trying to represent the 'strength' of a material by a single parameter seems an impossible one in view of the completely different modes of failure which materials exhibit. Often a material may fail in more than one manner, depending on the stress system applied. For brittle and semi-brittle materials, both of which exhibit macroscopic brittleness, fracture proceeds through the propagation of a crack, and for these materials normal tensile and bending rupture stresses are

controlled by surface rather than bulk properties. In order to overcome this difficulty 'fracture energy' is proposed as a more suitable measure of material 'strength' for materials which show a macroscopically brittle mode of failure.

1.2 Bonding within solids

The origin of the cohesive forces within solids lies in the electrical forces which exist between atoms. The attractive forces between electrons and the nucleus are equilibrated in individual atoms by the repulsive forces which arise out of the kinetic energy of localisation and the limitation of quantum states as the electrons near the nucleus. Attractive forces between atoms are similarly electrical in nature. In inert gases all the electrons interpenetrate the field of the nucleus to a large extent and the atoms are chemically inert; even so the unsymmetrical charge distribution produces a fluctuating dipole field which results in a general net attraction. These weak attractive forces are called Van der Waals forces.

Solids in which the atoms have unfilled electronic shells may exhibit one of three types of bonds: ionic, covalent or metallic. The ionic bond is the simplest and exists when unequal electron sharing takes place. Typically sodium chloride coheres as an ionic molecule, the sodium atom giving up an electron and becoming positively charged, and the chlorine atom accepting an electron and becoming negatively charged, and the two ions bonding through coulombic forces.

The ionic bond is moderately strong, the smaller ions being most strongly bonded. Stronger ionic bonds are obtained when two or more electrons are donated or accepted. Sapphire, Al_2O_3, exhibits multivalent ionic bonding, and is a hard, high melting point material. Another factor which increases the cohesion in ionic solids is polarizability, the distortion of the electron field by the positive ion. The electrons are pulled back towards the parent positive ion, the tendency being higher in the higher valency elements and in the limit the bonding becomes covalent. The structure of ionic compounds is determined by three main factors: the valency, the polarizability and the size of the ions. A pure ionic bond is non-directional and the crystal structure depends on the valency and the ion size. The packing factor is determined simply by the size of the positive ion, and complicated ionic structures are formed in the silicates, for example, which are based on the negative SiO_4 molecular ion.

Covalent bonding is the result of the sharing of electrons between two or more nuclei. The covalent bond is closely controlled by the quantum states which govern the atomic structures of the individual atoms. Predominantly an electron-pair bond because each bonding state can be occupied by two electrons of opposite spins, it is often a directional bond dependent on the spacial distribution of the quantum states. An important feature of the covalent bond is its ability to become saturated: a limited number of bonding quantum states exist between atoms. Many organic solids are chemically

saturated covalent compounds held together by Van der Waals forces. An examination of the number of valence electrons allows us to predict the structure of covalent compounds. Elements with one valence electron tend to join up in pairs, for example I_2. Two valence electrons generally produce two covalent bonds and long chain structures result; sulphur is an example. Bonding with three neighbours produced the sheet structure exhibited by Arsenic, and in which the sheets are loosely bonded by Van der Waals forces. Covalent compounds with four bonds to neighbours illustrate the limit of this type of bonding, the entire crystal consisting of a single covalent molecule.

Metallic bonds are peculiar in that the bonding electrons are non-localized. Atoms in which the metallic bond is preferred to the covalent often have weakly bonded electrons together with many alternative quantum states of similar energies for the outer electrons. The metallic bond can be considered to be an unsaturated covalent bond, and so without limits on the number or type of neighbours. The tendency for close-packed structures to occur is the cause of the simple crystal structures exhibited by metals.

The mechanical properties of materials depend upon the arrangement of their atoms which varies according to the bonding as described above. Solid structures may be divided into two general groups: crystalline and non-crystalline. The former group is composed of metals, semi-conductors, ionic crystals, valence and molecular crystals. Molecules exhibit a structural regularity because the atoms composing

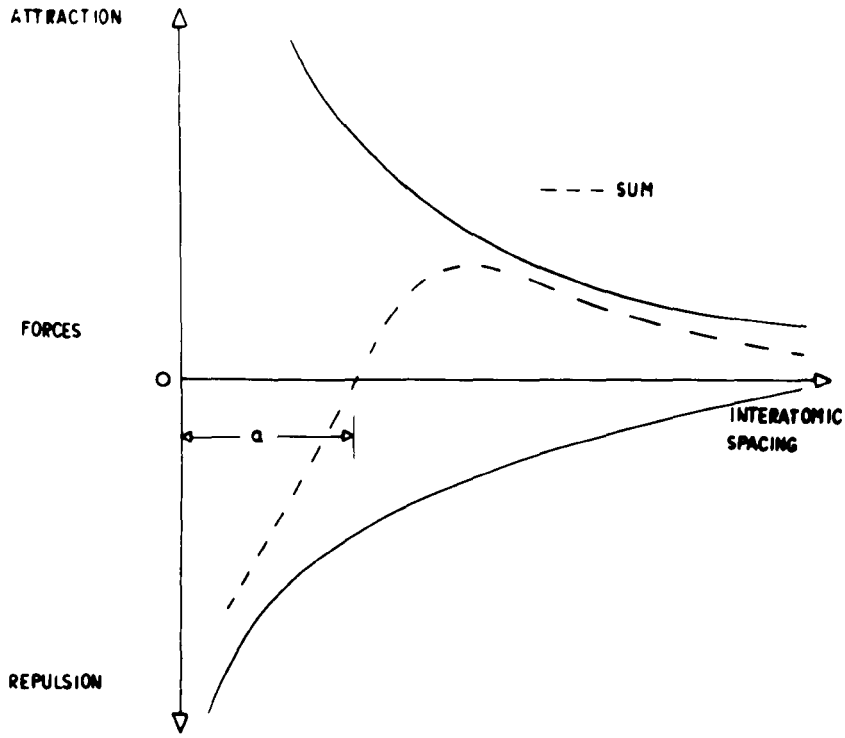

Fig. 1A

The forces of interaction between two atoms

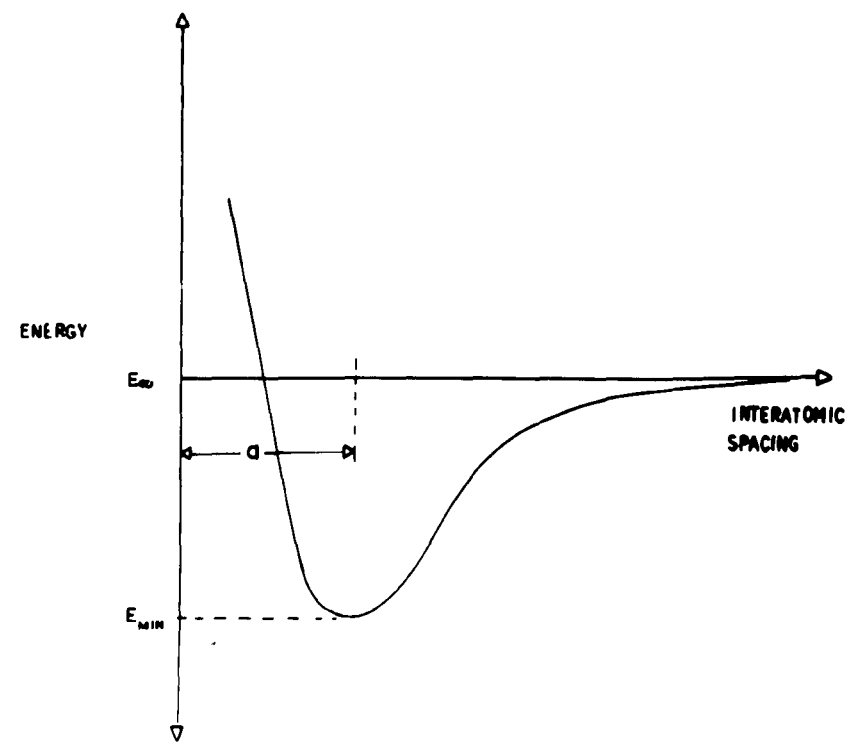

Fig. 1B

The energy of interaction between two atoms

them maintain by bonds a specific number and orientation of neighbours. Crystalline materials are those in which the molecules are arranged in a pattern that repeats periodically in three dimensions. The range of the extension of this order necessary to define a crystal is a subject of much discussion. The absence of obvious long range order is a feature of non-crystalline solids. Glass is considered to be amorphous, lacking in regular form above about 100Å, and exhibiting a considerable variation in the bond lengths, unlike metals, so that the energy required to break the bonds varies. Glasses, as a result, do not have a sharp melting point but soften gradually.

1.3 Theoretical strength

The forces of attraction and repulsion that determine the equilibrium position of two atoms bonded together are represented in Fig. 1A, and the corresponding energy, a Morse curve, in Fig. 1B. To a zeroth approximation a row of atoms within a crystal can be represented by a series of these potential wells. Elastic deformation can then be associated with the movement of the atom from its equilibrium position, up the side of the potential well. The shape of the curve determines the energy change for a given displacement, or expressed in another way, it fixes the elastic constant of the material. For non-crystalline solids the lattice approximation of a series of potential wells is not appropriate since the random arrangement of atoms produces a range of potential distributions of various shapes

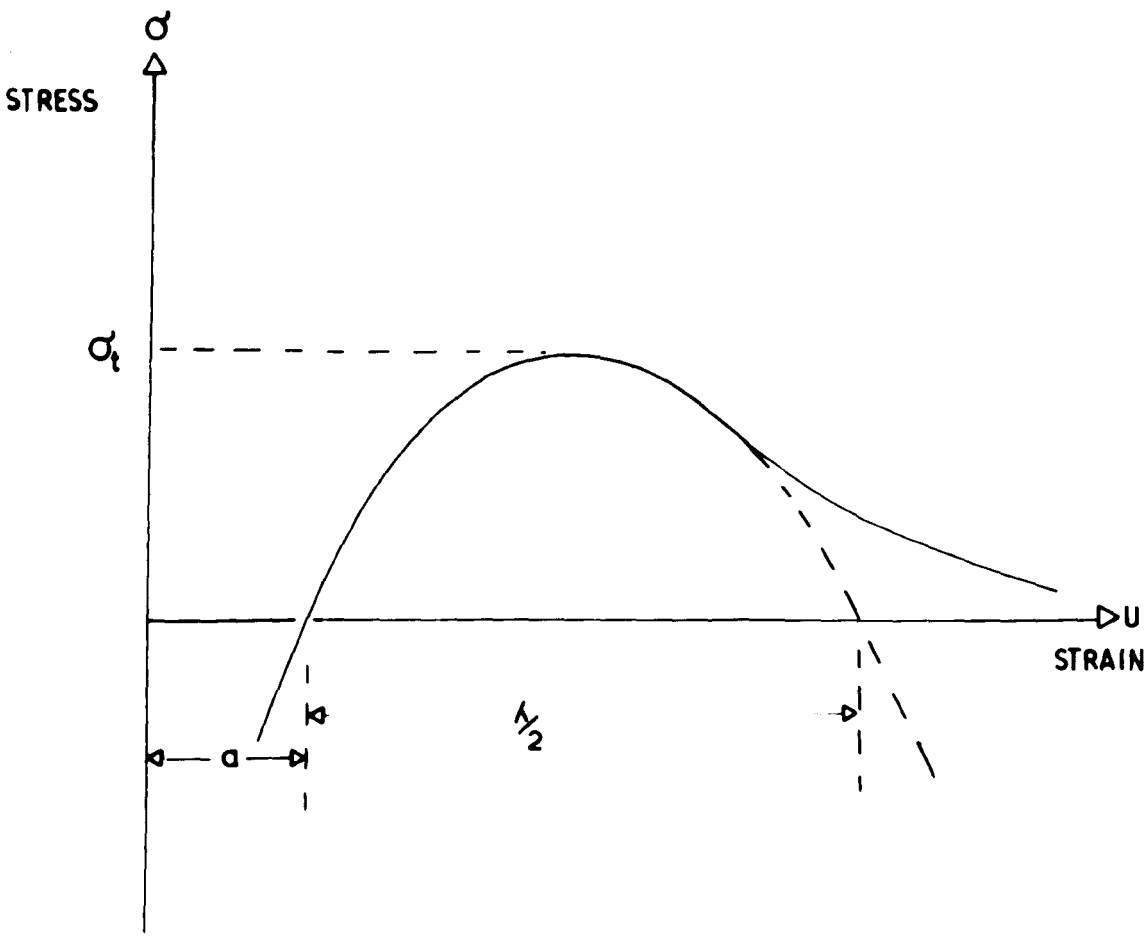

Fig. 1C

Atomic stress-strain curve

and depths. An approximate value of σ_m, the ultimate tensile strength, can be obtained if the atomic stress-strain curve is approximated to a sine wave (Fig. 1C). The area under the curve is 2T, where T is the surface energy and the initial slope is E, Young's modulus.

Then

$$\sigma = \sigma_m \sin\left(\frac{2\pi u}{\lambda}\right) \qquad 1.3.1$$

where λ is the wavelength of the sine curve and u is the displacement from the equilibrium spacing 'a'.

For small strains

$$\sigma = \sigma_m \frac{2\pi u}{\lambda} \qquad 1.3.2$$

and since $\sigma = \frac{Eu}{a}$ (Hooke's Law)

$$\sigma_m = \frac{\lambda E}{2\pi a} \qquad 1.3.3$$

Then

$$T = \int_0^{\lambda/2} \sigma_m \sin\left(\frac{2\pi u}{\lambda}\right) du = \frac{\lambda \sigma_m}{2\pi} \qquad 1.3.4$$

$$\sigma_m \simeq \frac{ET}{a} \qquad 1.3.5$$

Other methods similarly based, but relating λ to the spacing a between the atomic planes, estimate σ_m the maximum of the sine curve using the initial slope. In this way it is possible to express σ_m approximately as $E/10$.

1.4 Surfaces

From equation 1.3.5 above it can be seen that the theoretical value of the tensile strength of a material is dependent not only on E but also on the surface energy T.

Surfaces of solids always differ in behaviour from the bulk of the solid because of the rapid structural changes which must occur at the boundaries. For example, in metals the energy distribution of free electrons is determined by the atomic energy levels and the influence of the crystal lattice; the departure from the ideal bulk structure at the surfaces changes the free electron distribution. In all solids at the surface the equilibrium bonding positions are different, leading to an excess energy associated with the surface, 'surface energy'. The tendency to minimise this energy leads to an apparent force, surface tension. For liquids this phenomenon is illustrated in the spherical form taken by droplets. For more viscous materials, a reduction of the surface energy by this means is not feasible, but the surface energy is often lowered by the segregation of components to and from the surface. This phenomenon, adsorption, was discovered in 1773 by Scheel who observed the condensation of gases on the surface of active charcoal. Clean surfaces are extremely reactive and combine spontaneously with most gases; the activation energies for these reactions are almost zero (Roberts 1937). The binding forces for the adsorbed layers vary considerably. The weaker process, called physical adsorption, is mainly due to Van der Waals forces, with binding energies of the order of 1Kcal/mole. This process is generally reversible and on decreasing the pressure the gas is desorbed. A stronger process of adsorption, named chemical adsorption, involves valence forces often with binding energies as high as 100Kcal/mole. Unlike physical

adsorption this process is specific, a reaction between one particular chemical species and another. Clean surfaces are very reactive and even at pressures as low as 10^{-7} torr they will adsorb a monolayer in seconds. The process of adsorption of many gases is thought to proceed by a physical process which acts as a reservoir for subsequent adsorption into a more strongly bound chemically adsorbed state. Surfaces may also differ from the interior of the solid in composition when adsorption from within occurs: diffusion of ions to or from the surface.

1.5 Real solids

The reactive nature of surfaces makes them susceptible to attack by environments. Surfaces of real solids are also liable to suffer mechanical damage in preparation or subsequent handling. As a result tensile and bending strength tests are frequently tests of surface flaws, rather than tests of the material. Similarly environmental effects on the strength of a material often cannot be separated from the effect on the flaw. This is particularly noticeable with brittle materials which contain cracks; a corrosive environment may reduce the intrinsic strength of the material, and yet the measured strength may be increased as the flaws are made more innocuous. The high theoretical strength $E/_{10}$ estimated from elastic theory is not reached in real bulk materials. Glassware fails at approximately $E/_{1000}$ and strong steels at $E/_{100}$, both well below their theoretical strengths. Generally bulk

solids fail at these lower stresses either because they are brittle and contain cracks or other stress concentrators, or because they are ductile and contain glissile dislocations. Real solids do not have ideal structures; they exhibit irregularities of structure and these imperfections frequently have a major influence on their properties. The influence of these imperfections coupled with the reactive nature of the surface can have disastrous effects upon strength as measured in the normal tensile or bending tests. In brittle solids fracture occurs while the material is behaving elastically and for these materials sharp notches and other flaws within the structure concentrate the applied stress. For a slit in the edge of a plate the applied stress σ is increased to

$$\sigma_m \simeq 2\sigma\sqrt{c/\rho} \qquad 1.5.1$$

where c is the length of the slit or crack and ρ is the radius at the tip. It is easy to see how surface cracks and inclusions can have such drastic effects on the tensile strength. For example, abraded glass rods break at approximately 10,000 psi while the same rods unabraded but drawn have strengths around 50,000 psi. If the surface cracks and inclusions are removed by etching, 500,000 psi can be attained.

Brittle fracture is observed mostly in minerals, ceramics and polymeric materials and is characterised by little or no apparent permanent deformation prior to rupture. Ductile fracture, which is a characteristic of metals, is identified with considerable deformation before fracture. Failure at lower than theoretical strengths in

ductile materials can also be attributed to structural imperfections. The simplest form of a fault is a point defect, such as a vacancy. Line defects, of which the dislocation is most common, are perhaps more serious lattice faults. The discovery by Taylor (1934) and Burger (1939-40) of the 'edge' and 'screw' dislocations identified two more flaws in real materials which give non-uniform strain. The line defect which occurs at the edge of an extra half-plane of atoms is called an 'edge' dislocation and is accompanied by zones of compression and tension so there is a net increase in energy along the dislocation. Propagation of this line through the crystal would lead to slip of one interatomic spacing. Slip in real solids occurs at lower than theoretical stresses because the dislocations allow it to take place progressively rather than simultaneously along a crystal plane. Just as the growth of incipient cracks is responsible for the brittle behaviour of solids, so is the dislocation responsible for the plastic behaviour of crystals.
This plastic deformation can be characterised by three features; its magnitude, permanence and an absence of volume changes. If only 1 in 10^4 atomic planes are involved in slip, strains of 10% are easily attained compared with 0.1% attainable by elastic strain. With the passage of each dislocation, the atoms move from one position of stable equilibrium to another and there is no tendency to recovery.

Many ductile materials can break in either a ductile or a brittle manner. Cleavage in metals often occurs where plastic deformation is restricted and leads to crack nucleation. Crack nucleation theories

have been proposed which suppose that piled up groups of dislocations can produce the stress concentration necessary for cleavage crack initiation. (Koehler (1952), Mott (1953), Kochendoefer (1953) modified by Stroh (1954, 1955), Petch (1953)). This process requires strong barriers, several of which have been proposed: grain boundaries, Westwood (1961), twinning planes, Biggs and Pratt (1958) and intercrystalline barriers at the crossing of two slip bands.

Sharp notches are particularly effective in changing the fracture from ductile to brittle, a phenomenon known as notch-brittleness. Plastic flow and brittleness are assumed to be independent processes each with its characteristic tensile stress. The notch can raise the yield stress by plastic constraint, by increasing the strain rate and by work hardening. In fairly ductile materials the stress concentration factor of the tip is usually large enough to activate neighbouring Frank-Read sources of dislocations and plastic relaxation occurs. In the more brittle materials work hardening may take place. The dislocations pile up and can harden in two ways, by increasing the internal stresses and hindering, by elastic interactions, the development of dislocation loops from active sources. Cracks are nucleated because the dislocations are immobilized and plastic relaxation can only take place now by new dislocations being punched out of the tip of the crack into the surrounding good crystal (Gilman, Knudsen and Walsh, 1958). Since the shear stress for punching is of the order of the tensile stress for fracture it is not possible in most materials.

The discrepancy between observed strengths of real materials and the theoretical strengths is determined not simply by the presence of an imperfection but specifically by the nature of the imperfection. The rôle of dislocations in ductile and semi-ductile materials as stress concentrators depends not on their presence so much as their ability to move. Peason, Read and Feldmann (1957) showed that silicon crystals containing immobile dislocations have the same strength as dislocation-free crystals. It has been mentioned that the important stress concentrators for nominally homogeneous brittle materials almost always lie on the surface of the material. In metals dislocations may determine not simply the stress at which fracture occurs but the mode of fracture. There is some evidence (Jackson, 1962) to suggest that the origin of dislocations may be the same as for flaws which occur in brittle materials: inclusions on the surface. In brittle materials the stress concentrator leads to a crack; in the ductile materials it may act as a source of mobile dislocations. Hedges and Mitchell (1953) observed that glass beads implanted within a crystal send off rings of dislocations under applied stress.

For real materials the structure and the inherent flaws are determined ultimately by the bonding and it is the structural condition of the material especially at its surface which determines its strength.

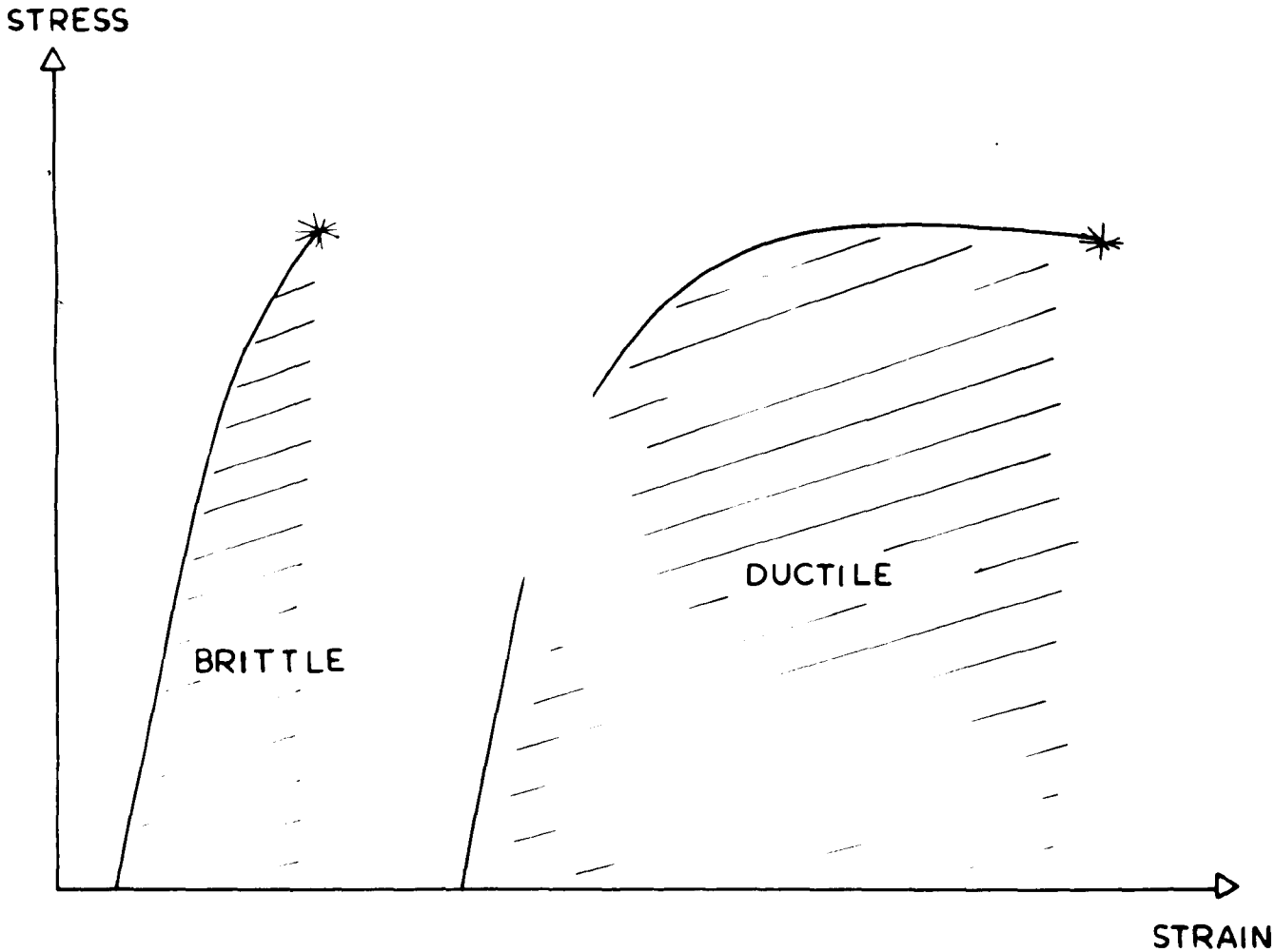

Fig. 2

Stress-strain curves of a ductile and a brittle material taken to failure

1.6 The measurement of strength

The notion of 'strength' as the resistance a material presents to fracture was suggested earlier. The task of measuring this resistance frequently depends upon the mode of fracture. The atoms may simply pull apart as in brittle failure, or slide off in the ductile mode of fracture. In a polycrystalline material failure may occur by a series of grain to grain cleavages or alternatively by grain boundary failure.
An examination of the critical stress for these processes might lead to the conclusion that ductile failure is a weaker mode of fracture than brittle failure. Fig. 2 shows the stress-strain curves for a ductile and a brittle material taken to failure. It can be seen that a ductile material with the same tensile strength will require more energy to fracture. This measure of the 'strength' of a material is often called toughness, and illustrates an aspect of tensile tests: the failure to provide an appropriate measure of 'strength' in all materials. A practical assessment of strength must include the reaction of the material to stress concentrators. For brittle solids the most potent stress raisers lie on the surface of the material, in general the result of abrasion, or corrosion. For more ductile materials the effectiveness of a crack is determined by the dislocations, not simply its depth. A new measurement of material strength is suggested: strength as the resistance of a material to the propagation of a brittle crack.

For a central crack of length 2c in an elastic material under tension σ the strain energy U obtained by integration of the strain field can be expressed as

$$U = \frac{\pi^2 c^2 \sigma}{E} \qquad 1.6.1$$

Griffith postulated that when the crack is on the point of growth the decrease of elastic energy, ΔU, is balanced by the increase of surface energy, ΔT, and we can write

$$\sigma = \sqrt{\frac{2TE}{\pi c}} \qquad 1.6.2$$

The Griffith equation may be generalised (Orowan 1948-9, Irwin 1948) and 2T is now interpreted as the total work of fracture. Because of this new interpretation the symbol γ will be adopted. γ, which may now include irreversible work can be represented by $\frac{\sigma_y \alpha}{2}$ where σ_y is the stress appropriate to the mode of fracture and α the displacement. For an ideally brittle material σ_y is the theoretical strength $E/10$ and α is the interatomic spacing.

The value of γ is determined by σ_y and α but the mode of fracture is determined entirely by the weakest value of σ_y. In this context a low σ_y value does not necessarily infer material weakness, high γ values can still be achieved by processes which require high α values. Ductile materials have extremely large values of α because dislocation movement prevents high stresses being maintained at the crack tip. The fracture energy concept of strength can readily be applied to real materials and offers a way of assessing materials which exhibit

totally different modes of fracture. The measurement of fracture energies can be carried out in a number of ways but in general they all involve the propagation of a crack through the material. Crack propagation in brittle materials is technically simple to achieve, but becomes extremely difficult in more ductile materials. At present the fracture energy concept of strength is somewhat academic when applied to ductile materials and will remain so until a technique for measuring γ has been determined. Suitable choice of test piece or notch often allows the propagation of a crack in normally ductile materials, large pieces of steel plate for example. It has been observed that when ordinarily ductile materials break in a 'brittle' fashion precise measurements reveal a high amount of flow in the vicinity of the fracture, which is reflected in the high fracture energy γ. In general the fracture energy represents the microscopic work although the overall behaviour is brittle in so far as there is no permanent bulk deformation.

In conclusion it is noted that fracture energy measurements have been carried out on an enormous range of materials from the truly brittle such as Potassium Chloride (Westwood and Hitch 1963) where the fracture energy γ is the surface energy T, to polymers such as poly methylmethacrylate (Broutman and McGarry 1965) where the fracture energy is very much greater than the surface energy. The usefulness of fracture energy is limited to 'brittle' fractures, but it has the advantage that it is not subject to the difficulty of

surface effects; the strength of the bulk material is measured directly. The measurement of the specific fracture energy of glass, in various environments, forms a large section of the experimental work described in the following chapters.

The fracture process for brittle and semi-brittle materials is essentially one of crack growth and is discussed in the following chapters. The prolonged crack growth observed in cleavage fracture experiments on glasses, described later in Chapter V, serves to illustrate an inherent advantage this type of study has over the usual uncontrolled tensile fracture studies. It would seem that this process of slow growth may be associated with a reduction in the specific fracture energy and identified with the phenomenon of delayed fracture observed in static tensile tests. The advantage of studying the crack directly rather than indirectly through a single parameter such as the breaking stress, is obvious. The following chapters describe the development of the cleavage technique of fracture study and its application to the measurement of the fracture energy of glass. The more detailed study of the slow prolonged crack growth is described in the second part of this thesis.

CHAPTER II

THE DEVELOPMENT OF THE CLEAVAGE TECHNIQUE

2.1 Introduction

Some of the difficulties of measuring the intrinsic strength of a material have been enumerated in the previous chapter. In this chapter the specific fracture energy is examined as a material property which is free from ambiguity. A brief resumé of some of the many methods of measurement is included and, in particular, the development of the cleavage technique is followed, together with the modifications made to apply the method to a variety of materials.

2.2 Fracture energy measurements

The earliest quantitative fracture measurements were simply tensile, bending, torsion or compression tests. It has been suggested in the previous chapter that these are not measurements of material constants. Indeed, Preston in a paper published in 1942 concluded that J.J. Littleton had been incorrect in commenting that "We never test the strength of glass: all we test is the weakness of the surface", and that this should be amended to read "We do not test the properties of glass at all, but only those of the surrounding atmosphere". Preston's experiments were subject to the difficulties described in the previous chapter, that is, the measurements were made on the system of (flaw + material) and separating the effects of environment on each

part was virtually impossible. The measurement of the work of fracture or specific fracture energy is proposed as a measure of the intrinsic strength of a material: a measure of its resistance to fracture. As we shall see later, a distinction may be made between the two terms 'work of fracture' and 'specific fracture energy'. The specific fracture energy is a material property, but the work of fracture may depend on the stress system applied to the material.

2.3 The Griffith Energy Balance Criterion

In 1920 Griffith suggested that the discrepancy which existed between actual strength and theoretical strength of glass was due to the existence of small cracks in the surface acting as stress concentrators. Griffith postulated that the determining factor in the fracture process was that the surface energy required for extension of a flaw (crack) must be less than the elastic energy lost by the body as a result of that extension. An energy balance criterion for fracture was thus established:

$$\frac{\partial U}{\partial A} > \frac{\partial S}{\partial A}$$

where U is the elastic energy, S the surface energy and A the area. Griffith tested this hypothesis by examination of the stresses necessary to fracture glass vessels containing cracks of known lengths. Using Inglis's solution for the stress around a crack in a two dimensional sheet an equation relating the breaking stress to the

crack length was derived

$$\sigma = \sqrt{2ET/\pi c} \qquad 2.3.1$$

where c is the half length of the crack, T the surface energy and σ the applied stress.

This relationship was verified experimentally and marked the beginning of the quantitative aspect of fracture mechanics. Within the experimental error Griffith was able to predict the breaking strengths of pre-cracked samples, using an experimentally determined value of the surface tension T. These results are questionable in the light of more recent experiments which suggest that γ, the fracture energy, cannot be equated to the surface energy, but is composed of other terms associated with the fracture process. Irwin (1948) and Orowan (1948-9) generalized the interpretation of T in the Griffith equation, suggesting that it may be replaced by γ, the total work to fracture per unit area done in propagating the crack.

Bilby, Cottrell and Swindon (1963) have derived a general expression for γ from elastic-plastic theory:

$$2\gamma = \int_0^{\alpha} \sigma_y d\alpha \qquad 2.3.2$$

σ_y is the stress in some element ahead of the crack front and α is the distance the element moves. In general σ_y is virtually zero beyond a charateristic fracture displacement α_f so that equation 2.3.2 can be evaluated:

$$2\gamma \simeq \sigma_y \alpha_f \qquad 2.3.3$$

σ_y is now the characteristic strength of the element for the particular mode of failure concerned.

The use of the energy balance criterion for fracture has been extended to cover a wide range of materials: mild and high strength steel (Irwin and Wells 1965), paper (Balodis 1963), mica (Obreimov 1930), glass (Shand 1965), ionic crystals (Gilman 1960), rubber (Rivlin and Thomas 1953) and polymers (Berry 1963).

From the Griffith energy balance criterion there have been two main approaches to the quantitative study of fracture, involving catastrophic or controlled fracture. The conditions applicable to the onset of fast fracture have been considered by many authors (Irwin, Kies, Griffith, Berry, Gilman). This approach to fracture mechanics will not be discussed in any detail, but as it offers an alternative method of measuring fracture energies particular references will be made to it in Chapter IV, in discussion of the results.

2.4 Stable fractures in glass

Following the work of Hertz (1882), Auerbach (1902) studied controlled fractures in glass. The results of this study of the stable cone shaped cracks produced by small hard steel balls was substantiated by Preston (1926). It was not until 1956 that the stability of cone cracks was utilized in an attempt to measure fracture energy. Roesler (1956) carried out a series of experiments on stable indentation fractures in silicate glass. In his introduction Roesler makes two points of direct relevance in fracture studies. The first is that Griffith's hypothesis is the assumption that the balance of surface energy

and mechanical energy controls the fracture process, and that this hypothesis is only likely to be true when the fracture grows slowly since the kinetic energy associated with a running crack may be larger than the surface energy. Roesler studied cone cracks produced from cylindrical flat ended punches restricted to certain dimensions by the crushing of the glass which occured at a limiting load. In order to calculate the specific fracture energy from the energy balance criterion, Roesler was forced to adopt an approximation method to find an expression for the elastic field around the cone crack: $\partial U/\partial A$ in equation 2.3.1. Two main points were that the specific fracture energy, γ, approximately 4000 ergs cm^{-2}, was much higher than the surface tension, and the cone size was found to depend upon the time of observation. The growth of the cone crack under constant load was followed for periods up to several days but the values of γ were calculated from data taken fifteen minutes after application of the load increment, when changes were taking place slowly. Crack sizes independent of previous growth were obtained by using loading increments of 10% of the initial load. These experiments were the first attempt to use an energy balance criterion in order to calculate the specific fracture energy of a material. Culf (1957) extended these measurements to cone cracks in plate glass in a variety of liquid and gaseous environments and the results are discussed in Chapter IV.

2.5 The Nakayama method of fracture energy measurement

A direct estimate of the work done during crack propagation is possible using the technique developed by Nakayama (1964) and Clarke et al. (1965). A specially notched specimen is broken in three point bending using a hard beam machine. The fracture which results is stable in that the strain imposed by the machine must be increased to extend the fracture. The fracture energy can be calculated from the force-time curve and a knowledge of the specimen dimensions. Nakayama's analysis of this problem is briefly as follows:

For a rectangular beam, length l, thickness d, and breadth b, bent in a three point bend apparatus, the total stored elastic energy in the conplete system can be expressed as

$$U_o = \frac{lbds^2}{18E}\left(1 + \frac{72bd^3E}{kl^3}\right) \qquad 2.5.1$$

where k is the apparent spring constant of the apparatus.

This is equivalent to expressing the total energy as:

$$U_o = U_s + U_a \qquad 2.5.2$$

where U_s is the energy stored in the specimen, and U_a that stored in the apparatus.

U_γ, the energy required to separate the test piece is:

$$U_\gamma = 2A\gamma \qquad 2.5.3$$

where A is the cross sectional area of the beam.

The mode of fracture is determined by the value of $(U_o - U_\gamma)$.

For $\Delta U > 0$, the fracture is catastrophic and the excess energy must be

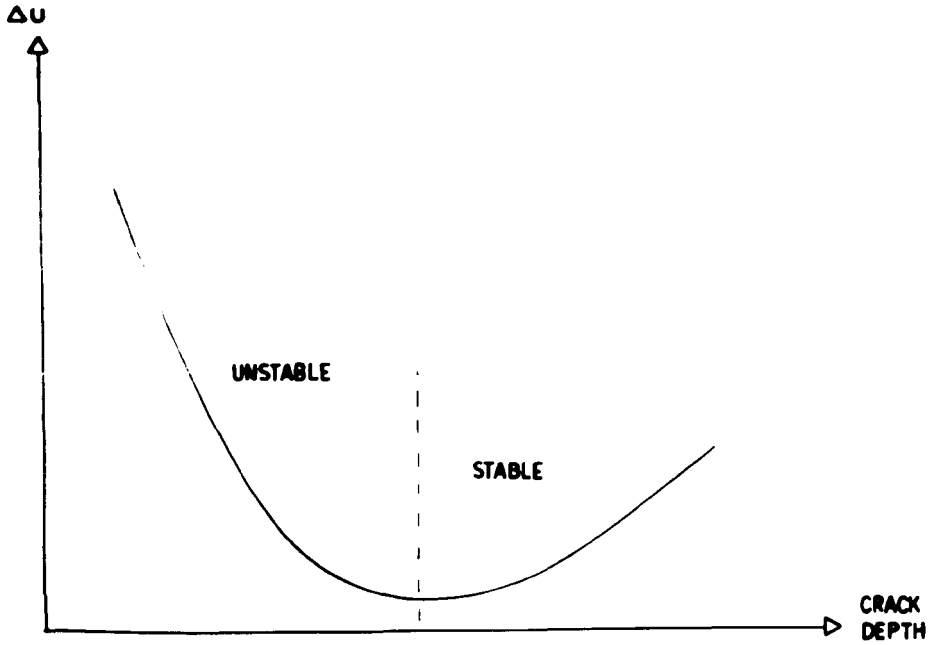

Fig. 3

Potential energy of the Nakayama system as a function of the depth of the shaped crack

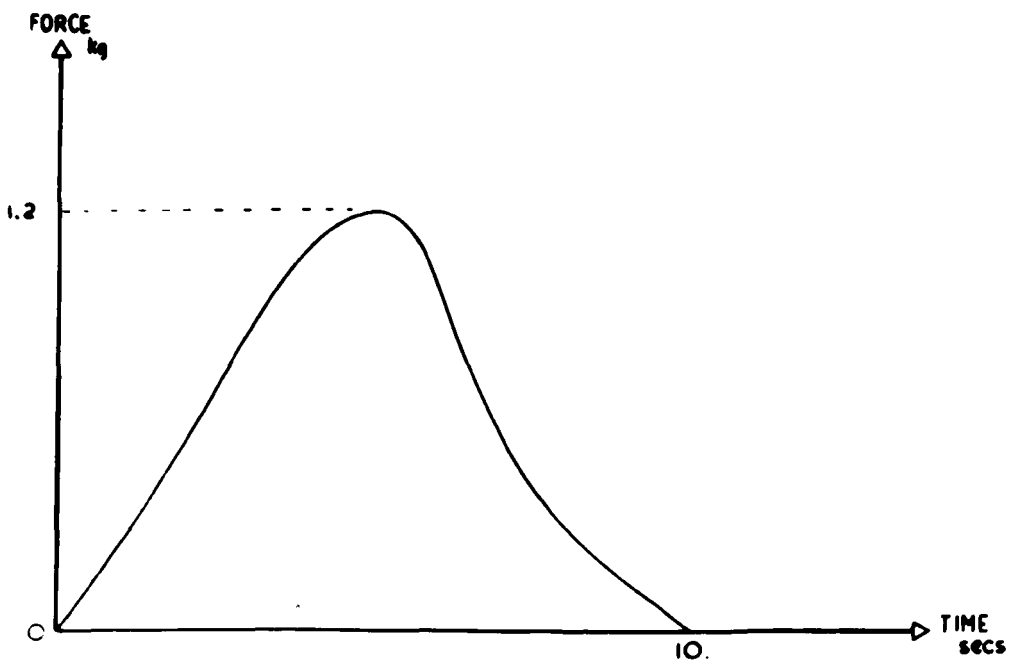

Fig. 4

A fracture curve for glass obtained using the Nakayama technique

dissipated in kinetic energy etc. When $\Delta U < 0$, additional external work must be provided and the fracture is stable. It is the use of the shaped notch and the hard machine (which reduces the energy stored in the machine) which allows the production of stable fractures.

For stable fractures the total work done by the external forces is transformed into fracture energy and can be calculated from the load-time curve.

$$U_\gamma = v \int_0^{t_c} F dt \qquad 2.5.4$$

where v is the speed of the overall deflection, t_c is the time to fracture and F is the bending force.

Hence

$$\gamma = \frac{U_\gamma}{2A} \text{ ergs cm}^{-2} \qquad 2.5.5$$

The main advantage in using this technique is that the specific fracture energy, γ, can be measured on a single specimen, although the accuracy of this measurement may not be very high. The disadvantage is that the production of a suitable notch or crack may prove to be difficult. Although the effect of the depth of the shaped crack is not fully understood, it is suggested by Nakayama that the possible potential energy distribution could be represented as in Fig. 3. The Nakayama technique in principle could be applied to test the energy balance criterion described earlier from a knowledge of the variation of crack length with time by relating this to the stress as a function of time: the second half of the curve (Fig. 4). In practice this could prove

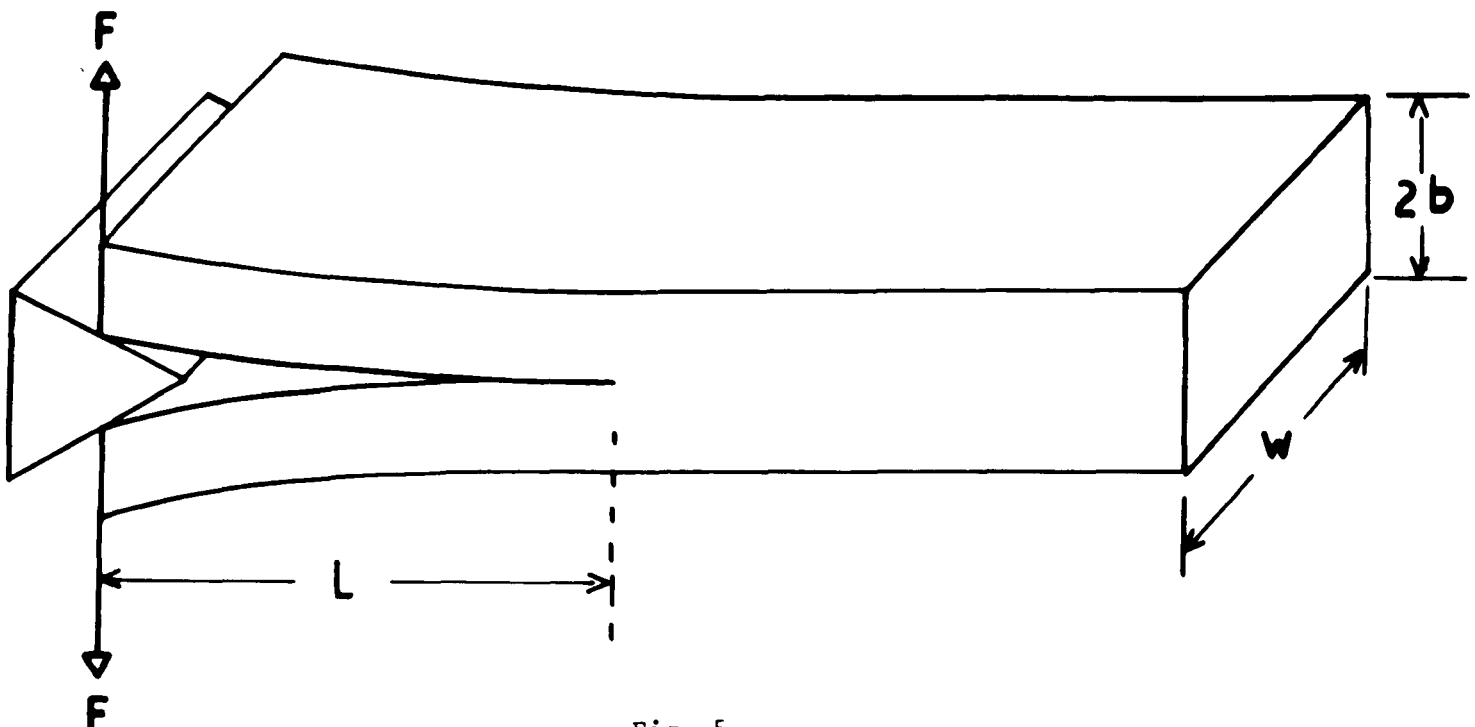

Fig. 5

Schematic representation of cleavage

extremely difficult, and would depend upon the response of the machine which controls the stability of the fracture.

2.6 Cleavage fractures

Examination of the fracture process is aided by the use of a system in which the fracture is controlled. Catastrophic failure tends to involve dynamic phenomena often beyond simple analysis. One method which has been used for a variety of materials has been described briefly above. The cleavage technique might be regarded as an extreme variation of this method. While the cleavage technique has many advantages, as will be discussed, it does impose more rigorous demands on the size and shape of the specimen. The form used by the author is the result of a number of modifications to Obreimov's original cleavage experiments on mica (1930). Before describing any of the experimental and analytical procedures adopted by various authors the basic mechanics of cleavage will be reviewed.

Mechanics of cleavage

Fig. 5 shows a schematic representation of a cleavage experiment. A discussion of the local effects of the cleaving chisel or wedge is not included, as to a first approximation the stress distribution some way down the specimen is independent of the form of the wedge. Indeed, in most cleavage experiments the wedge is replaced by grips. For the most elementary analysis we assume that the specimen is split along the

median plane and each half acts as a cantilever beam whose length is determined by the particular crack length at that instant. The cleavage force F produces a bending moment M(x) along one of the beams distributed so that:

$$M(x) = F(L - x) \qquad 0 < x < L \qquad 2.6.1$$

From simple beam theory neglecting shear, the strain energy in the beam U is given by:

$$U = \frac{1}{2EI}\int_0^L M^2(x)dx = \frac{F^2L^3}{6EI} \qquad 2.6.2$$

where I is the moment of inertia of the cross section $I = \frac{wb^3}{12}$ where b is the width and w the thickness.

Castigliano's theorem gives the deflection of the beam δ at the point of application of the force

$$\delta = \frac{\partial U}{\partial F}\bigg|_{x=L} = \frac{FL^3}{3EI} \qquad 2.6.3$$

Substituting for δ in equation 2.6.2:

$$U = \frac{3EI\delta^2}{2L^3} \qquad 2.6.4$$

The surface energy S of one side of the crack is given by:

$$S = \gamma Lw \qquad 2.6.5$$

From the energy balance criterion for fracture, $ds = - dU$ we can write:

$$\gamma w dL = \frac{9EI\delta^2}{2L^4}dL \qquad 2.6.6$$

Thus

$$\gamma_\delta = \frac{3Eb^3\delta^2}{8L^4} \qquad 2.6.7$$

or in terms of the cleavage force

$$\gamma_F = \frac{F^2L^2}{2EIw} \qquad 2.6.8$$

A more rigorous analysis of the cleavage technique will be discussed later in the chapter with particular reference to a paper by Gillis and Gilman (1964) in which the possible errors are assessed. Meanwhile several features of the cleavage technique may be revealed using the elementary treatment. The first feature is that when the crack is just beginning to move, the stresses at the tip are independent of the crack length. At that instant $dS = - dU$ and we can write

$$F = \frac{\sqrt{2\gamma wEI}}{L} \qquad 2.6.8$$

and since $M = FL$ it follows that $M = \sqrt{2\gamma wEI}$, which is independent of L. It is reasonable to suppose that the bending moment at the crack tip determines the local stresses so that the stresses are always the same when the applied force or deflection is just sufficient to propagate the crack. Thus in order to determine whether γ is independent of variations in the magnitude of the stress (i.e. the criterion for crack propagation is energy) it is necessary to vary the width of the specimen, b, which must change M even for constant γ.

2.7 Previous cleavage experiments

It was not until 1930 that a direct measurement of fracture energy by cleavage was undertaken. Obreimov (1930) measured what he called "the splitting strength of mica" utilising the laminated structure to provide the stability in crack direction needed to carry out a cleavage experiment. The mica was cleaved in air and under vacuum by means of a glass wedge, and the fracture energy calculated from observations of the crack separation and length for a particular thickness of cleaved flake. Values of 1500 ergs cm^{-2} and 20,000 ergs cm^{-2} are quoted by Obreimov for mica in air and vacuum respectively. These values appear to be in error. Obreimov calculated the fracture energy using in principle the simple theory outlined above, but he expressed the radius of curvature of a section of the beam ρ as

$$\frac{1}{\rho} = \frac{3M}{Ewb^3} \qquad 2.7.1$$

instead of

$$\frac{1}{\rho} = \frac{12M}{Ewb^3} \qquad 2.7.2$$

which is the correct elasticity relationship (Newman and Searle). This introduced an error amounting to a factor of $\frac{1}{4}$ into his published values of the fracture energy, and when corrected, the values of γ are 375 ergs cm^{-2} and 5000 ergs cm^{-2} for mica in air and vacua respectively. The discrepancy in the quoted values of fracture energy was also remarked on by Bailey (1957) who quoted Obreimov as having obtained a

value of 375 ergs cm^{-2}, for the fracture energy of mica in air, in agreement with her experimental results.

Stabilization of the crack direction is the essence of the cleavage technique developed by Obreimov. The crack is stable in two respects; first it is confined by natural weaknesses (crystallographic planes) within the material, and secondly, for a given position of the wedge, the longer the crack the greater the amount of strain required for movement. Gilman (1960) has also used a cleavage technique to measure the surface energies of a variety of crystals. The technique adopted involved measuring the minimum load F_o to propagate a previously initiated crack of length L_o in a specimen of known dimensions and γ calculated from equation 2.6.8:

$$\gamma = \frac{6F_o^2L_o^2}{Ewb^3} \qquad 2.6.8$$

The above equation neglects the effects due to shear, an approximation only feasible at large crack length to beam width ratios, $L_o/b > 3$. Driving in a wedge gave poor reproducibility and so the force was applied by attaching a small yoke to each arm by means of pivot pins.

Westwood and Hitch (1963) made use of the technique to measure the {100} surface energy of potassium chloride. Unlike the brittle crystals examined by Gilman, KCl is relatively ductile. It was observed experimentally that if the initial crack length L_o was greater than about three times the beam width, anomalously high values of γ_o were obtained. It was suggested that the propagation of long cracks in this material

is preceded by plastic relaxation at the tip, and so requires a greater stress to induce repropagation. The use of short specimens necessitated an analysis, still based on simple beam theory, but taking into consideration the contributions of shearing forces. The equation for the deflection δ given by Castigliano's theorem becomes:

$$\delta = \frac{FL_o^3}{3EI} + \frac{\alpha F L_o b^2}{4GI} \qquad 2.7.3$$

where α is an experimental constant and G is the shear modulus, and γ can be written:

$$\frac{1}{\gamma_A} = \frac{1}{\gamma_o} + \left(\frac{\alpha E}{4\gamma_o G}\right)\left(\frac{b}{L_o}\right)^2 \qquad 2.7.4$$

where γ_A is regarded as the experimentally measured surface energy:

$$\gamma_A = \frac{6F^2L_o^2}{Ew^2b^3} \qquad 2.6.8$$

and the true surface energy γ_o is obtained from the intercept of a plot of $1/\gamma_A$ versus $(\frac{b}{L_o})^2$.

Cleavage of isotropic materials

In principle the cleavage technique of fracture can be applied to any macroscopically brittle material, since it is essentially the gradual opening of a crack by means of a wedge or its equivalent. For adequate control of the direction of the crack however, some kind of anisotropy is essential. In an isotropic specimen the crack direction is unstable and one of the beams breaks off. Guernsey and Gilman (1959) carried out a photo-elastic study of the stress distribution around a cleavage crack. The results showed that unlike a crack in a uniformly

stressed, infinite plate, the steepest gradient of the maximum tensile stress lies in a direction almost perpendicular to the plane of the crack. This distribution is attributed to the presence of a bending moment at the tip of the crack. Cracks follow the line of steepest gradient of the tensile stress and it is a direct result of this stress distribution that, as is observed in practice, a cleavage crack in an isotropic solid will run out to the side of the specimen. The natural anisotropy of certain crystals produces straight plane cleavages. Several techniques have been adopted to overcome the difficulty of directional instability of cracks in naturally isotropic materials. Some of the different approaches will be described and a preliminary assessment made.

Benbow and Roesler (1957) carried out a series of experiments on isotropic polymeric materials using a cleavage type experiment in which the crack was stabilized by holding the specimen in a state of lengthwise compression. Long rectangular specimens of various widths were used and for the long narrow specimens, the compression necessary for crack stabilization was above the buckling limit. These specimens were therefore confined within guides so that they could not leave the plane of the apparatus. A wedge was used to control the length of the crack, but unlike Obreimov's experiments on mica, the wedge was applied to a pair of clamps fastened to the material, and not directly to the material. The clamps were guided to prevent any rotation. The crack was started from a saw cut, which had been finished in the shape of a

swallow tail to facilitate the formation of a real crack. Although the analysis is similar to the Gilman method described above, there is a difference in the form of the bending beam equations. The clamping of the free end of the beams, which prevents rotation, produces a complex cantilever system as shown in Fig. 6. The resulting equation relating the specific fracture energy γ to the experimental parameters becomes:

$$\gamma = \frac{3E\delta^2 b^3}{64L^4} \qquad 2.7.5$$

compared with

$$\gamma = \frac{3E\delta^2 b^3}{8L^4} \qquad 2.7.6$$

The effect of the compressive forces was assessed by the authors as contributing about ±10% to the value of γ. This is discussed in the Appendix to this thesis where the possible magnitudes of the effects are re-assessed in the light of more recent experiments. One important new factor which is apparent in the cleavage technique described above is the technique of incremental displacement loading, in contrast to the procedure of Gilman and others who used a constant loading rate. In these experiments, Benbow and Roesler increased the displacement δ in small increments just sufficient to cause crack growth. The values of the crack lengths and the corresponding deflections δ, were measured and in this way a number of experimental points collected from each specimen.

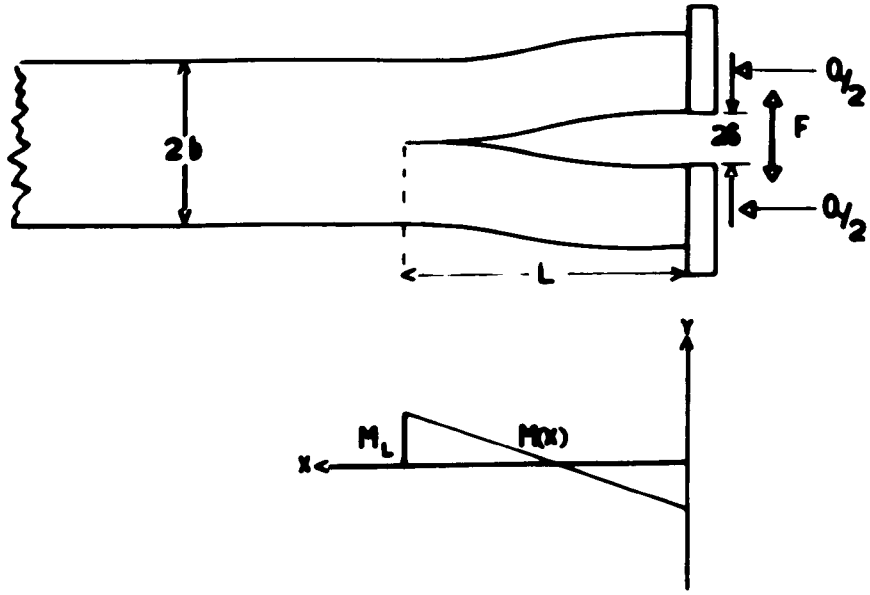

Fig. 6

The complex cleavage system used by Benbow and Roesler and the moment distribution

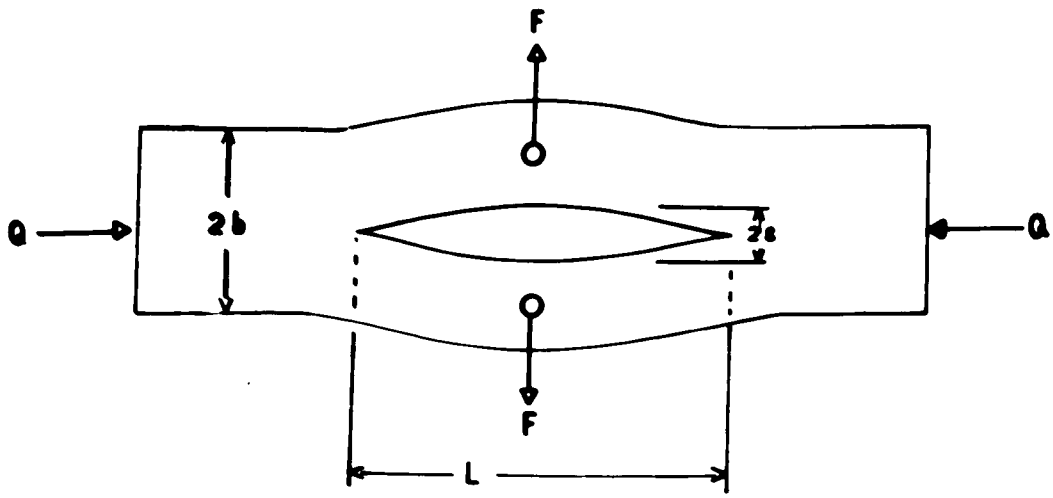

Fig. 7

The cleavage test piece used by Svennsson in fracture energy determinations

Svennsson (1960) used a modified version of the apparatus designed by Benbow and Roesler, to measure the effects of temperature on the specific fracture energy of some polymeric materials. The specimen length was doubled and the crack started from the centre, and although crack stabilization was by axial loading, in Svennsson's apparatus this load was measurable. A sketch of the apparatus is shown in Fig. 7. Account was taken of the compressive forces and also of the effect of shearing stresses. The specific fracture energy was calculated from:

$$\gamma = \frac{Eb^3\delta^2}{L^4}. S \qquad 2.7.7$$

where S is a function of the crack length whose magnitude is determined by the compressive forces and the shearing stresses. A more detailed examination of Svennsson's analysis is included in the Appendix, but two general features are noted here. The inclusion of compressive forces appears to have the effect of increasing γ by approximately a factor of two. The second point noted by Svennsson was that γ can be calculated from the gradient of the plot of δ versus $L^2/\sqrt{S}$ and so measurements can be made on a continually moving crack.

The systems developed to stabilize the direction of the cleavage crack in an isotropic material described above are somewhat clumsy and present difficulties in the analysis. A simpler method of overcoming the tendency of the cleavage crack to turn out of the median plane was adopted by Berry (1961). Stabilization is achieved

by the presence of a slot down the centre of each face along the length of the specimen, (Fig.13). The narrowing of the centre portion and the high stresses near the slot edges produce a directionally stable crack. Berry made use of the inherent stability of the system which exists under conditions of constant deflection, pointing out that the crack will grow only until it has attained an equilibrium length determined by the appropriate energy balance criterion for fracture.

This system for crack stabilization was used by Broutman and McGarry (1965) who also carried out a series of experiments on the fracture of poly methylmethacrylate. The only difference from Berry's technique was that Broutman and McGarry used a constant strain rate, and made observations of δ and L on a continuously moving crack. For both systems the equations relating the specific fracture energy γ to the beam dimensions were adjusted to take account of the narrow section of the specimen, w_1, produced by grooving.

Now $$dS = w_1 \gamma dL$$

and $$dU = \frac{9}{2} \frac{EI\delta^2}{L^4} d.L$$

where $$I = \frac{w_2 b^3}{12}$$

Hence $$\gamma = \frac{3Ew_2 b^3 \delta^2}{8w_1 L^4} \qquad 2.7.8$$

or $$\gamma = \frac{6F^2 L^2}{w_2 w_1 b^3} \qquad 2.7.9$$

This assumes that the effect of the slot is to reduce the surface area of fracture only, and that it has a negligible effect on the strain energy of the beam. In practice this was achieved by the use of a narrow slot.

The cleavage system used by the author and described in Chapter III is based on the technique introduced by Berry: stabilization of the crack direction by grooving. The use of this system during fracture energy measurements was restricted to conditions of constant deflection, allowing γ to be calculated from a series of experimental observations on a single specimen. The specimen was cleaved using a system of chucks and pins, rather than by a wedge.

2.8 Analysis of the cleavage technique

The measurements of fracture energy described above have been based on a study of the conditions necessary to produce crack growth. Using the Irwin-Orowan generalization of the Griffith criterion for mechanical instability which may be written

$$-\frac{\partial U}{\partial L} = \frac{\partial S}{\partial L}$$

then fracture energy measurements can be summarized as the examination and evaluation of the term $\partial U/\partial L$ for a given mechanical environment. In particular it may be said that the cleavage method makes use of the approximation of the specimen to two "built in" cantilever beams in calculating $\partial U/\partial L$. The evaluation of this approximation has been

approached in two ways: from a theoretical examination of the possible errors involved, and semi-empirically by assuming the overall form of the errors and assessing them experimentally. The former approach has been adopted by Gilman, Svennsson, Westwood and Hitch, whereas Berry and Broutman and McGarry utilised the second approach.

Theoretical analysis of cleavage experiments

Following Gilman's cleavage experiments on crystals, Gillis and Gilman (1964) carried out a comprehensive analytical investigation of the possible sources of errorinvolved in the simple double cantilever cleavage description of the crack propagation. This work will be summarized here together with some of the points made by other authors, and this survey will be taken as representing the theoretical approach to the analysis. Because of its relevance, use of the specific equations derived here will be referred to again in Chapter IV of this thesis in a discussion of the results obtained from fracture energy experiments carried out by the author. The effects of shear and the use of simple beam theory together with an examination of the boundary conditions at the fixed end of the beam will be assessed. It will be shown that shear effects are negligible for large L:b ratios and that under these conditions for slow moving cracks, the kinetic energy is small compared with the strain energy. The procedure of simultaneous force and deflection measurement is suggested as a method of estimating the elastic linearity of beam material and the effect of strains past the tip of the crack.

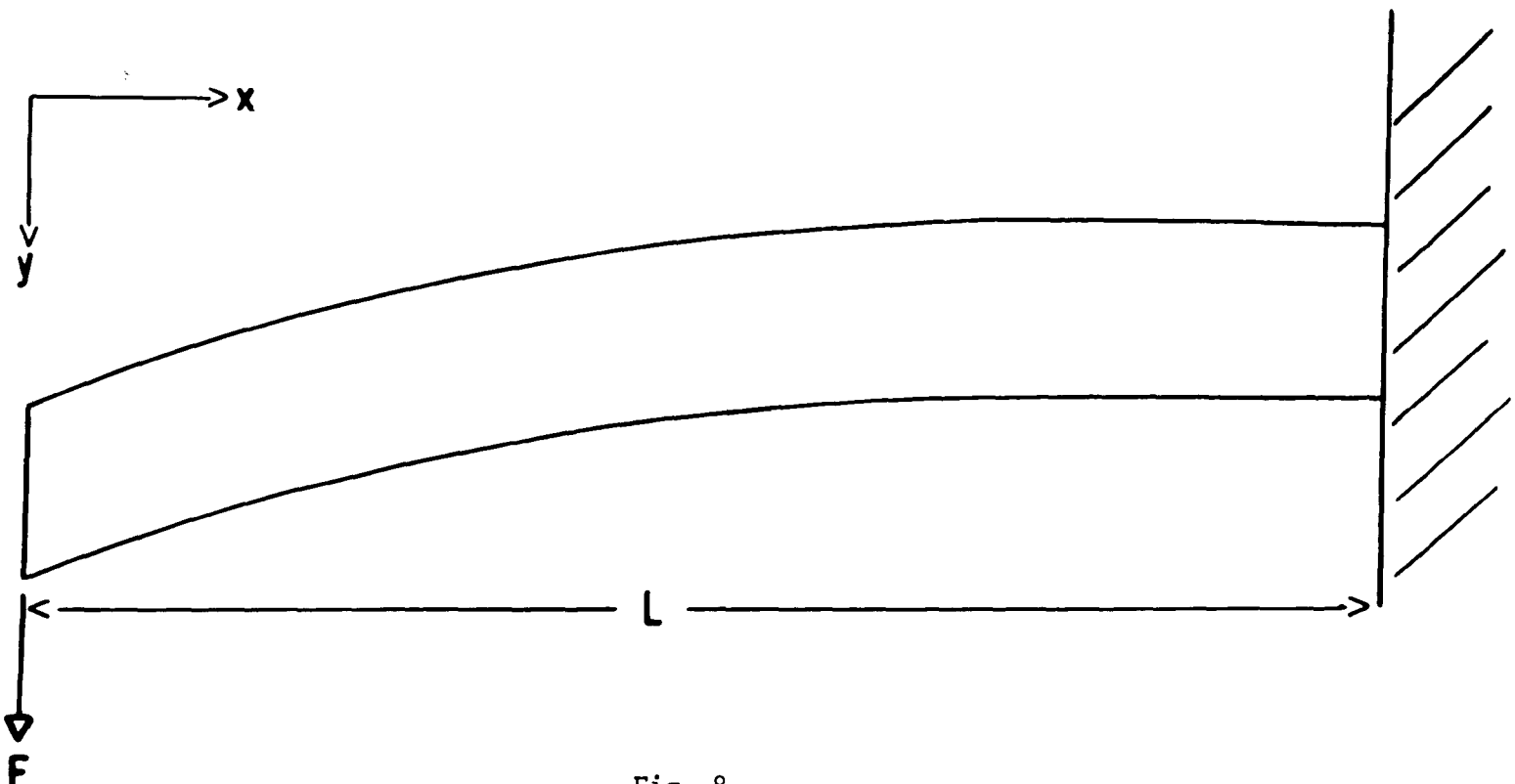

Fig. 8

End loaded cantilever

The simple equation

$$\gamma = \frac{F^2L^2}{2EIw} \qquad 2.6.8.$$

derived earlier was obtained by assuming that the arms of the crack acted as simple cantilever beams. In order to assess the magnitude of these approximations a more sophisticated examination of the bending beams, applicable to the cleavage situation, will be made.

For such a cantilever beam of an isotropic material, with a rectangular cross section which is loaded with a force F at the free end, the bending moment at a distance x from the load (see Fig. 8) is given by

$$M = -Fx$$

and the shearing force by

$$V = -F$$

The deflection curve can be obtained from elasticity theory (Timoshenko)

$$\frac{d^2y}{dx^2} = -\left(\frac{M}{EI}\right) + \frac{K}{AG}\left(\frac{dV}{dx}\right) \qquad 2.8.1$$

where A is the cross sectional area of the beam

G is the shear modulus

and K is a numerical constant = 1.

After integration and substitution

$$\frac{dy}{dx} = -\frac{Fx^2}{2EI} - \frac{KF}{AG} + C_1 \qquad 2.8.2$$

The constant C_1 can be evaluated by an examination of the conditions at x = L. Rotations of $-\frac{KF}{AG}$ can be identified with shear and an additional

rotation at x = L is included to allow for the restriction af anticlastic curvature and the strains past the tip of the crack; i.e. at x = L

$$\frac{dy}{dx} = -\frac{KF}{AG} - \theta \qquad 2.8.3$$

Thus

$$\frac{dy}{dx} = -\frac{FL^2}{2EI} + \frac{Fx^2}{2EI} - \frac{KF}{AG} - \theta \qquad 2.8.4$$

and

$$C_1 = -\frac{FL^2}{2EI} - \theta \qquad 2.8.5$$

A second integration yields

$$y = -\{F(3L^2x - x^3)/6EI\} - (KFx/AG) - \theta x + C_2 \qquad 2.8.6$$

C_2 can be determined from y = 0 at x = L:

$$C_2 = F\left(\frac{3L^3 - L^3}{6EI}\right) + \frac{KFL}{AG} + \theta L \qquad 2.8.7$$

$$\therefore \quad y = F\left(\frac{2L^3 - 3L^2x + x^3}{6EI}\right) + \frac{KF(L - x)}{AG} + \theta(L - x) \qquad 2.8.8$$

Thus

$$\delta = \frac{FL^3}{3EI} + \frac{KFL}{AG} + \theta L \qquad 2.8.9$$

Then still following Gillis and Gilman's analysis closely, the strain energy of the cantilever part of the beam can be evaluated from first principles and expressed as

$$U_b = \int_o^L \frac{M^2dx}{2EI} + \int_o^L \frac{KV^2dx}{2AG} \qquad 2.8.10$$

Since M = - Fx and V = - F, we can write

$$U_b = \frac{F^2L^3}{6EI} + \frac{KF^2L}{2AG} \qquad 2.8.11$$

If half the strain energy past the tip is denoted by U_a, Castigliano's theorem states

$$\delta = \left(\frac{\partial U}{\partial F}\right) = \left(\frac{\partial U_a}{\partial F}\right) + \left(\frac{\partial U_b}{\partial F}\right) \qquad 2.8.12$$

Thus

$$\delta = \frac{FL^3}{3EI} + \frac{KFL}{AG} + \frac{\partial U_a}{\partial F} \qquad 2.8.13$$

Comparing equations 2.8.13 and 2.8.9, we must have:-

$$\frac{\partial U_a}{\partial F} = \theta L \qquad 2.8.14$$

By the conservation of energy the work done by the grips must be equal to the total stored energy (before the propagation of the crack).

Thus

$$\frac{F\delta}{2} = U_a + U_b \qquad 2.8.15$$

Substituting for δ, U_a and U_b we can write

$$\frac{F}{2}\left(\frac{FL^3}{3EI} + \frac{KFL}{AG} + \theta L\right) = \frac{F^2L^3}{6EI} + \frac{KF^2L}{2AG} + U_a \qquad 2.8.16$$

$$\therefore \quad U_a = \frac{F}{2}\theta L \qquad 2.8.17$$

but from equation 2.8.14, $\frac{\partial U_a}{\partial F} = \theta L$

$$\therefore \quad \theta L = \frac{\theta L}{2} + \frac{FL}{2}\frac{\partial \theta}{\partial F} \qquad 2.8.18$$

$$\text{and} \quad F\frac{\partial \theta}{\partial F} = \theta \qquad 2.8.19$$

$$\text{therefore} \quad \theta = C^{*}F \qquad 2.8.20$$

i.e. depends linearly upon F which implies that the total end deflection is a linear function of the force F and

$$U_a = \frac{C^{*}F^2L}{2}$$

Gillis and Gilman then argue that C^{*} is a function of L and assuming a simple power relationship

$$C^{*} = \frac{CL^n}{EI} \qquad 2.8.21$$

Then the total energy stored in each arm of the beam will be:

$$U = \frac{F^2L^2}{6EI} + \frac{KF^2L}{2AG} + \frac{CL^{n+1}}{EI}\frac{F^2}{2} \qquad 2.8.22$$

and the end deflection δ of each arm of the specimen will be

$$\delta = \frac{FL^3}{3EI} + \frac{KFL}{AG} + \frac{CFL^{n+1}}{EI} \qquad 2.8.23$$

Before relating the stored strain energy to the fracture energy as in the simple analysis by equating $\partial U/\partial L$ to $\partial S/\partial L$, Gillis and Gilman consider the possible contributions to the total energy of the kinetic energy of the moving crack. However, as we shall see in the next sub-section, the effect of this term is negligible. For completeness the argument will be summarized now before continuing the main development of the more sophisticated expression for the specific fracture energy.

Kinetic energy effects

A moving cleavage crack has associated with it a certain amount of kinetic energy produced by the sideways motion of the cantilevers. The mass of an elemental volume in one of the cantilevers can be expressed as

$$m = \rho w t dx \qquad 2.8.24$$

where ρ is the density of the material of the beam and w and t are as previously defined. The velocity is $\frac{d\delta}{dt}$ and the kinetic energy

$$dK = \tfrac{1}{2}\rho w t . dx . (\frac{d\delta}{dt})^2 \qquad 2.8.25$$

The kinetic energy of the whole cantilever K can be written

$$K = \frac{\rho w t}{2} \int_0^L (\frac{d\delta}{dt})^2 dx \qquad 2.8.26$$

Now

$$\frac{d\delta}{dt} = \frac{d\delta}{dL} \cdot \frac{dL}{dt} = \frac{d\delta}{dL} V_c \qquad 2.8.27$$

where V_c is the crack velocity.

And K can now be evaluated in terms of the crack velocity:-

$$K = \frac{\rho w t}{2} V_c \int_0^L (\frac{d\delta}{dL})^2 dx \qquad 2.8.28$$

Neglecting shear and end rotation effects

$$\delta = \frac{F}{6EI}(2L^3 - 3L^3 x + x^3) \qquad 2.2.29$$

$$\frac{d\delta}{dL} = \frac{F}{6EI}(6L^2 - 6Lx) = \frac{FL}{EI}(L - x) \qquad 2.8.30$$

$$(\frac{d\delta}{dL})^2 = \frac{F^2L^2}{(EI)^2}(L^2 + x^2 - 2Lx) \qquad 2.8.31$$

$$\int_o^L (\frac{d\delta}{dL})^2 dx = \frac{F^2L^5}{3(EI)^2} \qquad 2.8.32$$

Thus $$K = \frac{\rho wb}{2} V_c \frac{F^2L^5}{3(EI)^2} \qquad 2.8.33$$

Now the velocity of sound in the medium $V_s = (E/\rho)^{\frac{1}{2}}$ and $U = \frac{F^2L^3}{6EI}$, where $I = \frac{wb^3}{12}$

Substituting and rearranging:-

$$K = 12(\frac{V_c}{V_s})^2 . U . (\frac{b}{L})^2 \qquad 2.8.34$$

Therefore for large (L : b) ratios the kinetic energy is small compared with the strain energy U and can be neglected for slow moving cracks, $V_c << V_s$. We are now in a position to return to the main argument to develop a more refined expression for γ.

The application of the principle of conservation of energy, assuming crack initiation under adiabatic conditions gives

$$dQ = dE + dW = 0 \qquad 2.8.35$$

dE, the isothermal energy change, is composed of strain energy, surface energy and kinetic energy terms. dW, the work done by the system, is the cleavage force multiplied by its displacement.

Thus

$$dU + dS + dK = Fd\delta \qquad 2.8.36$$

where $S = \gamma wL$

If F and L are independent variables

$$\left(\frac{\partial U}{\partial L}\right)_F + w\gamma + \left(\frac{\partial K}{\partial L}\right)_F = F\left(\frac{\partial \delta}{\partial L}\right)_F \qquad 2.8.37$$

At the instant of propagation $V_c = 0$ and the term $\frac{\partial K}{\partial L}$ is equal to zero, thus the kinetic energy under these conditions cannot contribute to γ. Substituting for $\left(\frac{\partial U}{\partial L}\right)_F$ and $\left(\frac{\partial \delta}{\partial L}\right)_F$ in equation 2.8.37:

$$\frac{F^2L^2}{2EI} + \frac{KF^2}{2AG} + \frac{(n+1)CF^2L^n}{2EI} + \gamma w = \frac{F^2L^2}{EI} + \frac{KF^2}{AG} + \frac{(n+1)CF^2L^n}{EI} \qquad 2.8.38$$

and rearranging:

$$\gamma = \frac{F^2L^2}{2EIw}\left[1 + \left(\frac{KEI}{AGL^2}\right) + (n+1)CL^{n-2}\right] \qquad 2.8.39$$

It is now possible to examine how the contributions to the strain energy from the bending beam, shear, and the end condition affect the value of fracture energy γ.

The term due to shear, $\frac{KEI}{AGL^2}$, can be approximated to $\frac{1}{4}\frac{b^2}{L^2}$ and for large L:b ratios this can be neglected.

Using the resulting expression for γ we can see at once that in an experiment, recording the force and end deflection simultaneously has two advantages. The first is that it can be determined whether the system is linear, i.e. $\delta \alpha F$, and thus whether the above analysis can be applied. Secondly the value of CL^{n-2}, the term due mainly to end rotation, can be evaluated as follows:

Neglecting shear, which we can do for large L:b ratios, we can express the end deflection as

$$\delta = \frac{FL^3}{3EI}(1 + 3CL^{n-2}) \qquad 2.8.40$$

and the fracture energy in terms of the cleavage force as

$$\gamma_F = \frac{F^2L^2}{2EIw}(1 + (n+1)CL^{n-2}) \qquad 2.8.41$$

or in terms of the deflection as

$$\gamma_\delta = \frac{9}{2}\frac{EI\delta^2}{L^4w}\frac{(1 + (n+1)CL^{n-2})}{(1 + 3CL^{n-2})^2} \qquad 2.8.42$$

Gillis and Gilman suggest that because the deformations past the tip of the crack are primarily due to the bending moment, it would be reasonable to expect n to have a value close to 2.

If $n \simeq 2$

$$\gamma_F = \frac{F^2L^2}{2EIw}(1 + 3CL^{n-2}) \qquad 2.8.43$$

and

$$\gamma_\delta = \frac{9}{2}\frac{EI\delta^2}{L^4w}(1 + 3CL^{n-2})^{-1} \qquad 2.8.44$$

The true value of γ corrected for end rotation effects can be obtained from $\gamma_{true} = (\gamma_F \cdot \gamma_\delta)^{\frac{1}{2}}$. It is expected that γ_δ will be too high and γ_F too low, a point which will be noted in the discussion of the fracture energy values for glass and p.m.m. obtained by the author (Chapter IV).

Gillis and Gilman concluded from the analysis that although beam theory is strictly an approximation, for large L:b ratios the difference between the strain energy estimated by the simple theory and the more rigorous theory is negligible although due to the prevention of anti-clastic curvature the strain energy density near the tip may be higher than simple theory suggests by as much as 10%. It was also noted

that the use of compressive forces as a means of crack stabilization could produce large errors in the calculated value of γ. The extent of the error being largely determined by the position and nature of the compressive forces with respect to the neutral axis.

In summary, the analytical investigation of the cleavage technique indicates that in practice errors can be minimised or allowed for by two procedures. The use of large L:b ratios will reduce shear effects, and simultaneous force and deflection observations allow end rotation effects to be estimated and to be checked for linearity.

The semi-empirical analysis of cleavage experiments

The approach used by Berry and later by Broutman and McGarry has been described as semi-empirical. The essential difference between their technique and that of Gillis and Gilman is that Berry assumes the form of the possible errors and determines the constants experimentally whereas Gillis and Gilman deduce the form of the errors theoretically and evaluate or eliminate them experimentally. Berry assumes that the specimen acts as two symmetrical cantilever beams but that the simple equations

$$U = \frac{F\delta}{2} \qquad 2.8.45$$

and

$$\delta = \frac{FL^3}{3EI} \qquad 2.8.46$$

are incorrect for two reasons: strain energy is stored in the uncracked region, the amount depending on the local stresses, and since the uncracked region is not rigid the equations used to describe the

characteristics of the deflected region, including the strain energy relationship, will be inexact. The first effect tends to increase the strain energy, while the second tends to decrease it.

The basic assumption adopted by Berry in his analysis is that the beam equation can be generalised to become:

$$\delta = \frac{FL^n}{a} \qquad \text{or} \qquad F = \frac{a\delta}{L^n} \qquad 2.8.47$$

where a and n are numerical constants.

Now $$U = \frac{F\delta}{2}$$

Substituting $$U = \tfrac{1}{2}a\delta^2 L^{-n} \qquad 2.8.48$$

$$\therefore \qquad \left(\frac{\partial U}{\partial L}\right) = -\frac{na\delta^2}{2L^{n+1}} \qquad 2.8.49$$

So that $$\frac{\partial U}{\partial L} = -\frac{nF\delta}{2L} = 2\gamma w$$

Rearranging: $$\frac{F\delta}{w} = \left(\frac{4\gamma}{n}\right)L \qquad 2.8.50$$

The constant n is determined experimentally from a plot of Log F/δ versus Log L, and the specific fracture energy γ calculated using this value of n. It is of interest to compare in some detail these two approaches to the problem of allowing for the behaviour of the real double cantilever. Gillis and Gilman suggest

$$\delta = \frac{FL^3}{3EI}\left(1 + \frac{3EIK}{AGL^2} + 3CL^{n-2}\right) \qquad 2.8.23$$

while Berry puts

$$\delta = \frac{FL^n}{a} \qquad 2.8.47$$

Both authors identify the properties of the uncracked region which contribute to the non-ideality of the arms as cantilever beams in terms of a lack of rigidity and a source of strain energy. The distinction is that Gillis and Gilman estimate the magnitude of the effects of these properties by summing them into an end rotation whereas Berry determines the experimental form of the modified beam equations. It is suggested that strain energy may be introduced into the uncracked region by processes other than end rotation. In practice for some materials, as we shall see for glass and p.m.m. in Chapter IV, it appears that experimentally it is very difficult to decide whether Berry's equation, with $n \neq 3$ or Gillis and Gilman's equation is a better description of the relationship between δ and L. Even so a significant difference exists in the values of γ obtained from the two equations since Berry's assumption has a first order effect on γ, while Gillis and Gilman's assumption has only a second order effect on γ.

2.9 Summary

The specific fracture energy γ has been proposed as a direct measure of material strength. An energy balance criterion for fracture has been assumed and its use in the calculation of specific fracture energies followed. It should be noted that even if an energy balance criterion is not applicable, the 'work to fracture', although no longer a material

constant like γ, may still provide a useful measure of the strength of any material that fails by crack propagation; even if this parameter does change, for example with the stress distribution, nevertheless it is not influenced by the surface flaws. The cleavage technique of measuring fracture energies has been shown to possess a number of advantages over the other techniques described. In particular the stability of the system under conditions of constant deflection allows a large quantity of data to be extracted from a single specimen. The method of slotting (due to Berry) as a means of stabilizing the crack direction is suggested as being preferable to the use of compressive axial forces. Stability is also a feature of Nakayama's method. However, the cleavage technique has the advantage that it provides a means of examining the energy balance criterion for fracture and also provides a number of checks on self-consistency of the fracture energy measurements. Possible sources of errors may be accounted for or eliminated analytically or experimentally and it is suggested that the analytical technique involves fewer basic assumptions. A modified cleavage technique has been adopted by the author, and used to measure the specific fracture energies of polymethylmethacrylate and glass. The results of these experiments are described in the following chapters.

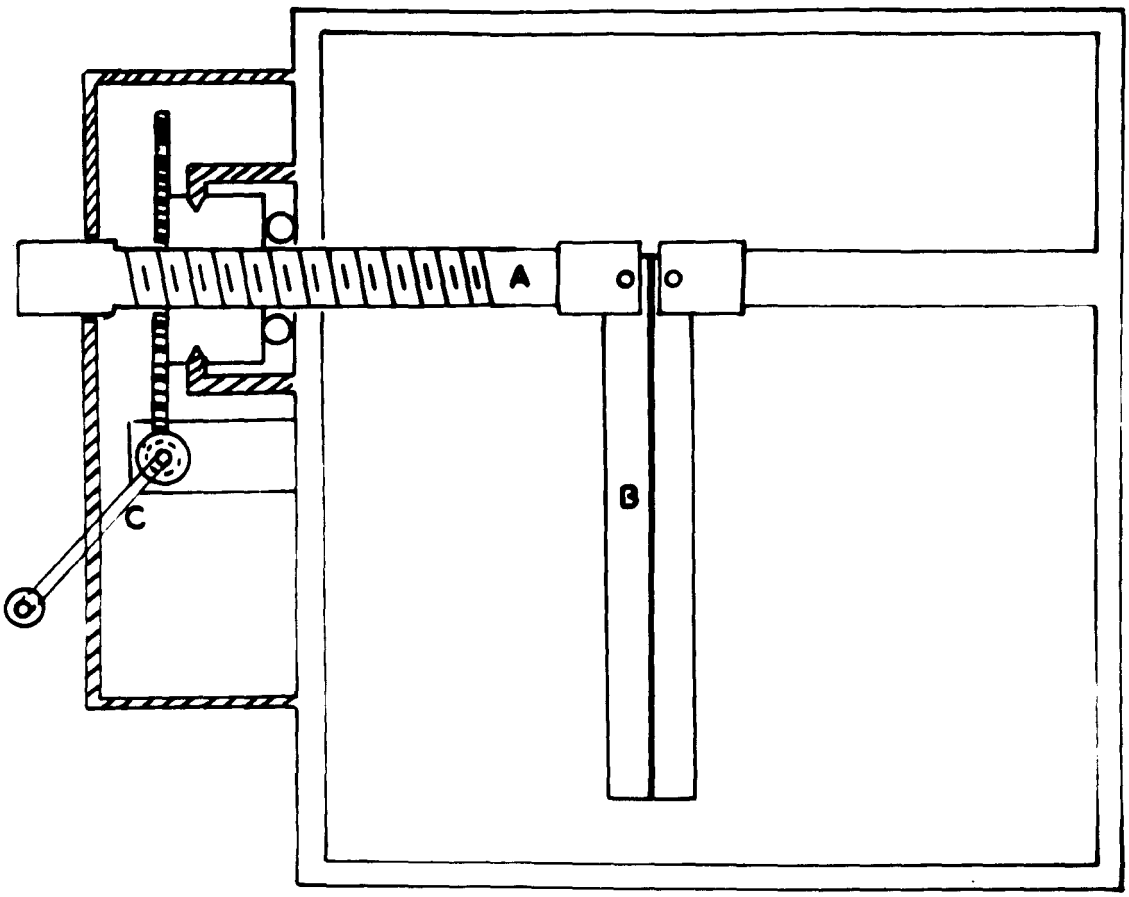

Fig. 9

Schematic representation of prototype cleavage machine

A - worm gear
B - specimen
C - hand drive mechanism

CHAPTER III

APPARATUS AND EXPERIMENTAL TECHNIQUES

3.1 Introduction

This chapter contains a description of the apparatus designed and used by the author to measure the specific fracture energies of polymethylmethacrylate and two glasses - a soda-lime silicate glass and a boro-silicate glass. The apparatus was initially designed so that fracture energy measurements could be carried out in various environments, but even so in order to facilitate this procedure additional apparatus was designed and constructed during the course of the work and incorporated into the basic cleaving machine.
The experimental techniques involved in the use of the basic and the and the ancillary apparatus are reported.

3.2 The basic apparatus

In order to gain the experience with which to design a versatile cleavage machine, initial measurements on polymethylmethacrylate (p.m.m.) were carried out with a prototype machine.
The prototype machine (Fig. 9) was simply a metal frame on which a pair of chucks had been mounted. One of the chucks was movable by means of a hand operated gear. In spite of the insensitivity of the hand operated drive, which limited the number of experimental points (often to three or four), the preliminary results were sufficiently close

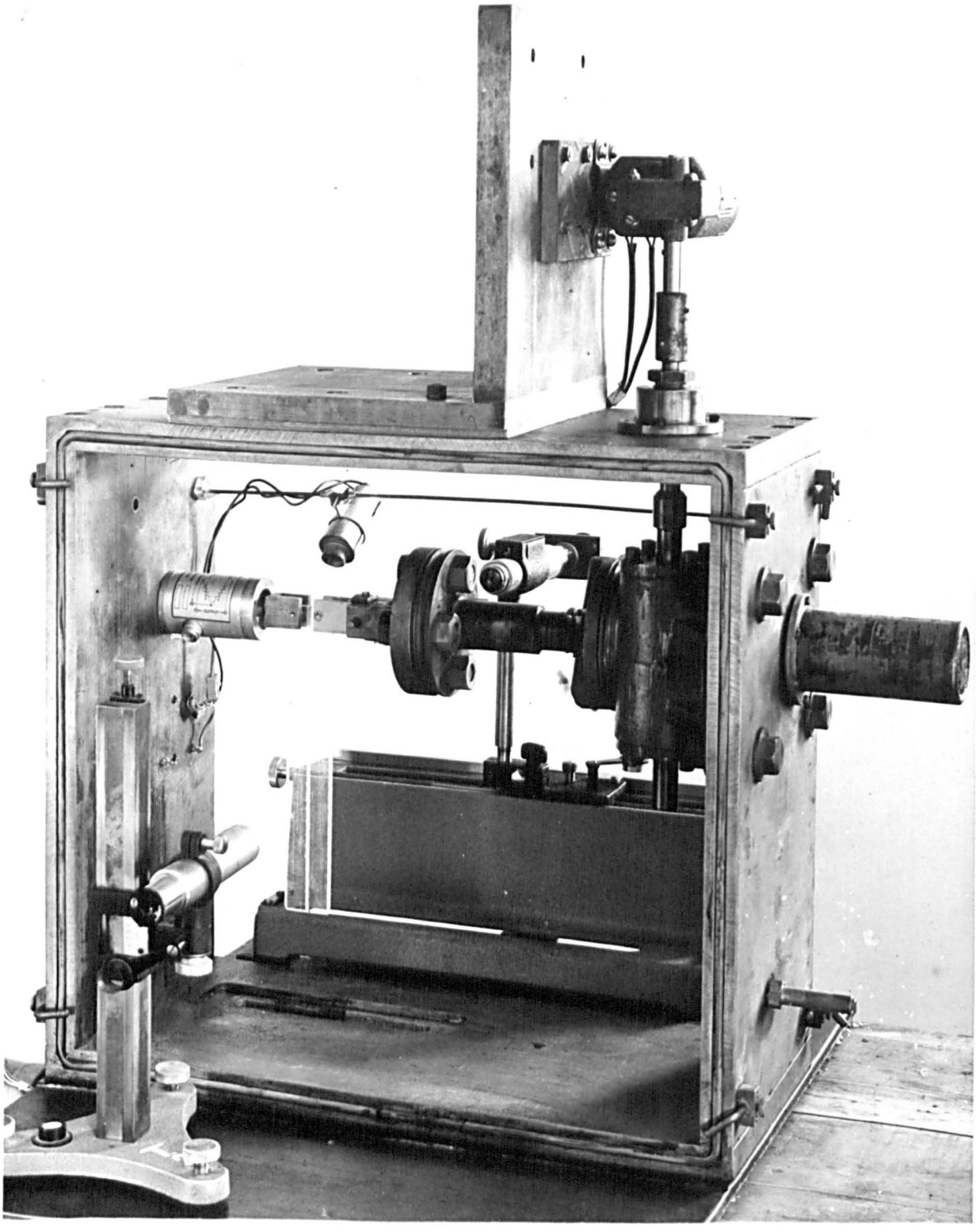

Fig. 10

Photograph of cleavage machine designed and used by the author

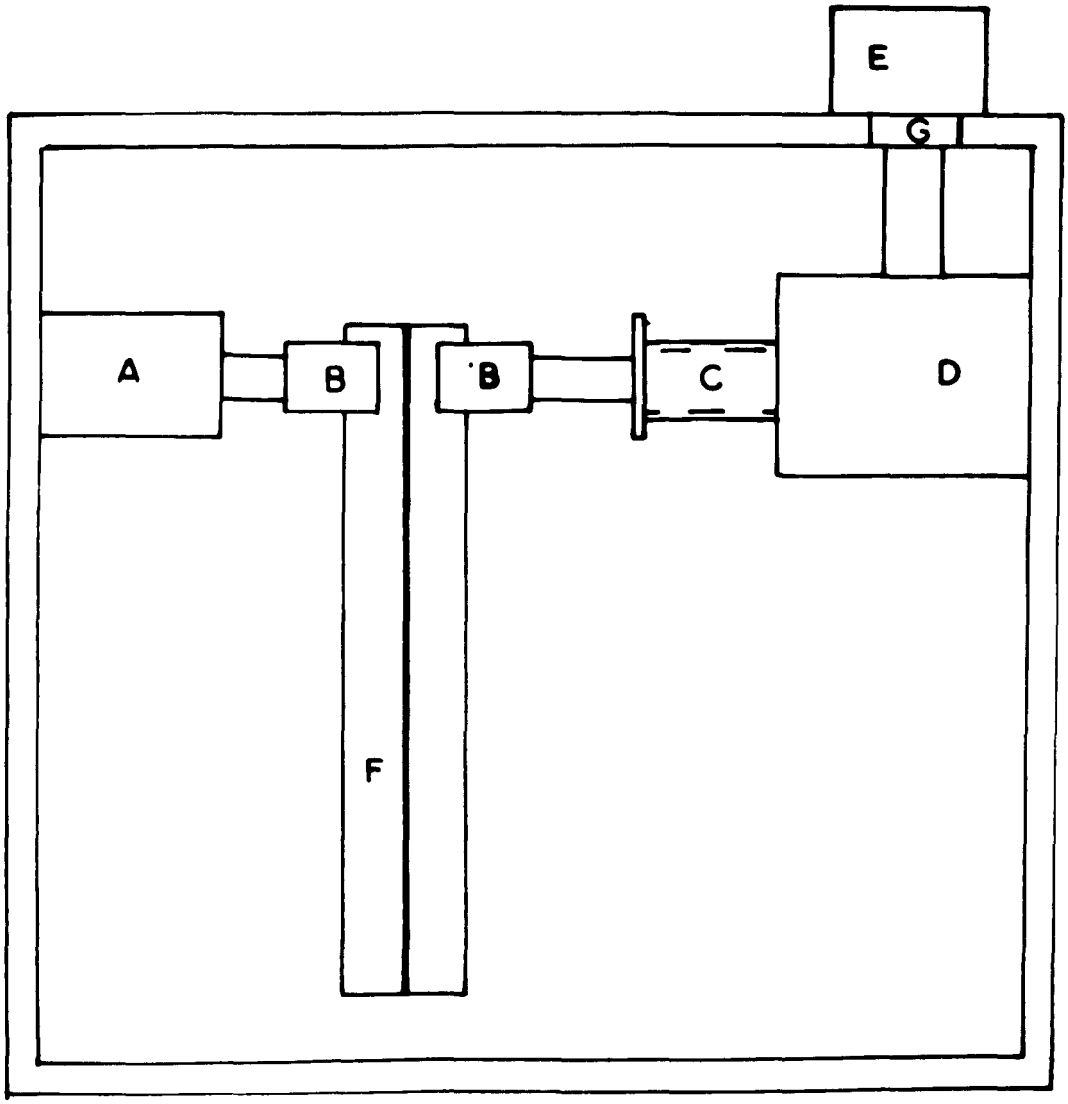

Fig. 10

Diagrammatic representation of the cleavage machine designed and used by the author

A - load cell
B - steel chucks
C - worm gear
D - worm gear housing
E - motor
F - specimen

to those obtained by previous workers (Berry 1963) to suggest that subsequent development of the apparatus would prove informative.

New features incorporated into the design of the new cleavage machine included the ability to control the environment and to control and measure the cleavage force, F, accurately. The new machine, shown diagrammatically in Fig. 10, is essentially an open-sided steel box 20" x 19" x 12" built of 1" thick mild steel plate in order to approximate as closely as possible to a rigid system. Mounted on one side of the box on the inner wall was a Duff-Norton worm gear (Model 1805-6-1) fitted with a steel chuck; opposite on the inner wall was a solid arm and chuck. The worm gear was driven by a variable speed reversing motor mounted on the top of the box and attached to the gear by means of a seal (Fig. 11) which was designed to limit gas flow around the drive shaft. The electrical system used to control the motor is shown in Fig. 12 and incorporated a reversing switch and push button which provided greater control over the loading. A variac was placed in the circuit to control the voltages on the motor and so its torque and speed. The solid arm and chuck were replaced by a load cell fitted with a steel chuck which was fastened to the end wall by means of an O.B.A. bolt, whenever the cleavage force was to be measured. The load cell was an Ether dynamometer type UF2, covering either the range 0 - 10 lbs or 0 - 100 lbs, and in use was coupled directly to a dial indicator. Before use in the machine and again after a period of months, each load cell, which consisted of four strain gauges mounted

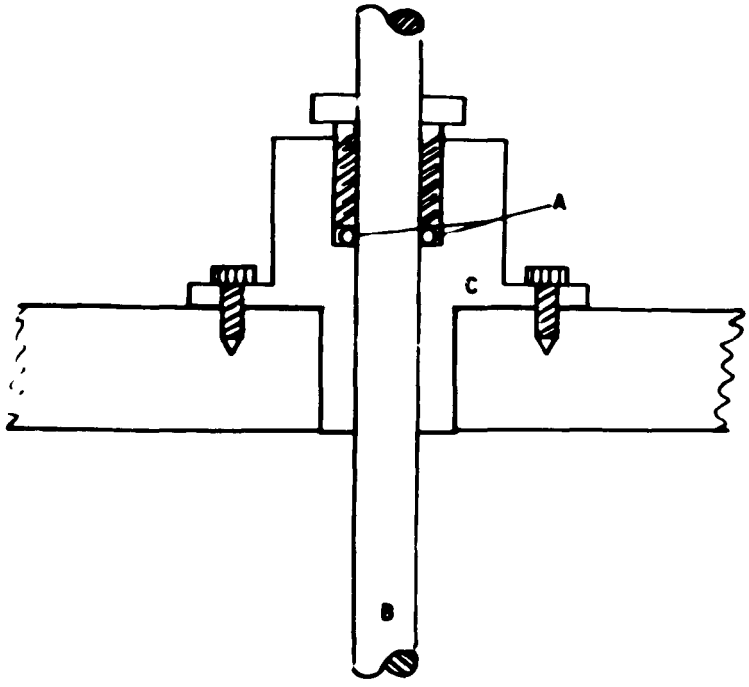

Fig. 11

Section through gas seal

A - neoprene ring
B - motor drive shaft
C - housing

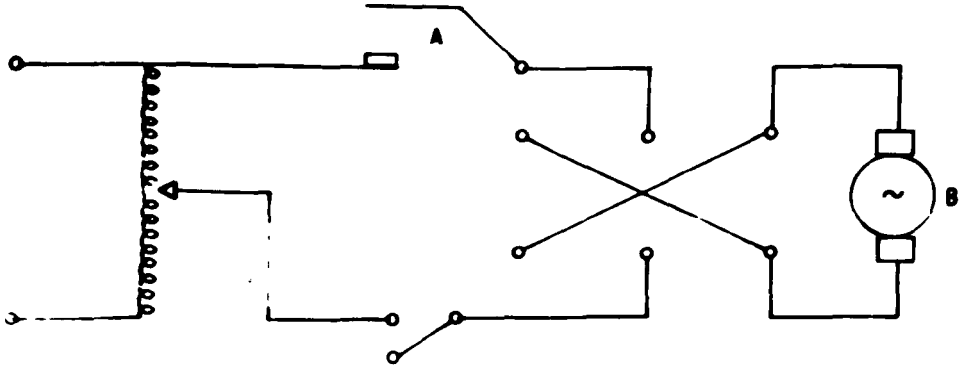

Fig. 12

Circuit diagram for motor control system

A - push button

to form a Wheatstone bridge, was calibrated directly in tension. Large changes in the cleavage force, corresponding to the propagation of the crack, occurred over very short periods of time, and so the output from the indicator was recorded continuously by a pen recorder. A Toa EPR 2TB potentiometric recorder was found to be suitable and this had a fast response: full scale in 0.3 seconds.

The open sides of the steel box were covered by $\frac{1}{2}$" thick perspex sheets sealed to the edges by neoprene rings and held in place by four clips on each side.

3.3 Production of specimens

As the majority of the experiments were on glass, only the techniques involved in the preparation of glass specimens will be described. In most cases the adaption of these techniques to the preparation of p.m.m. specimens, used in the preliminary experiments is obvious.

Specimens of the form shown in Fig. 13 were produced from either Pilkington 'Float glass' plate or from pyrex plate* (Corning 7740), having the nominal compositions shown in Table 1.

---

* We should like to acknowledge the gift of a quantity of pyrex plate through the courtesy of Mr. P.P. Jaram of Q.V.F. Ltd.

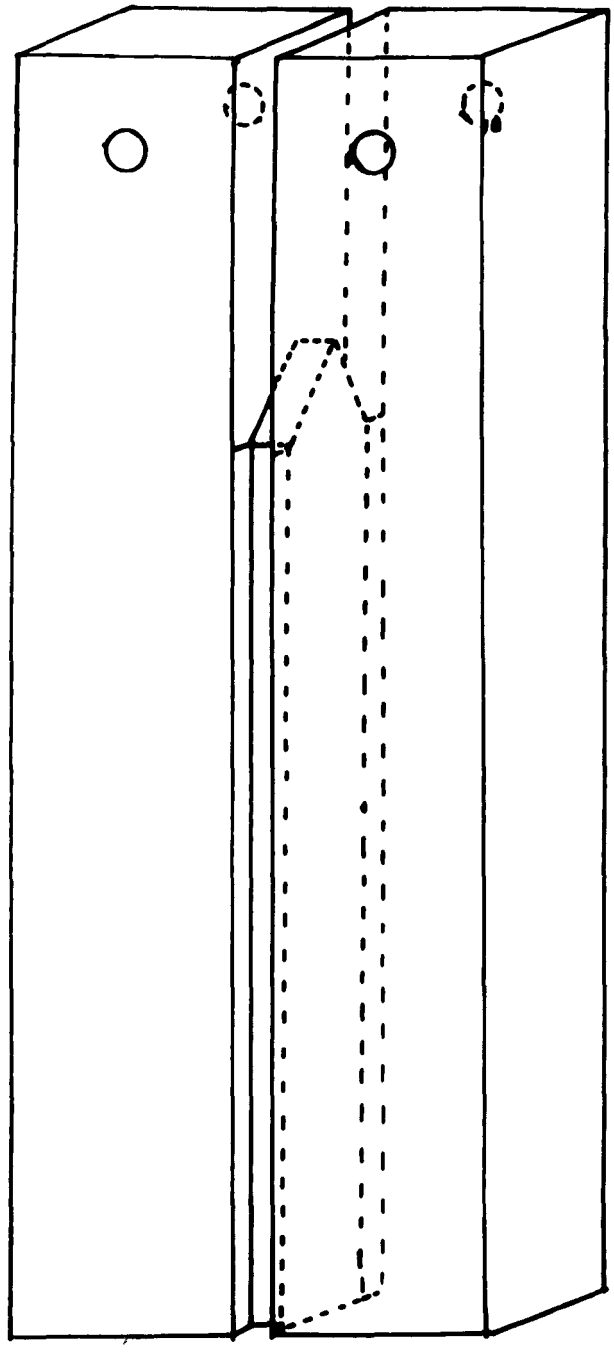

Fig. 13

Cleavage specimen showing groove

TABLE 1

Composition of Glasses

Composition	Float Glass Plate Author 1967	Pyrex Plate Author 1967	Soda-lime-silica Wiederhorn 1966	Soda-lime Culf 1957
SiO_2 (wt %)	72.7	80.6	72.13	72.7
CaO	9.0		7.2	9.3
Al_2O_3	1.0	2.0	1.70	1.1
Na_2O	12.9	4.2	14.12	13.2
MgO	3.1		3.97	3.1
Fe_2O_3	0.1		0.04	0.1
K_2O	0.6		0.45	
SO_3	0.2			0.5
B_2O_3		12.6		
Others	0.4	0.5		

Usually the specimens, 30 cm long and of various widths from 2.0 to 9.0 cm., were broken from $\frac{1}{4}$" or $\frac{1}{8}$" sheet after scoring with a diamond and then ground to give an accurately rectangular shape. Later specimens were cut directly from the bulk sheet with a Heathway glass cutting machine which utilised a diamond impregnated alloy wheel. This eliminated the tedious and time consuming grinding stage, and more important produced more accurately rectangular specimens.

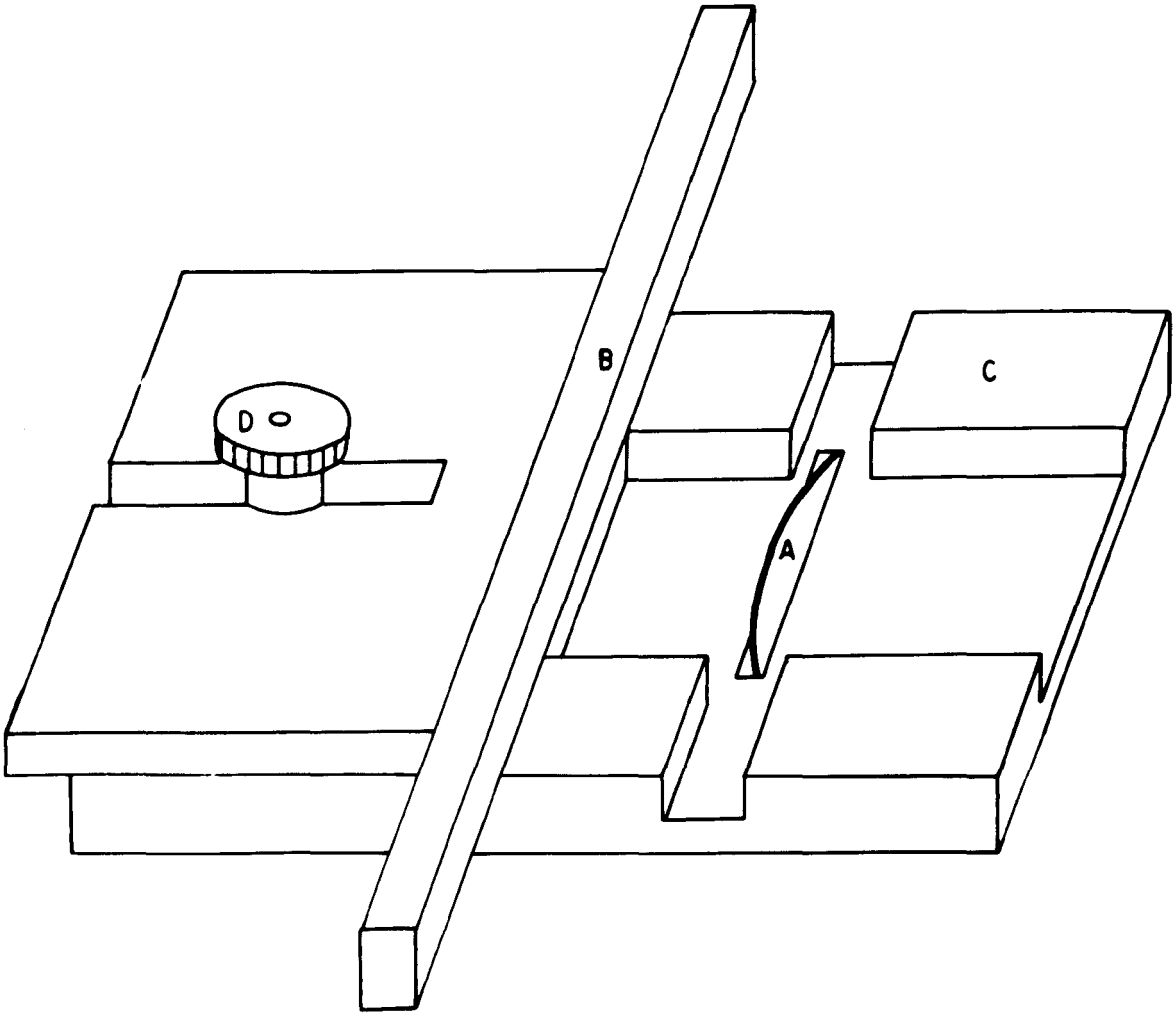

Fig. 14

Apparatus used for slotting specimens

A - copper/diamond wheel
B - guide
C - cutting bench
D - locking nut

Stabilizing slots of approximately 0.05 cm width and 0.1 cm depth were then cut down the centres of the faces of the glass rectangles parallel to the long edges, by means of a jig mounted on an Anderman glass cutter (Fig. 14). This cutter uses a very fine copper wheel, the periphery of which is impregnated with diamond, and which protrudes above the cutting table; removal of the jig allowed the "swallow-tail" cuts (Fig. 15A) to be made at the top of the specimen simply by feeding the specimen into the wheel. The specimen was strained by a system of chucks attached by pins through two holes, one on either side of the groove near the top of the specimen. The holes were drilled with a tungsten-carbide tipped drill of diameter 0.3 cm and water was used as a combined coolant and lubricant during the drilling process.

In order to examine the possibility of undue stresses having been introduced into the specimens during their preparation it was decided to subject them to a heat treatment. For this purpose a long stainless steel lined oven was designed and built. Stainless steel lining was used to ensure a clean environment during the heat treatment. The inner lining was constructed from a $^{1}/16"$ stainless steel sheet folded into a box open at one end. Around this, thin asbestos tape was wrapped both to hold it together and to insulate it from the nichrome wire which formed the heater. The wire was wound around the inner oven and more closely spaced at the ends in order to produce a more nearly uniform temperature along the length of the oven. Two shelves of flat $\frac{1}{8}"$ stainless steel sheet were cut and placed inside the oven lining to rest on

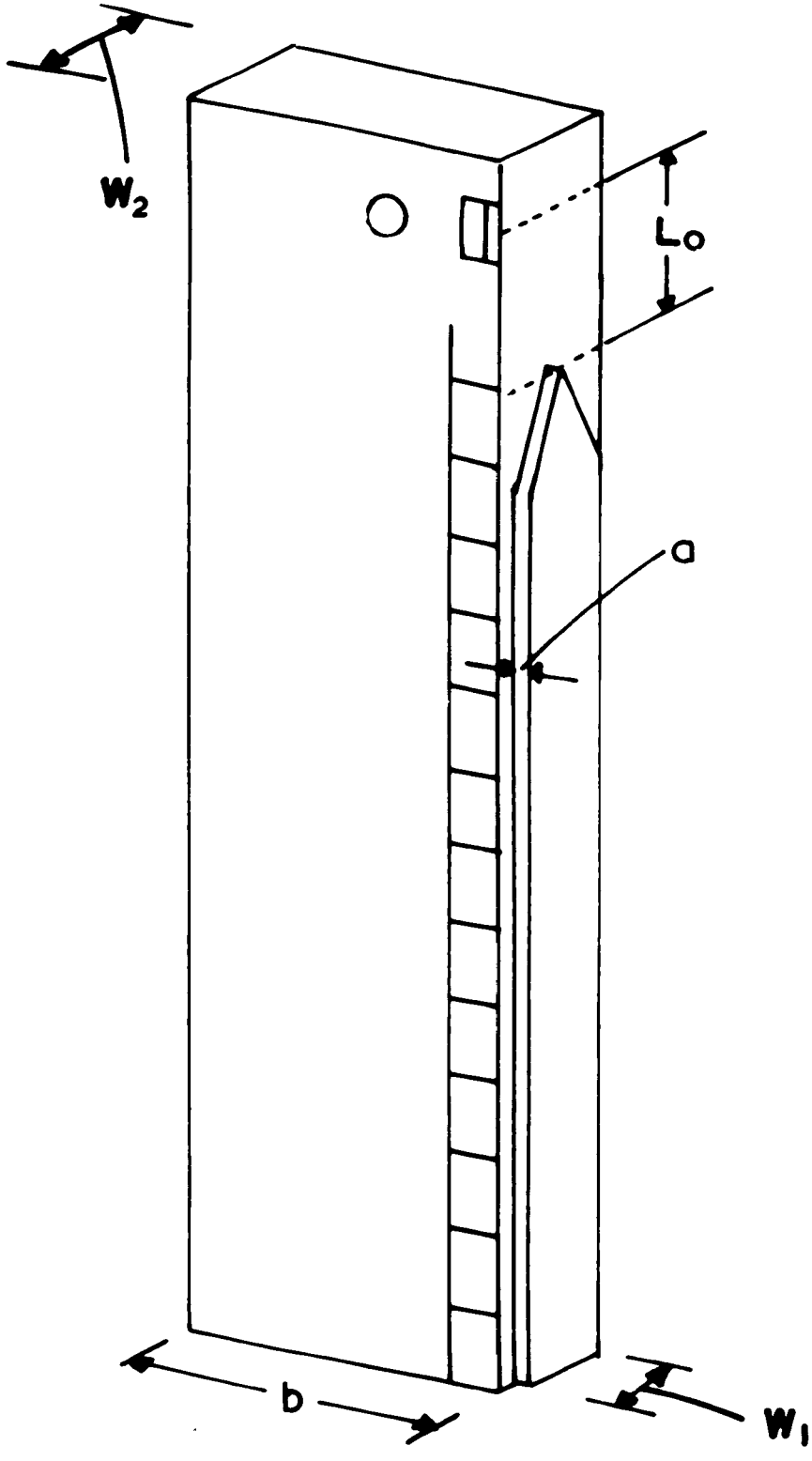

Fig. 15A

Half specimen illustrating "swallow-tail" cut,
scale and beam dimensions

bolts fastened onto the sides. The inner oven was then placed in a box constructed from 1" thick asbestos sheet and dexion, open at one end, and then packed with exfolliated mica to insulate it. The ends of the heater were drawn through the outer asbestos and a stainless steel/ asbestos door fitted at the open end. The oven was used in conjunction with a temperature controlling device already in service in the laboratory. This consisted of an Ether temperature recorder and controller coupled to a motor driven variac which, by lowering the voltage on the oven at a fixed rate, allowed the oven to cool at approximately $1C^{o}$ per minute. The temperature of the oven was measured by means of a copper-constanton thermocouple, inserted into the oven via a hole in the door, the output of which was fed directly into the Ether controller. The mode of operation was to set the control at the required temperature and to switch on; once the temperature was reached it was regulated thermostatically and maintained for several hours. A temperature of $550^{o}C$ was used, this was $40C^{o}$ below the softening temperature for a typical specimen which was determined experimentally. The motor driven variac mechanism was then switched on and the specimens removed from the oven only when the temperature had reached that of the room.

After annealing, examination of the specimens between crossed polaroids gave no indication of residual stresses, and preliminary cleavage experiments showed that the only apparent effect of the heat treatment was marginally to reduce the scatter in the results. Nevertheless, as a precautionary measure the heat treatment was incorporated into the routine preparation.

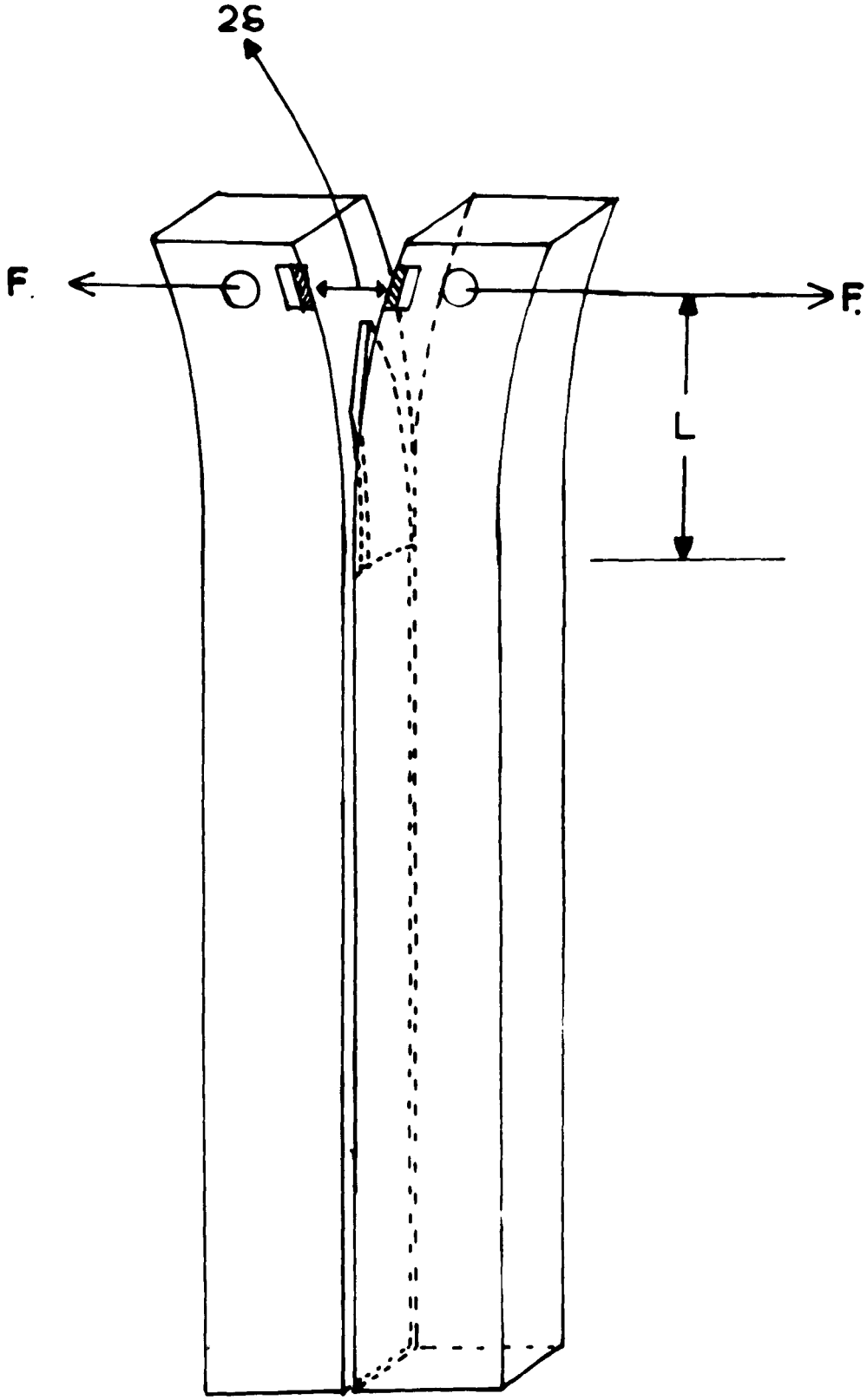

Fig. 15B

Specimen under cleavage showing separation of the ends (2δ) and fiducial markers

After annealing, small groups of specimens were etched in 4% HF solution in order to produce smoother surfaces at the bottom of the stabilizing grooves. They were etched for various times using ultrasonic agitation. The results obtained from such specimens were indistinguishable from those from the normal unetched ones, and it was concluded that the roughness of the groove did not affect the crack position.

3.4 Experimental technique

The specimen to be cleaved was suspended vertically by two steel pins which passed through the holes in the top of the specimen and those in the steel chucks (Fig. 10). As the chucks were separated, using a fixed strain rate, a crack started at the tip of the "swallow-tail" and propagated down the specimen. Provided that the specimen was rectangular and that the grooves in the faces were accurately aligned opposite to one another and parallel to the edges of the specimen, the crack would propagate smoothly down the whole length of the specimen as the displacement of the chucks was increased, leaving a smooth fracture surface. Failure to achieve any one of these conditions resulted in a rough fracture surface or occasionally in the crack running through one arm of the specimen. The length of the cleavage crack was measured after each incremental increase of the displacement of the chucks, against a paper scale affixed to the surface of the specimen adjacent to one of the grooves (Fig. 15A). The crack front was located accurately by means of a 6" focal length telescope mounted on a

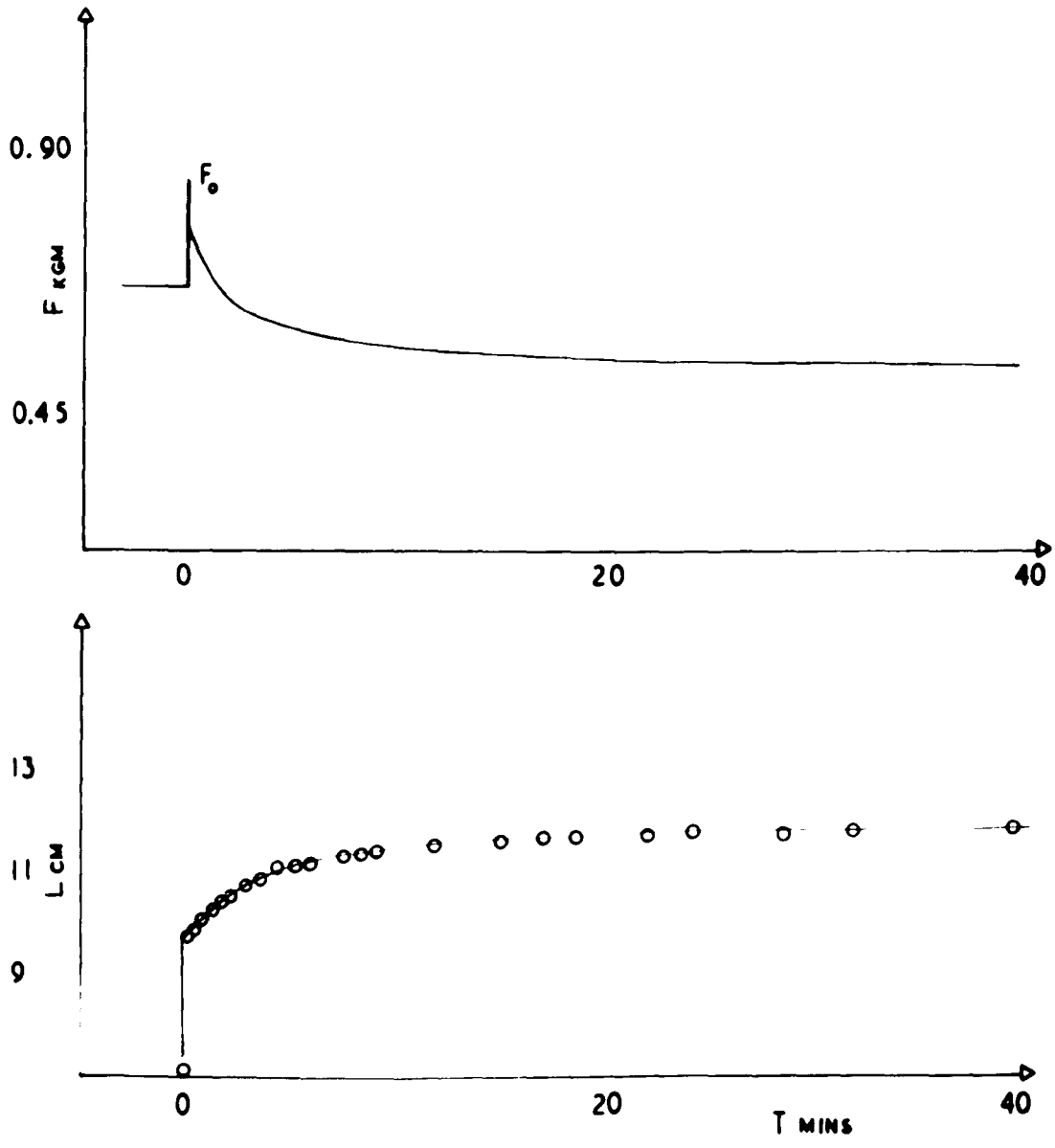

Fig. 16

The variation of cleavage force and crack length with time at constant deflection (2δ)

cathatometer. In some corrosive environments it was not possible to use a paper scale and in these cases the crack length was measured directly on the cathatometer. The separation of the ends of the cantilever arms, 2δ, (Fig. 15B) was measured using a low powered microscope fitted with a Watson micrometer eye-piece (x 15 overall magnification) and mounted on a travelling microscope bench. The microscope was focussed onto fiducial markers (pieces of razor blade) aligned with the centres of the holes drilled in the top of the specimen.

The cleavage force F was recorded continuously during the experiment, using the polyrecorder set typically at 500mV or 1Volt range and chart speeds of 180mm per hour or 20mm per minute. Throughout these experiments it was noted that after each normal increment in the displacement δ the length of the crack increased continuously with time. As the crack length increases at constant, δ, the force on the loading pins decreases. These changes are illustrated in Fig. 16A and B. Normally readings of L, δ and F were taken at the instant of propagation of after two, or in some cases fifteen, minutes of crack growth.

After the specimen had been cleaved completely, the value of b, the beam width, was measured with a ruler at ten points on each half of the specimen. The thickness of the specimen, w_2, was measured using a micrometer and the mean of ten readings calculated. Although w_1, the width of the fracture surface, was approximately constant down the whole specimen, the values corresponding to the measured crack lengths were always determined; a requirement of the differential energy balance

criterion. Values of w_1 were measured using a Watson microscope fitted with a vernier eye piece.

Young's modulus was determined in a separate experiment using 'three-point' and cantilever bending systems; the results are shown in Table 2.

TABLE 2

Young's Modulus for Glasses determined experimentally

	Three point bend	Cantilever	Cleavage
"Float Glass" Plate	7.14 x 10"dynes cm^{-2}	6.86 x 10"	6.5 x 10"
Pyrex plate	6.32 x 10"	6.22 x 10"	

3.5 Controlled environment

The initial measurements of fracture energy were carried out in air and the humidity and composition remained uncontrolled. Later tests involved the use of controlled environments and for these, particular techniques were evolved which will be described in the following sections of this chapter.

Gaseous environments

For tests in gaseous environments the box was simply sealed off by means of the two perspex plates and flushed with the required gas for several hours using the inlet and outlet gas ports in the end walls.

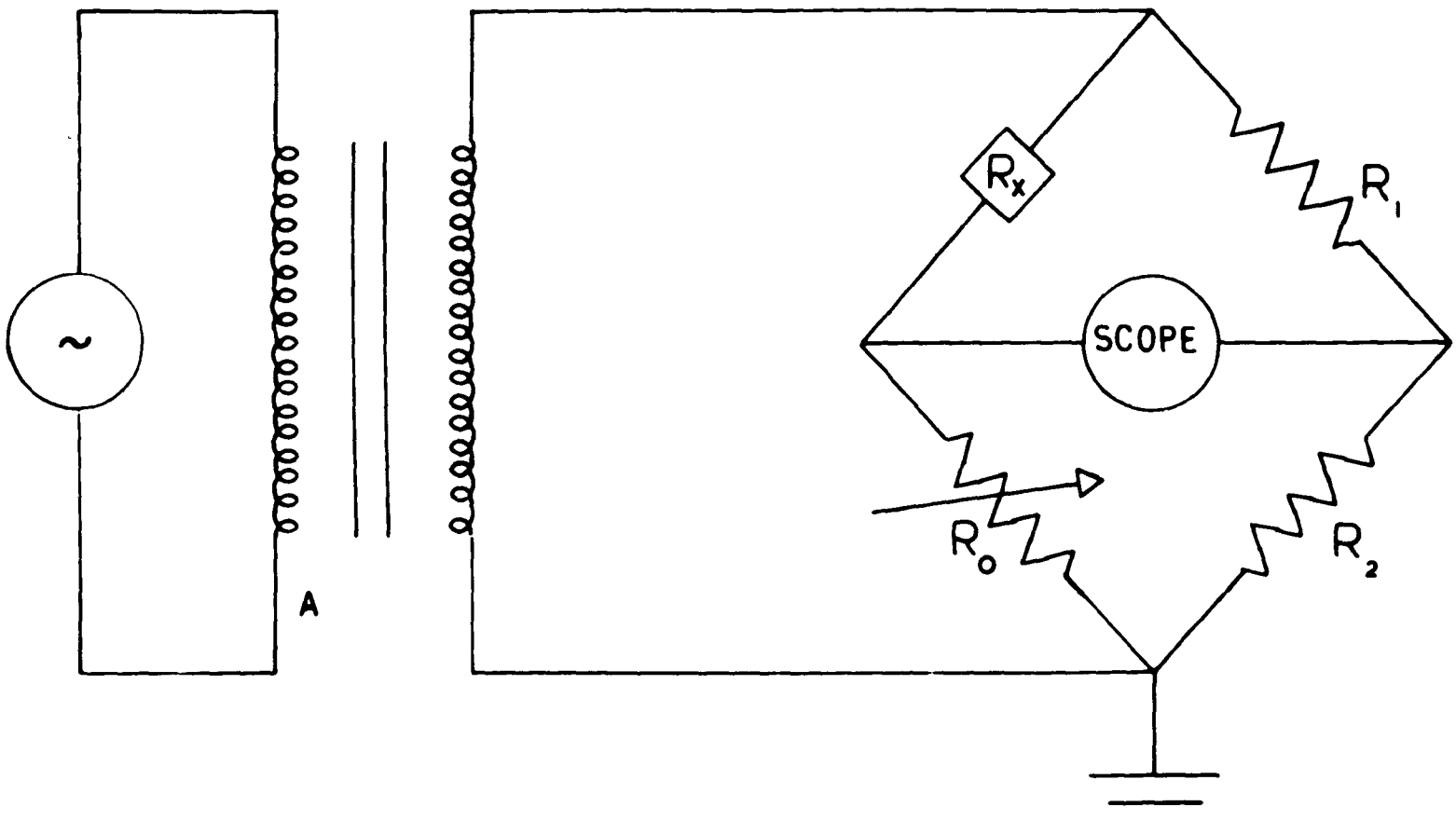

Fig. 17

Circuit diagram for humidity transducer

If the gas was to be dried then it was passed through a liquid nitrogen trap and then over the specific drying agent. Some of the drying agent was also placed inside the box before sealing and the system was left for several hours, after flushing with the gas, to allow the drying agent and environment to reach an equilibrium. Tests were carried out in this way in Air, Nitrogen, Carbon dioxide and Ammonia. Calcium oxide (anhydrous) was used to dry the ammonia and Phosphoric oxide (P_2O_5) for the other gases. Measurements of the relative humidity were carried out using a P.C.R.C.-33* humidity transducer. The transducer is a processed plastic wafer - a chemically treated styrene co polymer - which has an electrically conducting surface layer. Changes in relative humidity cause the surface resistivity to vary. The transducer was only useful within the range 4 → 100% R.H. since its resistance at 4% was already 10MΩ and increased rapidly with further reduction in relative humidity. The transducer was used with a standard A.C. Wheatstone bridge capable of measuring up to 10MΩ; the circuit is shown in Fig. 17. The bridge was balanced for each environment and the relative humidity determined from the calibration chart provided with the transducer.

Liquid environments

Whenever tests required a liquid environment, the specimen was suspended from the chucks so that the bulk of the specimen was immersed

---

* Supplied by the Phys-Chemical Research Corporation

in a bath of liquid; particular care was taken to ensure that the liquid covered the "swallow-tail" cut in the top of the specimen. In this way the crack was initiated in the test environment. The liquids were dried, when required, by an appropriate drying agent which was left in the liquid during the test. Tests were carried out at room temperature in distilled water, liquid paraffin, glycerol-water solutions, 4% HF solution and silicone oil. In gaseous environments the crack front was easily visible by virtue of the difference in refractive indices of the glass and gas; in liquids, however, the crack front was almost invisible but could be located by the position of its strain field detected with the aid of crossed polaroids. A check was made in air to verify that the crack front coincided with the position of the strain field located with the crossed polaroids.

3.6 The variation of fracture energy with temperature

The bulk of the fracture energy measurements were made at room temperature (20°C), which was recorded at intervals during the experiment using a mercury-in-glass thermometer. Because of the difficulties involved in producing uniform heating, variations in the temperature of the environment were restricted to the use of selected liquid baths. Two extremes of temperature were used, liquid nitrogen (-196°C) and a silicone oil heated to 200°C. For the low temperature tests specimens were immersed in liquid nitrogen contained in a clear dewar. To prevent the specimen from cracking up due to thermal shock on

immersion, a procedure of gradual cooling was adopted. First the specimen was suspended in the dewar and pre-cooled nitrogen gas passed around it for some time. Liquid nitrogen vapour from a dewar partially full of liquid nitrogen was then poured around the specimen and finally small quantities of liquid nitrogen, until the liquid level was just above the bottom of the specimen. Once this level had been reached, cooling through conduction could also take place and so liquid nitrogen was added at a reasonable rate until the dewar was full. In these experiments, ice formation on the part of the specimen exposed to the air and on the dewar was a major problem. The crack front was located by means of crossed polaroids and a strong light source but the specimen was only visible when the sides of the dewar were wiped with acetone. The ice on the top of the specimen eventually formed a link between the two sides of the crack and had to be broken every time the crack was repropagated. This made force measurements unreliable and introduced complex strains into the beam system. However, this was not important for fracture energy measurements where the total testing time was not more than about thirty minutes. The liquid nitrogen had to be replenished at regular intervals throughout the experiment.

Several high temperature tests were carried out at 200°C using an inert silicone oil (M.S.550) bath. The bath was heated by a finely wound 25Ω nichrome resistor placed inside a U-shaped pyrex tube and packed with alumina. The temperature was maintained at 200°C ± 2°C by the Ether control unit mentioned earlier and the temperature measured by

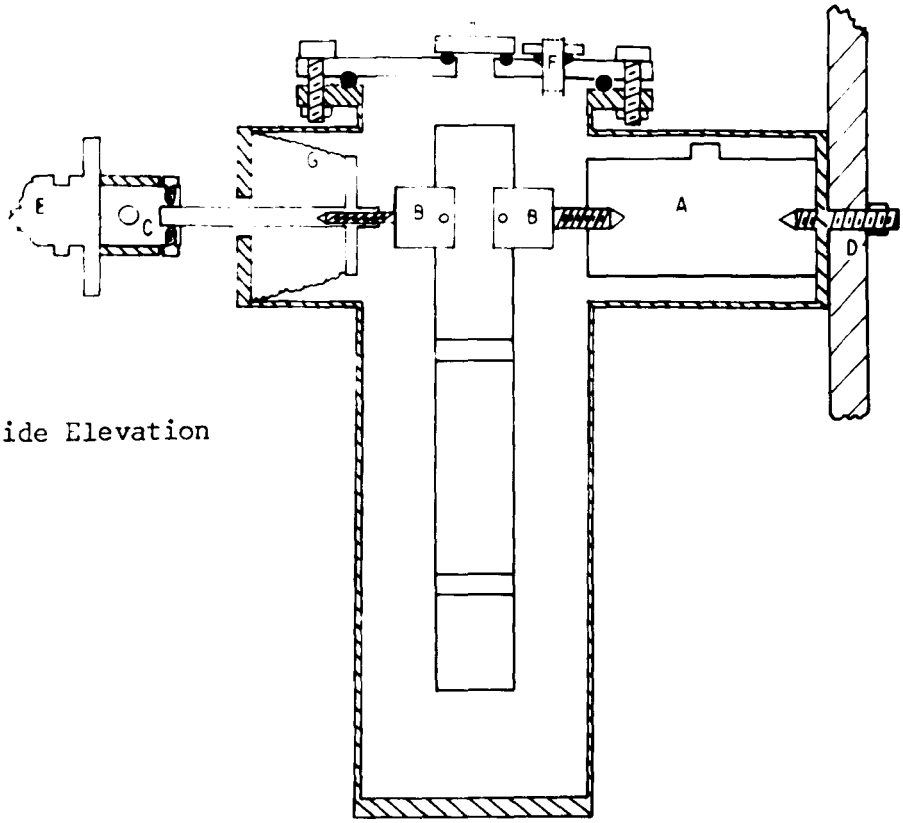

A - Side Elevation

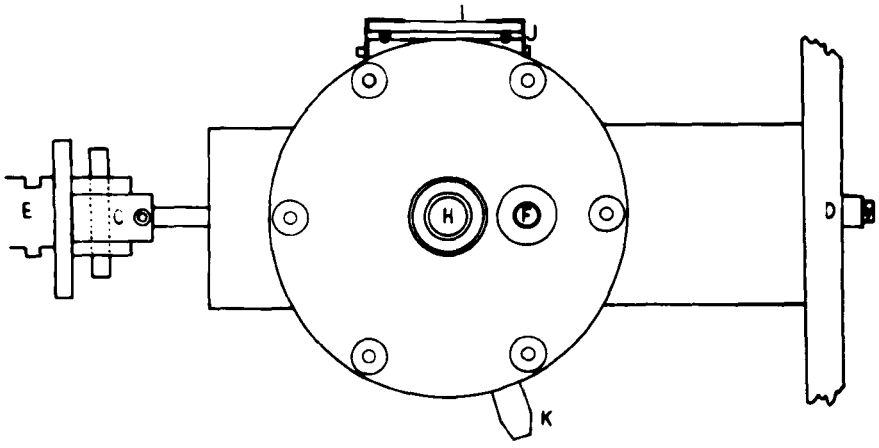

B - Plan

Fig. 18

Vacuum system designed for cleavage experiments

A - load cell, B - chucks, C - chuck insert,
D - end wall of cleavage machine,
E - worm gear & plate, F - araldite/brass plug,
G - flexible bellows, H - window, I - long window,
J - window clips, K - pumping arm.

a copper-constantan thermocouple placed inside a pyrex tube and immersed in the liquid bath. Previously tests had been carried out in this oil at room temperature, so that a direct comparison of the results would indicate any temperature effects.

3.7 The measurement of fracture energies in a vacuum

In the preliminary series of tests a marked variation of the specific fracture energy of glass with environment was observed. In order to identify the effects of the environment more critically it was decided to carry out a series of tests under vacuum. This involved the design and production of a vacuum system which could be coupled directly into the existing cleavage machine without any major alterations. The main problems were the transmission and measurement of the cleavage force F. Figs. 18 A and B illustrate the system, which is essentially a copper cylinder with two side arms opposite one another and near to the top. One side arm housed the load cell, which was fastened through the end wall of the arm directly to the machine, as shown. The other side arm contained a flexible bellows which coupled the worm gear to a movable chuck inside the main vessel. In this way it was possible to transmit the cleavage force to the specimen directly. The deflection of the beams, δ, and the crack length, L, were observed through a long $\frac{1}{4}$" plate glass window sealed to a raised section of the main tube by means of neoprene rings. A second window in the top was used to illuminate the specimen; this was circular in shape and also sealed by a neoprene ring fitted into a groove cut in the flanged lid.

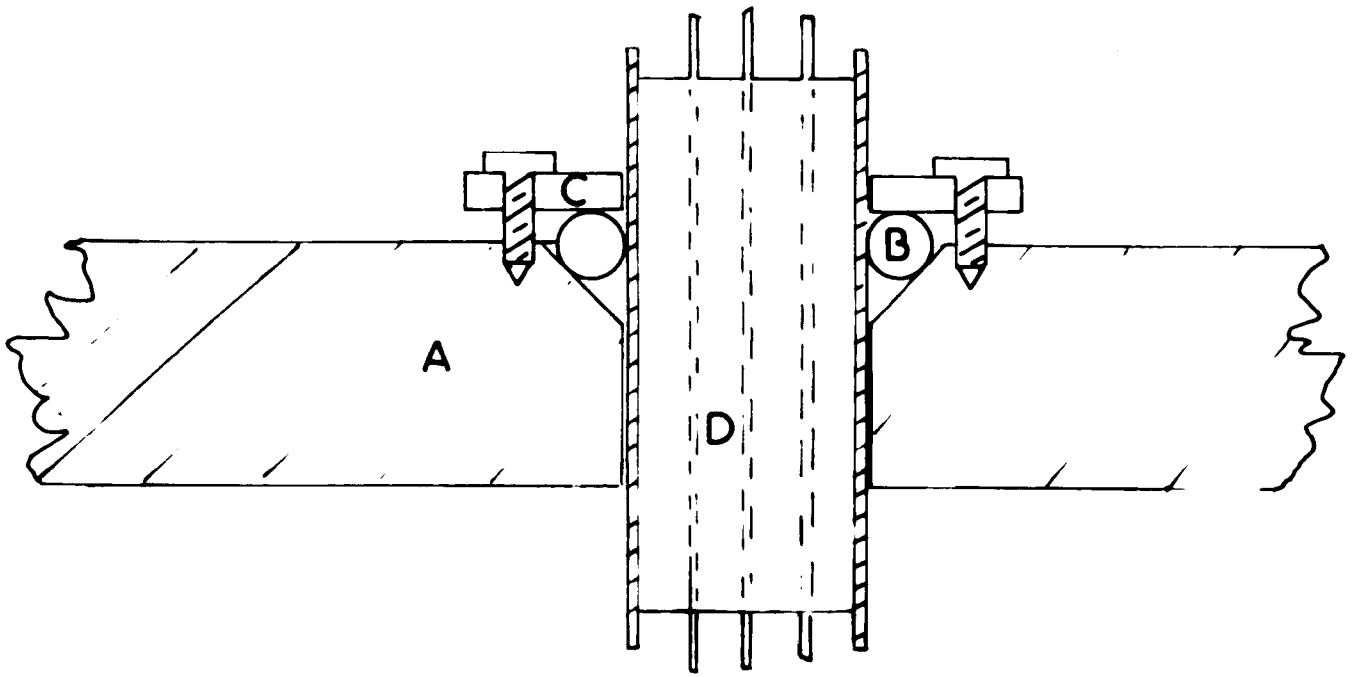

Fig. 19

Araldite/brass vacuum plug, connection to load cell

A - lid of vacuum system
B - neoprene ring
C - brass retaining ring
D - araldite and copper wires

For tests in vacuum it was necessary to assemble the system in a strict sequence. First the load cell was placed inside the side arm and screwed into position. A long lead from the load cell to the connection in the lid of the system was necessary so that the lid itself did not obstruct the initial stages of assembly. The two chucks were then screwed into position, one into the load cell and one into the connecting rod which was fastened to the bellows and linked the chuck to the worm gear. The vacuum vessel was then placed in the cleavage machine and the end of the bellows connecting rod clamped into a chuck insert by two grub-screws. This insert was then fastened to the chuck on the worm gear by means of a pin which passed through the insert and the chuck. The system was then locked into position by bolting the arm containing the strain gauge to the end wall of the cleavage machine as illustrated, (Figs. 18). The chucks inside the vacuum vessel were then adjusted by the worm gear so that the specimen could hang freely from them.
The flanged top was then replaced and carefully bolted down, sealing against the neoprene O-ring in the flange. The connection to the load cell was by means of an araldite/brass vacuum plug (Fig. 19).
The chamber was evacuated using an oil filled rotary pump and a molecular absorption pump filled with $^{1}/16$" pellets of Aluminium Calcium Silicate (Fig. 20). The "backing" pump was used first to evacuate both the chamber and the molecular pump to approximately 10^{-2}cm Hg. The molecular pump was then isolated from the pumping system and completely immersed in liquid nitrogen contained in a large dewar. The rotary pump was then

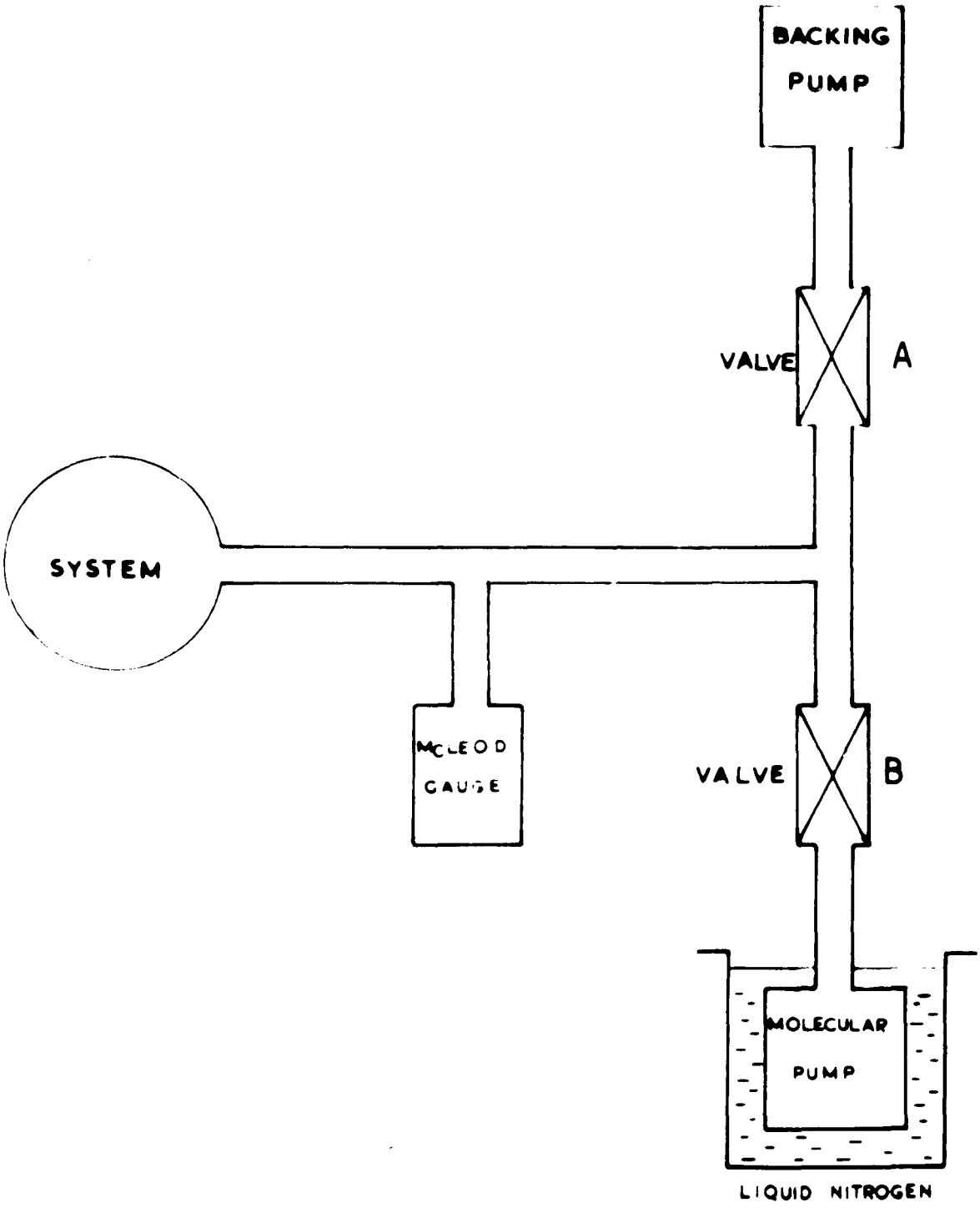

Fig. 20

Pumping unit

isolated and switched off and the molecular pump opened to the system. Within 30 minutes the pressure was approximately 2×10^{-4} cm Hg, measured directly with a McCleod gauge. Cleavage tests were then carried out using the technique of incremental displacement loading described in Chapter II, recording δ, F and L for positions down the specimen.

3.8 Tensile measurements of the specific fracture energy

In view of the apparent conflict between the high fracture energies ($\sim 4.0 \times 10^3$ ergs cm^{-2}) obtained using the cleavage technique described above, and that obtained by Griffith ($\sim 5.0 \times 10^2$ ergs cm^{-2}) in tensile tests, it was decided to carry out a few tensile tests on some glass specimens. Tests were carried out on rectangular plate glass specimens containing cracks of known length introduced by mechanical cleavage or by thermal shock. These specimens were prepared from the usual cleavage specimens in two ways. Either a cleavage crack was introduced into a specimen as usual and the specimen was then cut to give a rectangular sample with a short crack. Or a crack was introduced into a normal cleavage specimen by pressing a white hot glass rod against the lower end of the specimen and a tensile specimen was produced by then cutting off both ends of the original cleavage type specimen. In both cases the crack propagated down the centre of the specimen controlled by the stabilizing grooves. The tensile specimens were approximately 6 cm long and of various widths, from 4 → 8 cm. Crack lengths ranged from 0.1 cm to 0.5 cm. Araldite grips were cast onto each half of the specimen, using polythene moulds; some care was taken to ensure that the top

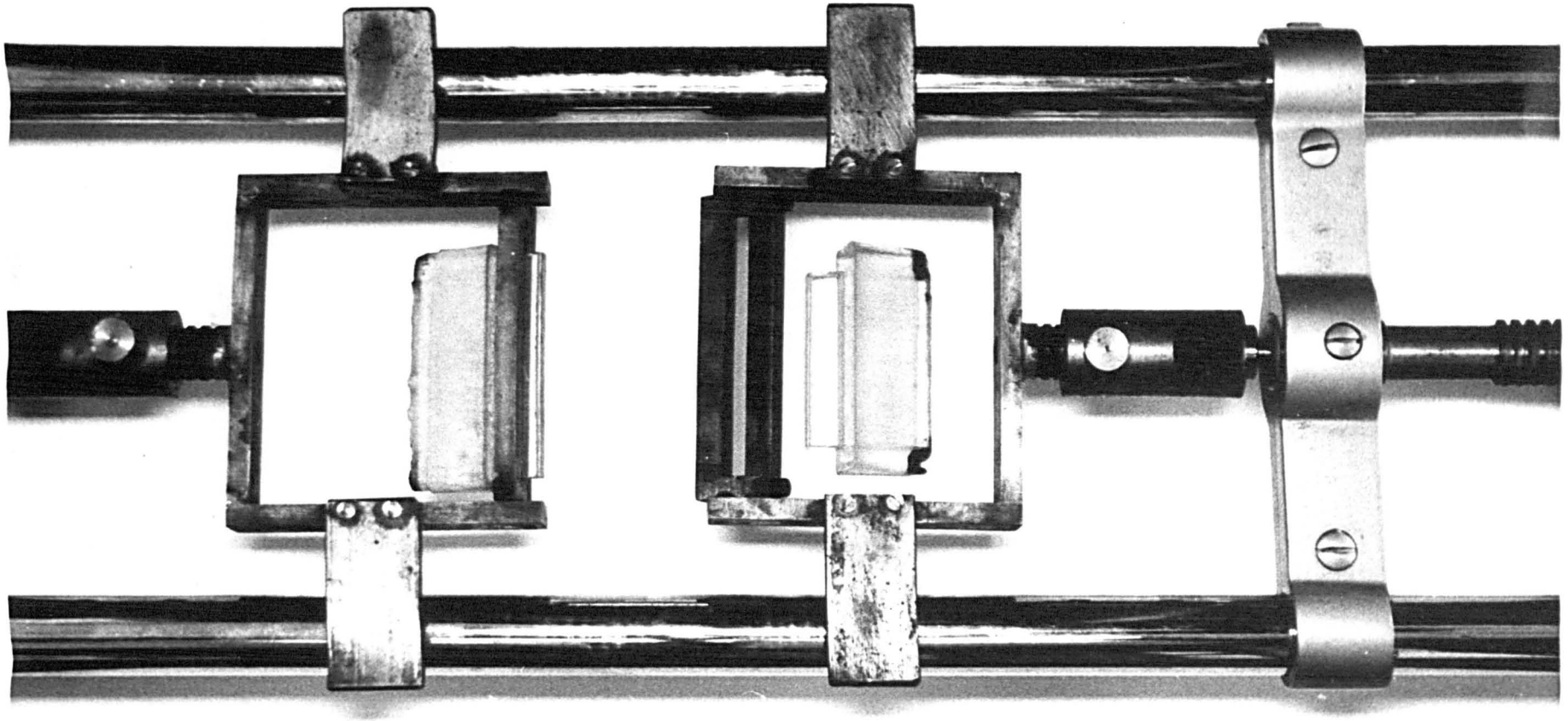

Fig. 21

Photograph of tensile specimen and chucks as used in Hounsfield Tensometer

surface of the grip was perpendicular to the specimen. The specimens were broken in tension on a Hounsfield Tensometer which had been fitted with chucks designed to take the araldite grips (Fig. 21). The rate of loading was such that fracture occurred after about 5 seconds. Values of the fracture energy were calculated from the Irwin-Orowan equation

$$\sigma = \sqrt{\frac{2E\gamma}{\pi c}} \qquad 3.8.1$$

using the measured breaking stress and the corresponding initial crack depth.

3.9 Summary

A series of cleavage experiments was carried out on soda-lime silicate and borosilicate glass in a variety of environments and at several different temperatures. A few experiments were undertaken to measure the specific fracture energy of polymethylmethacrylate specimens prepared from $\frac{1}{4}$" sheets obtained from I.C.I. Tests in specific environments, especially under vacuum, required additional apparatus and techniques which have been described. Tensile tests were carried out on a few specimens. In all the cleavage experiments described above, the technique of incremental displacement loading was adopted and the detailed results of these experiments together with an analysis of the errors are described in the following chapter. The experiments designed to investigate the phenomenon of prolonged crack growth observed in the cleavage fracture energy measurements are described later, in Chapter V.

CHAPTER IV

RESULTS AND A PRELIMINARY ANALYSIS AND DISCUSSION

4.1 Introduction

In this chapter the results obtained in the initial phase of the experimental work to measure the fracture energy of glass are described together with the few results for polymethylmethacrylate. As has been mentioned earlier (Chapter III) a complication appeared in these experiments in that within reasonable experimental time spans the cracks did not reach an equilibrium position. It is nevertheless possible to measure the crack length at a selected, if somewhat arbitrary, time after the increase in displacement. The very rapid transient growth following the change in displacement occurred within a few seconds. A standard time of two minutes was selected; in addition crack lengths at fifteen minutes were also recorded on occasion. The results presented here for the fracture energy of glass and p.m.m. are those calculated using simple theory and the crack lengths at selected times. As we have seen in Chapter II, this treatment involves a number of approximations and the magnitude of these are evaluated in the discussion. A comparison with previously published values of the fracture energy is included and the effects of environment, temperature and possible effects due to composition, on γ are discussed briefly. Some of the interesting features of crack propagation revealed in these experiments will be described and discussed briefly although a comprehensive interpretation of cleavage fracture

energies and detailed discussion cannot be made until the full significance of the prolonged crack growth is known.

4.2 Analysis of the Results

The basic experimental data collected during a cleavage experiment consisted of a series of values of crack separation (2δ) or cleavage force (F) and the corresponding values of the crack length L. Values of the crack width (w_1) and the beam dimensions, w_2 and b, were taken after cleavage.

As we have seen in Chapter II, application of the Irwin-Orowan criterion for mechanical instability with the assumption that simple beam theory can be applied to calculate the strain energy of the cleavage specimen leads to expressions relating the specific fracture energy γ to the beam dimensions

$$\gamma_\delta = \frac{3Ew_2b^3\delta^2}{8w_1L^4} \qquad 2.7.8$$

$$\gamma_F = \frac{6F^2L^2}{Ew_1w_2b^3} \qquad 2.7.9$$

where the symbols are as described above and the effects due to shear have been neglected. The results of cleavage tests are generally shown graphically in the form of a plot of $\delta(w_2b^3/w_1)^{\frac{1}{2}}$ versus L^2 or as a plot of $L/(w_2b^3w_1)^{\frac{1}{2}}$ versus F^{-1}. These forms can be directly related to equations 2.7.8 and 2.7.9. above.

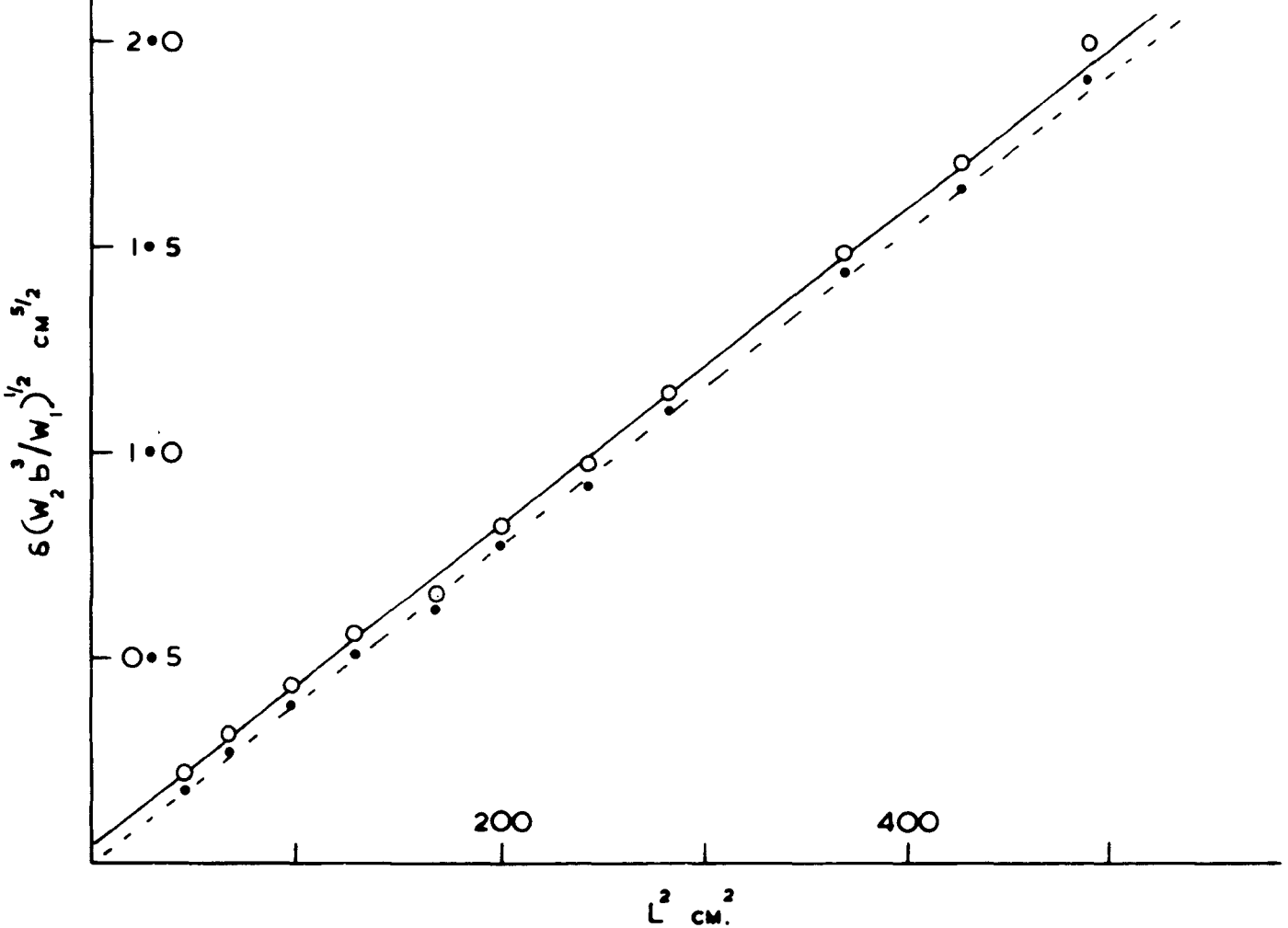

Fig. 22A

Typical reduced plot for p.m.m. cleaved in air

O - original data; ● - data corrected for end rotation

4.3 Cleavage of polymethylmethacrylate

The results of cleavage experiments carried out on p.m.m. in air are shown in Table 3 together with some previously published values. Figs. 22 A and B show the results of the cleavage of a typical specimen in the reduced graphical forms. From these graphs γ_δ was 2.20×10^5 and γ_F was 3.0×10^5 using the value of E as 3.1×10^{10} dynes cm^{-2} measured in a separate three point bend apparatus. Following Gillis and Gilman's analysis (Chapter II) we may write:

$$\gamma_{true} = (\gamma_\delta . \gamma_f)^{\frac{1}{2}} = 2.6 \times 10^5 \text{ ergs cm}^{-2}$$

The initial experiments on p.m.m. were carried out on the prototype machine and instead of using a value of Young's modulus determined separately, a three point bend experiment was carried out on each half of the cleaved specimen to determine directly the effective stiffness of the beam. Values of the specific fracture energy were calculated from the slope of a plot of δ versus L^2 using the experimentally determined constant. A mean value of 2.75×10^5 ergs cm^{-2} with a standard deviation over the group (15 specimens) of 0.18×10^5 ergs cm^{-2} was obtained.

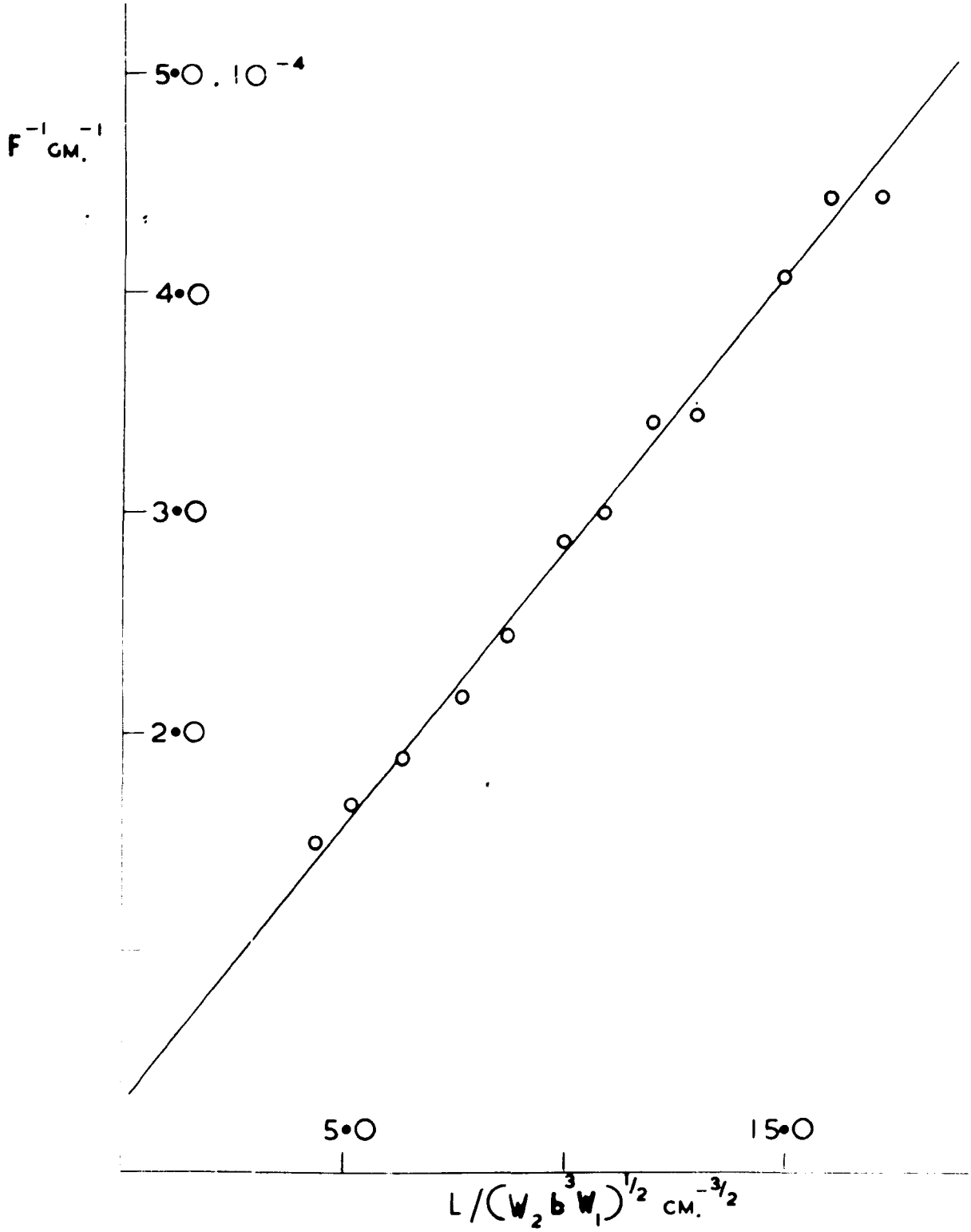

Fig. 22B

Typical reduced plot for p.m.m. cleaved in air

TABLE 3

Published values of the specific fracture energy of p.m.m. tested in air at R.T.

Author	Technique	γ ergs cm^{-2}
Benbow & Roesler (1956)	Wedge cleavage	$4.9 \pm 0.5 \times 10^5$
Svennsson (1960)	" "	4.4 "
Benbow (1961)	" "	4.2 "
Irwin & Kies (1958)	Central notch	4.4 "
Van den Boogart (1966)	" "	1.65 "
Berry (1961)	Tensile	2.1 "
Berry (1963)	Cleavage	1.4 "
Broutman & McGarry (1965)	"	1.25 "
This work (1966)	"	2.7 ± 0.2 "

4.4 Comparison of previously published results for polymethylmethacrylate

Although the experimental work with p.m.m. formed only a very small section of the results to be described it will be useful to discuss them and the previously published figures in some detail, for as we shall see, several points of principle emerge directly. The values of the fracture energy of p.m.m. shown in Table 3 above have been obtained by a variety of techniques and yet differ only by a factor of four. It is significant that all these values are well above the calculated surface

energy for this material (Kambour 1965). Some of the variation between the values in Table 3 may be attributed to changes in composition but it is suggested that generally the main differences are due either to the method of testing or to the subsequent analysis of the data.

In the experiments of Benbow and Roesler (1956) which were described briefly in Chapter II, the cleavage crack was stabilized by axial compression. It has subsequently been suggested by Svennsson (1960) and Gillis and Gilman (1964) that this method of stabilization can produce large positive errors in the calculated value of the fracture energy. The strain energy of the system is underestimated if contribution of the compressive stresses is ignored, and Svennsson's analysis indicates that this may amount to a factor of two in $\frac{\partial U}{\partial L}$, the strain energy gradient. A correction of this order would reduce the value of γ obtained by Benbow and Roesler to the value obtained by the author.

Svennsson, who modified Benbow and Roesler's technique, took into account the effect of the compressive forces. In view of this it may seem somewhat surprising that Svennsson quotes a value of 4.4×10^5 ergs cm^{-2} for the specific fracture energy of p.m.m. which compares with 4.9×10^5 ergs cm^{-2} obtained by Benbow and Roesler. Svennsson in fact makes a rather elementary error in writing his energy balance equations in terms of the differential coefficients, and thereby overestimates the strain energy in his analysis by approximately a factor of two. (A critique of Svennsson's analysis is given in Appendix 1).

The method used by Irwin and Kies (1958) and Van den Boogart (1966) is based on the fact that for linear elastic materials stable crack growth in a centrally notched specimen occurs when a tensile load is applied close to the notch (Barenblatt 1962). In their experiments, specimens of p.m.m. sheet containing a central saw cut were loaded until crack extension occurred. After a certain crack extension, the specimen was unloaded, then reloaded to perform the next measurement and so on. The fracture energy was calculated from a knowledge of the load and extension values at the start of the crack growth. It is interesting to note that a large discrepancy exists between the two published values of the fracture energy obtained by this technique, and that the value of 2.7×10^5 ergs cm^{-2}, obtained in the present work, falls between the two. In this respect it is noted that the figures published by Berry for the cleavage fracture energy of p.m.m. and the value he obtained from tensile tests on precracked specimens differ by a factor of two. This difference may be a fundamental one in that it could be revealing that the work of fracture and not the fracture energy has been measured in these experiments. As discussed in Chapter II, although the work of fracture, as defined there, is a constant for a given mode of fracture and a given stress distribution, it is not a material constant.

The differences which exist between the author's value and those obtained by Berry and Broutman and McGarry cannot be attributed to the method of measurement, but may be associated with the subsequent analysis of the experimental cleavage data as we shall see. In Chapter II

two methods of analysis were described, the theoretical analysis of Gillis and Gilman, and the more empirical analysis due to Berry. Using the former method, the basic experimental data recorded for cleavage experiments with p.m.m. was plotted in the forms shown in Fig. 22, and the values of γ_δ and γ_F calculated from the slopes. It has previously been shown that provided L > 3b shear effects can be neglected and the effects of end rotation eliminated by the calculation of

$$\gamma_{true} = (\gamma_\delta \cdot \gamma_F)^{\frac{1}{2}}$$

Writing the equations for γ_δ and γ_F more fully:-

$$\gamma_F = \frac{F^2L^2}{2EIw_1}(1 + 3CL^{n-2}) \qquad 2.8.43$$

$$\gamma_\delta = \frac{9}{2}\frac{EI\delta^2}{L^4w_1}(1 + 3CL^{n-2})^{-1} \qquad 2.8.44$$

we can see that the calculation of γ_t eliminates the term due to end rotation ($3CL^{n-2}$). However, this is an approximation which is only applicable if n ≈ 2, as we have shown in Chapter II. The expression for the deflection δ corrected for end-rotation is:-

$$\delta = \frac{FL}{3EI}(1 + 3CL^{n-2}) \qquad 2.8.40$$

By rearranging and taking logarithms we may write

$$\log\left(\frac{3EI\delta}{FL^3} - 1\right) = \log 3C + (n-2)\log L$$

and by plotting $\log\left(\frac{3EI\delta}{FL^3} - 1\right)$ as the ordinate and log L as the abscissa it is possible to evaluate n from the slopewhile the constant C can

be obtained from the intercept on the ordinate axis. This procedure was carried out for the data obtained from the specimen represented in Fig. 22 above. The value of n was approximately 0 and of C - 8. The corrected values of δ were then used in a second reduced plot which is shown as the dotted line in Fig. 22A. We may surmise that as expected the correction has little effect on the value of γ which is calculated from the slope, but it is satisfying to note that it explains the small positive intercept obtained in the previous plot.

A completely different value for the specific fracture energy can be obtained from the same experimental data if the analysis due to Berry is used. As described in Chapter II, Berry assumes that the non-ideality of the crack walls as cantilever beams can be represented by a general beam equation

$$F = \frac{a\delta}{L^n} \qquad 2.8.47$$

and by applying an energy balance criterion for fracture the expression becomes:-

$$\frac{F\delta}{W_1} = \frac{2\gamma L}{n} \qquad 2.8.50$$

The value of n may be determined experimentally from the slope of a plot of Log F/δ versus Log L which follows equation 2.8.47 above. For the experimental data used previously in Fig. 22, the value of n obtained was 2.6 giving a value for γ of 1.91×10^5 ergs cm^{-2}. If the arms of the crack had acted as true cantilevers then a = 3EI and n would have had a value of 3. The difference between the experimental value of

2.6 and the ideal of 3 is directly reflected in the value of γ . Clearly because of the small ranges involved in both Log L and Log F/δ , the value of n must be subject to large probable errors, and unlike the similar log plot used to calculate the end-rotation effects these errors will appear in the calculated value of the specific fracture energy, The similarity of the values obtained by Broutman and McGarry and Berry is not surprising as the same technique and method of analysis was used in both cases.

Apart from the major differences due to technique or analysis the fracture energies listed in this chapter differ slightly in terms of definition. Benbow and Roesler, Svennsson, and Berry all report that an equilibrium crack position was never observed: slow continuous crack growth occurred in all cases. Each author adopted a different definition of a stationary crack. Benbow and Roesler took the crack length when the velocity had fallen below 10^{-2}cm sec^{-1} while Svennsson recorded and used the length of the crack after five minutes of growth. Berry opted for a velocity less than 10^{-4}cm sec^{-1} and Broutman and McGarry adopted a completely different procedure - propagating the crack continuously and recording the force, deflection and crack length at intervals down the specimen. For all these cases a true energy balance cannot be defined as equilibrium does not exist, and convenience appears to be the only justification for the particular definition adopted. Slow crack growth was observed in the cleavage experiments described in the previous chapter. For the specific fracture energies calculated from deflection

measurements (γ_δ) the crack length was measured two minutes after each loading increment when the crack velocity was approximately 10^{-3}cm sec^{-1}. Calculations of γ_p were carried out using the peak force (Fig. 16A) and the crack length previous to the load increment.

In seeking a value for the specific fracture energy of p.m.m., it would appear that the cleavage value obtained by the present author might be free from serious errors. Svennsson's analysis has indicated that the previous value of Benbow and Roesler could be subject to errors arising from the compressional forces; his own published figure may have confirmed this indication had his analysis not been subject to a different, rather trivial, error. From the tensile-type measurements of Kies and others it is only possible to suggest that γ lies between 2 and 3 x 10^5 ergs cm^{-2}. We conclude that the assumptions of Berry have not been justified and that by taking a preferred value of ~ 2.5 x 10^5 ergs cm^{-2} for the fracture energy of p.m.m. it is possible to correlate the cleavage and tensile tests.

4.5 The value of the fracture energy of polymethylmethacrylate

Not withstanding the small discrepancy in the published figures, it is quite clear that the observed value of fracture energy is roughly three orders of magnitude larger than the calculated surface energy of p.m.m. (Kambour 1965). This discrepancy was first explained by Berry (1960) as being due to the irreversible work involved in aligning the polymer chains ahead of the crack tip. This hypothesis is supported by the interference colours exhibited by p.m.m. fracture surfaces. It has also

been established that they are thermolabile. Kambour (1965) has shown that these interference colours arise from a layer of craze material. The phenomenon of crazing in a material may be defined as the occurrence of localized zones which develop with time in a direction normal to the principle tension when some polymeric materials are stressed. These zones have every appearance of cracks. Spurr and Heigisch (1962) first showed that these apparent cracks are thin abruptly bounded regions with different optical properties from the bulk material but that in contrast to a true crack a craze is still load bearing. Kambour (1964) has examined crazes in glassy polymers and identified them as regions containing orientated polymer interconnecting the craze walls. Refractive indices determined from the measurements of the critical angle for total internal reflection showed crazes in polycarbonates to be approximately 50% void. Electron micrograph studies suggested that the void content appeared to be distributed in the form of holes, most of which had the dimensions 20 - 200Å. Kambour (1965) demonstrated that fracture surface layers of p.m.m. were craze-like in nature. From determinations of the refractive indices and the surface colours it was possible to calculate the thickness of the craze layer. It was established that the thickness of this layer varied with the fracture velocity. Van den Boogart (1966) studied crack propagation in p.m.m. and also concluded that the crack progresses through crazed material.

The high fracture energy of p.m.m. is thought to be due to the result of the craze process which involves the dissipation of strain

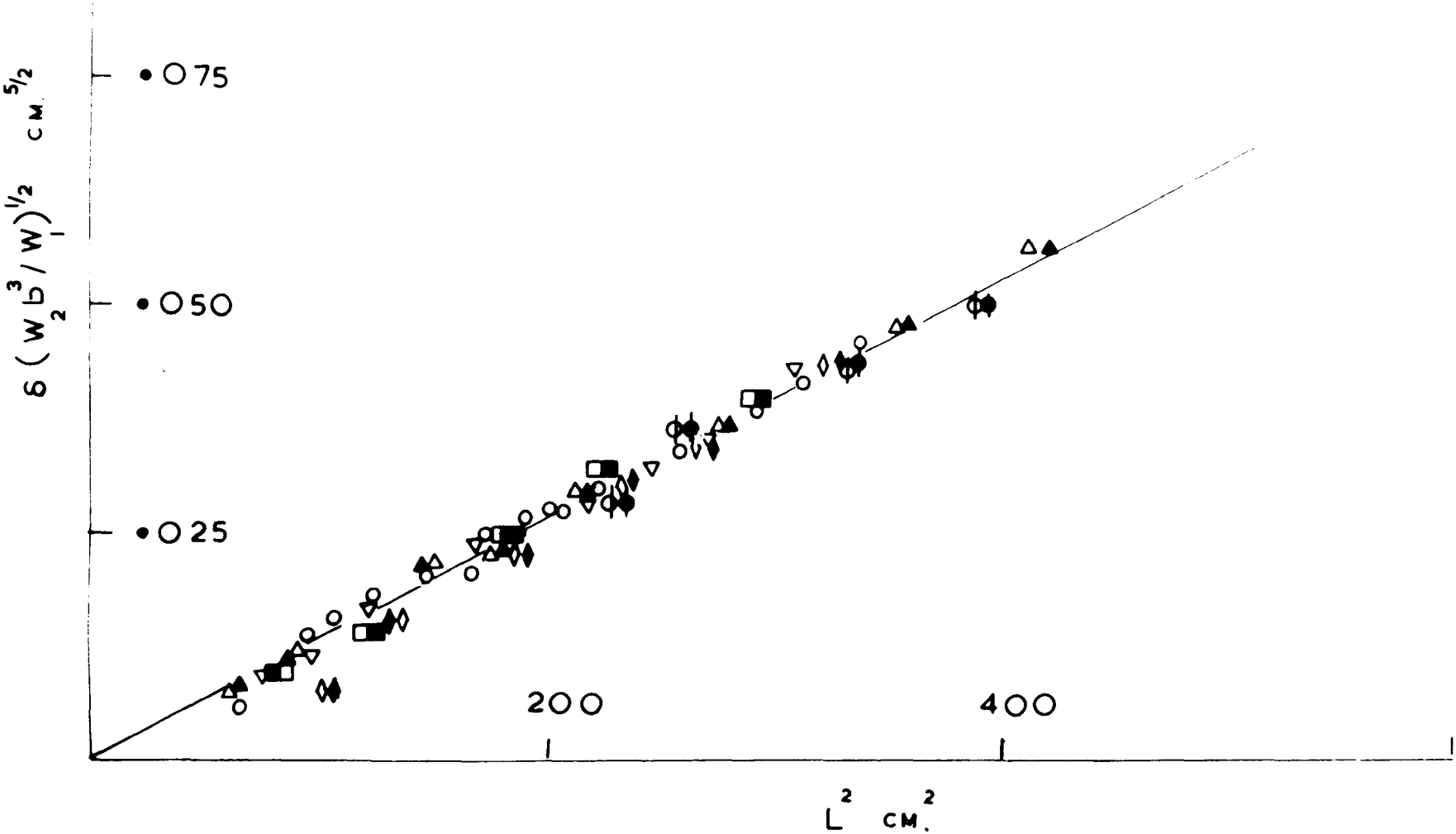

Fig. 23

A typical reduced plot for "Float" glass cleaved in liquid nitrogen.

Each symbol represents a different specimen; open symbols correspond to data collected at 2 mins. and closed symbols to 15 mins.

energy by plastic work as well as the production of extra surface free energy through hole formation. The formation of voids was calculated by Kambour (1965) to account for only 3% of the observed γ while the plastic work calculated from the craze thickness and an assumed yield stress amounted to ~20%. It is evident that the plastic flow hypothesis explains to a large extent the phenomena observed in fracture of p.m.m. Any small differences observed between fracture energies obtained by cleavage or tensile tests might be explicable in terms of different craze thickness. Kambour has observed that different crack velocities can produce thicknesses varying by as much as 20%, which might produce changes in the fracture energy of the same order. Although it seems likely that crack propagation involves plastic work it must be emphasized that nothing is known of the mechanism of the process. In this respect it is interesting to note that interference colours have been observed on fracture surfaces of p.m.m. at liquid nitrogen temperatures (Berry 1961, Broutman and McGarry 1965), an observation which must surely restrict the number of possible flow mechanisms.

The cleavage experiments on p.m.m. served two useful purposes. Apart from familiarizing the author with the intricacies of the cleavage technique they also allowed a comparison of the applicability of the analyses and interpretations to be made to two different materials - glass and p.m.m.

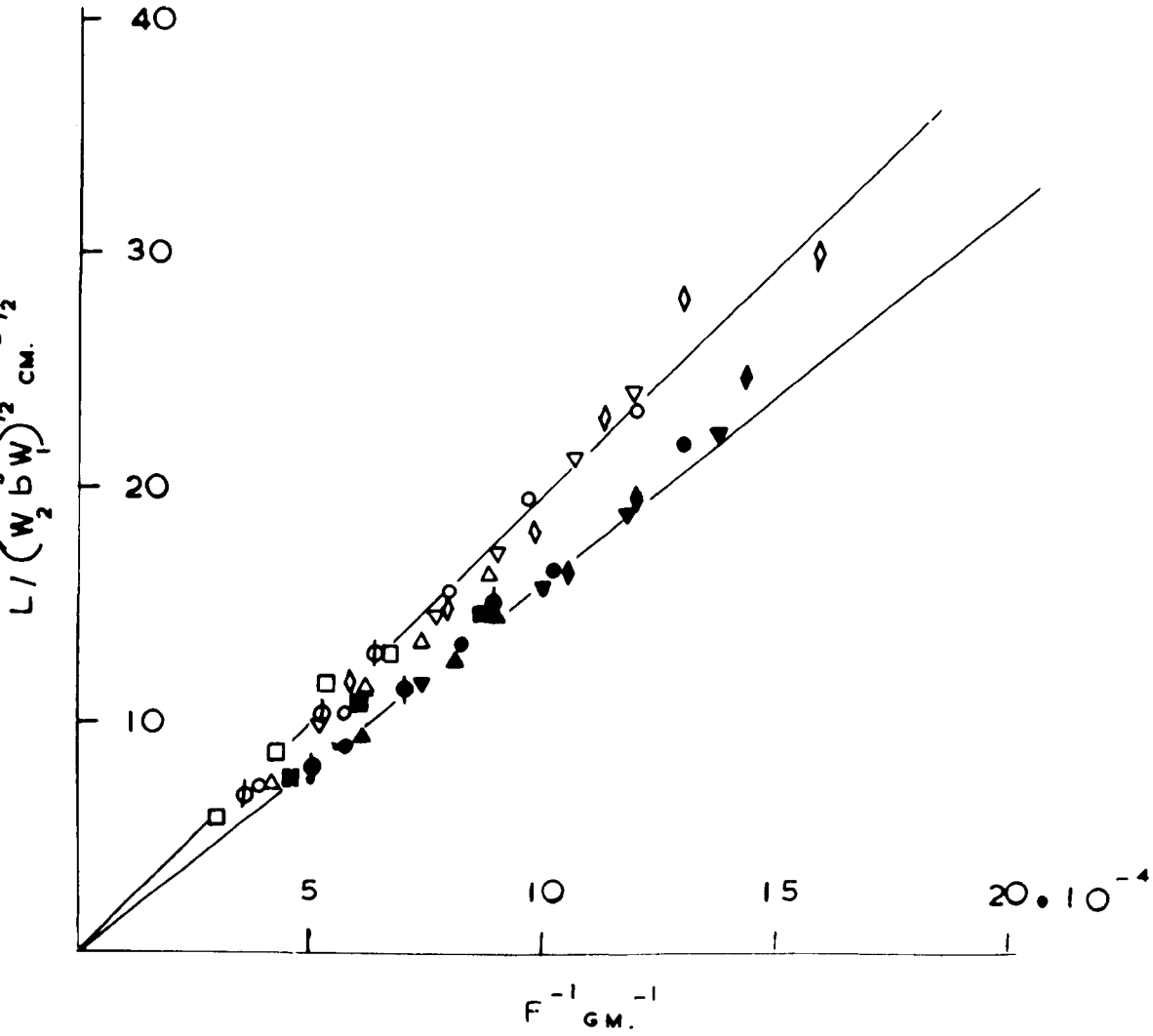

Fig. 24

Reduced plots for "Float" glass cleaved in air using crack lengths and forces at 2 and 15 minutes

4.6 Cleavage of Soda-lime-silica and Boro-silicate glasses

An extensive series of soda-lime-silica glass specimens with a range of widths was prepared and cleaved in various environments. A more limited series of borosilicate glass specimens was prepared and these cleaved in selected environments to serve as a comparison with soda-lime-silica glass.

In Chapter II, it was pointed out that the stress at the tip of a cleavage crack of the form used in these experiments is the same for all equilibrium positions of the crack on a given specimen. The linearity of a δ versus L^2 plot for a given specimen cannot then be used to distinguish between a critical stress criterion and an energy balance criterion for fracture. Since the stresses around the tip and the rate of release of strain energy will be different functions of the beam width b, coincidence of points from specimens of different widths would suggest an energy criterion might be appropriate. This is why the results from each series of tests were plotted in one of the reduced forms $\delta(w_2 b^3/w_1)^{\frac{1}{2}}$ versus L^2 or $L/(w_2 b^3 w_1)^{\frac{1}{2}}$ versus F^{-1} which can be derived from equations 2.7.8 and 2.7.9, as mentioned earlier in the chapter. Figs. 23 - 25 show typical examples of such plots. It is expected that in these reduced forms the experimental points from all specimens cleaved in the same environment should be on single straight lines, from which γ may be calculated directly. For all specimens tested in cleavage, shear effects were avoided by considering only crack lengths which were greater than three times the specimen half width, following the analysis of Gillis and Gilman (1964) described in Chapter II.

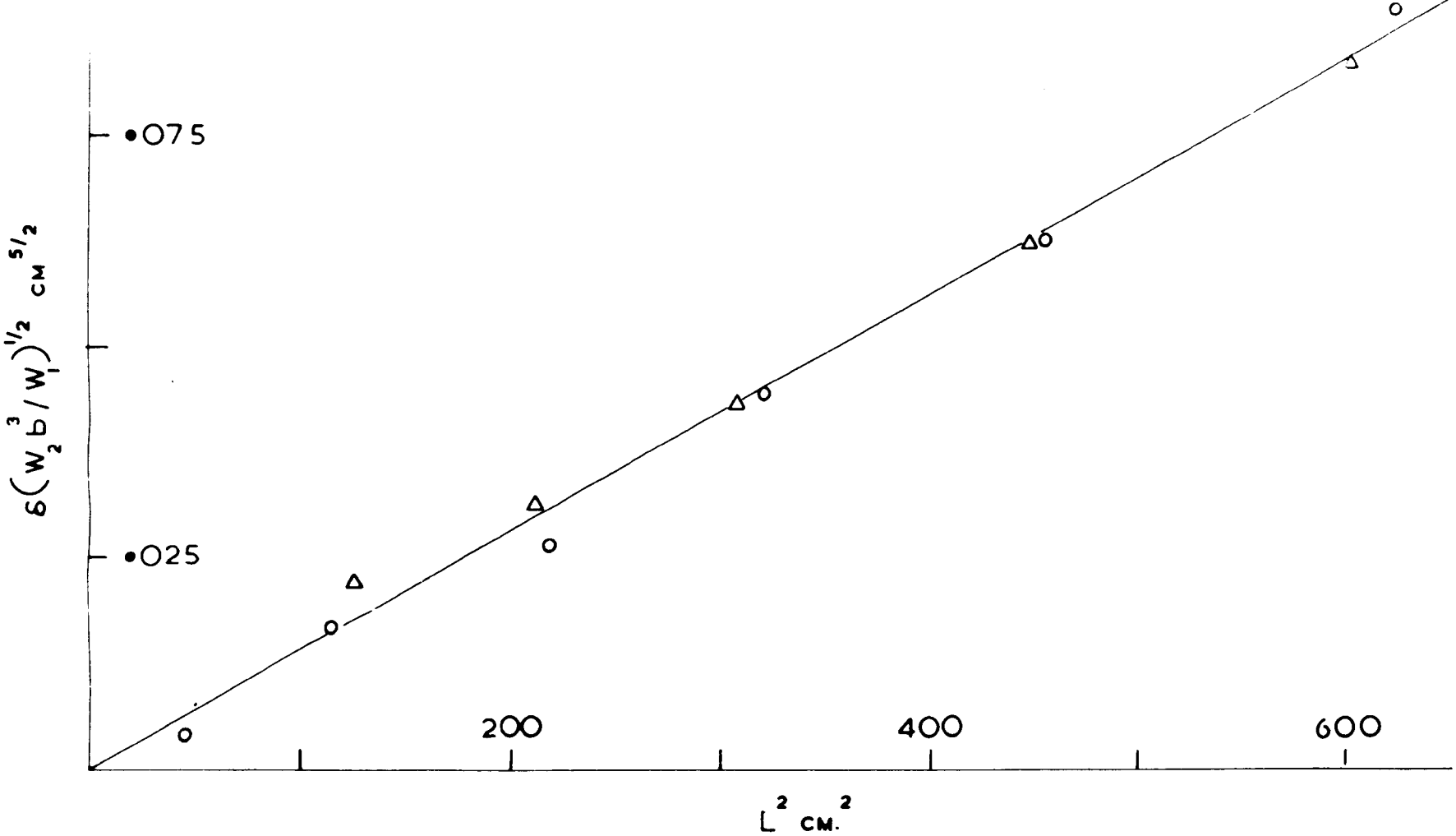

Fig. 25

Reduced plot for Pyrex glass cleaved in air

(Data collected at 2 mins.)

Throughout these experiments, it was observed that as with p.m.m., after each increment of strain the crack length increased continuously with time. It was established that provided the increments of deflection were sufficiently large the position of the crack was independent of any previous slow growth. An investigation of some characteristics of this prolonged growth is described in the second part of this thesis. The influence of the first part of the prolonged crack growth on the calculated value of the specific fracture energy of soda-lime-silica glass in various environments is illustrated in Table 4, which compares γ_δ values calculated from the crack displacement and length determined two and fifteen minutes after each incremental increase in strain.

TABLE 4

Values of γ_δ calculated from the displacement and crack length taken after 2 or 15 minutes

Environment	$\gamma_{2\ \text{mins}}$	$\gamma_{15\ \text{mins}}$
HF (4% soln.)	2.58×10^3	1.98×10^3
Water (R.T.)	2.52×10^3	1.99×10^3
Air (R.T.)	3.87×10^3	2.58×10^3
N_2 gas (dry)	3.72×10^3	3.72×10^3
CO_2 gas (dry)	3.78×10^3	
Ammonia (dry)	3.3×10^3	
Liquid paraffin (R.T.) (dry)	4.17×10^3	4.17×10^3
Glycerol (dry)	4.17×10^3	
Silicone oil (R.T.)	3.72×10^3	
Silicone oil (200°C)	4.04×10^3	4.04×10^3
Vac. ($<2.10^{-4}$cm)	5.0×10^3	5.0×10^3

The values of the fracture energy calculated from measurements of the cleavage force and the crack length at the instant of propagation, and from the force and crack length two minutes later are summarized in Table 5.

TABLE 5

Values of γ_F calculated from the cleavage force and crack length at 0, 2 and 15 minutes

Environment	γ_0	$\gamma_{2\ mins}$	$\gamma_{15\ mins}$
H.F. 4% Soln.	3.17×10^3	1.98×10^3	
Water R.T.	3.3×10^3	2.98×10^3	2.38×10^3
Air R.T.	3.82×10^3	3.23×10^3	2.11×10^3
H_2 gas (dry)	4.48×10^3		
CO_2 gas (dry)			
Ammonia (dry)	4.67×10^3		
Liquid Paraffin (dry)	4.90×10^3	4.90×10^3	4.90×10^3
Glycerol (dry)			
Silicone oil R.T.	4.67×10^3		
Silicone oil 200°C			
Liquid H_2	4.66×10^3	4.36×10^3	4.36×10^3
Vac < 2.10^{-4} cm Hg	4.75×10^3		

A comparison is made with previously published values for the fracture energy in Table 6. In this table, values of γ_F (instantaneous) are used whereas strictly γ_t calculated from $(\gamma_\delta . \gamma_F)^{\frac{1}{2}}$ is expected to be rather a better estimate of the fracture energy (see Chapter II), but as we shall see later there is little difference in practice between these two values for glass.

TABLE 6

A comparison of fracture energy values for glass

Environment	This work γ_F Cleavage	Culf (1959) Cone crack	Wiederhorn Cleavage (const.load)	Shand Bending	Griffith (1920) Tensile
HF 4% soln.	3.17×10^3				
Water R.T.	3.30×10^3	2.9×10^3	0.96×10^3		
Air R.T.	3.82×10^3	$3.7 \rightarrow 4.3 \times 10^3$	2.58×10^3	1.7×10^3	0.58×10^3
N_2 gas (dry)	4.48×10^3	7.6×10^3	2.85×10^3		
CO_2 (dry)		7.8×10^3			
Ammonia (dry)	4.67×10^3	4.2×10^3			
Liquid Paraffin	4.88×10^3	6.9×10^3			
Glycerol (dry)		6.6×10^3			
Silicone oil R.T.	4.67×10^3	7.1×10^3			
Silicone oil 200°C					
Liquid N_2	4.66×10^3		3.20×10^3		
Vac $<2 \times 10^{-4}$ cm Hg	4.75×10^3		4.06×10^3		

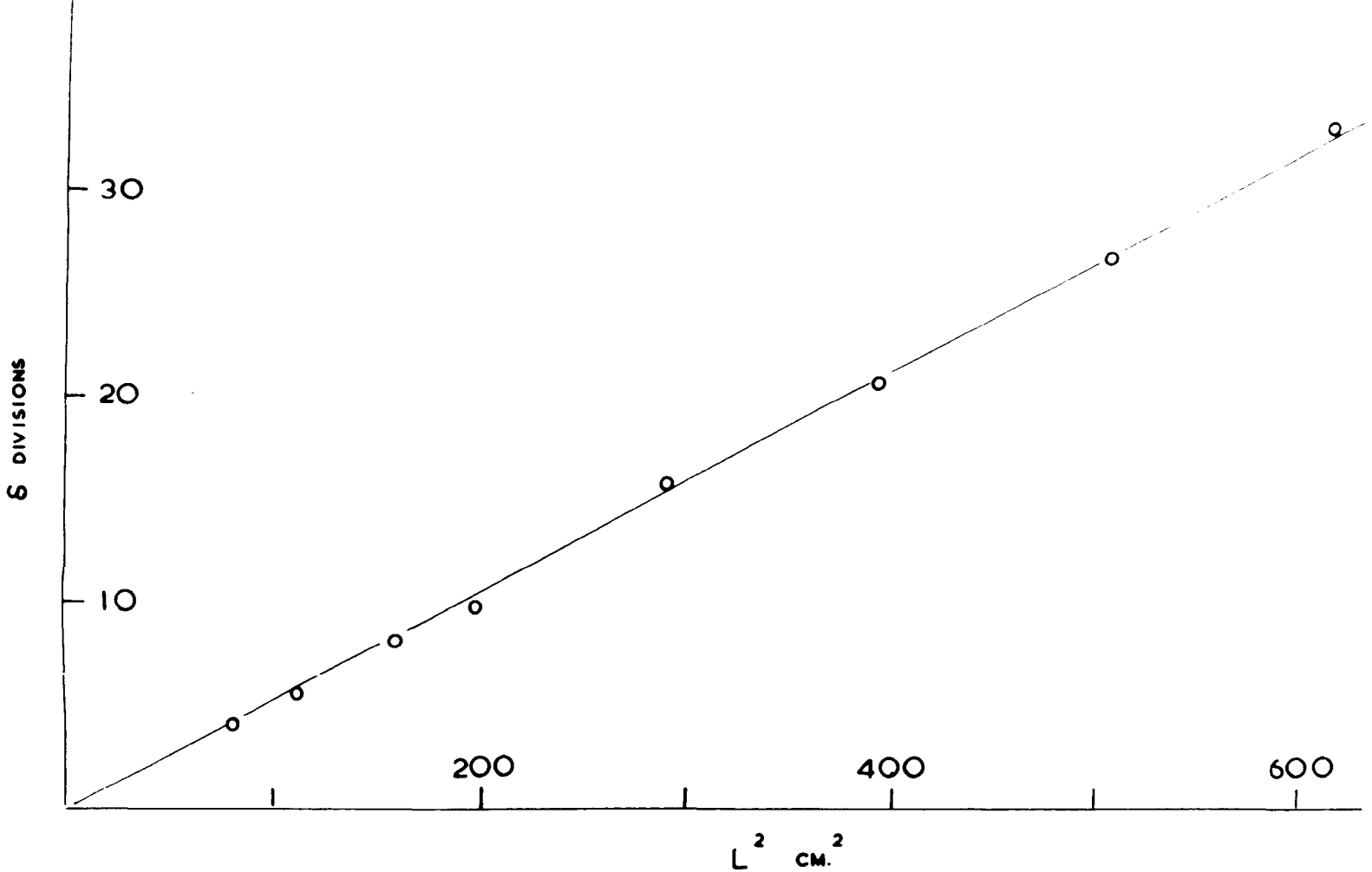

Fig. 26

Single "Float" glass specimen cleaved in air

4.7 Analysis of errors

The scatter in the individual points taken from a typical series of different specimens tested in the same environment was calculated, using the Gaussian method of least squares, to lead to an uncertainty in the slope of the order of 5%. The overall precision of the value of the fracture energy in any given environment was therefore about ±10%. Examination of a plot of δ versus L^2 for a single specimen (Fig. 26) suggests that the between sample variance is significantly greater than the within sample variance.

In order to calculate values of γ_t and so eliminate the effects of end-rotation it is necessary to use the appropriate values of both γ_δ and γ_F. To estimate values of the fracture energy free from both end-rotation and extended growth effects, two specific tests were carried out. Two specimens, 45 cm long, were prepared from the soda-lime-silica glass, one of width 1.25 cm and the other the largest beam width tested (4.0 cm). The length of the specimens was increased in order to increase the number of 'equilibrium' points obtainable; this number decreases as the beam width increases. These long specimens could be accommodated in the cleavage machine because a 15 cm slot had been cut in the base directly under the chucks which allowed the long specimens to hang freely; the slot was normally sealed with araldite for the experiments with normal length specimens in controlled environments. The long specimens were tested in air, in which a significant difference between the instantaneous and two minute values of γ_δ was expected. To estimate the

instantaneous value of γ_δ, the crack length was recorded immediately after each increment of strain had been applied. Values of γ_F corresponding to crack lengths taken instantaneously and after two minutes of growth were also obtained. The results of these tests are summarized in Table 7.

TABLE 7

Values of the fracture energy of "Float Plate" Glass

A. Theoretical Analysis

Time	Specimen A (b = 1.25cm)			Specimen B (b = 4.0cm)		
	γ_δ x10^3	γ_F x10^3	γ_t x10^3	γ_δ x10^3	γ_F x10^3	γ_t x10^3
t = 0	4.04	3.99	4.01	4.60	3.61	4.07
t = 2mins	3.48	3.05	3.26	3.91	3.10	3.48

B. Semi-empirical Analysis (determination of n for generalised beam)

Time	n	γ	n	γ
t = 0	2.76	3.66 x 10^3	2.60	3.51 x 10^3

From a comparison of the instantaneous and two minute values of either γ_δ or γ_F, it is possible to suggest that a 15% difference in the calculated values can arise out of two minutes of crack growth in air. It is important to note that although the differences in the individual γ_δ and γ_F values obtained for the different specimens is large (up to 15%)

the difference in the values of γ_t for the two specimens, both the instantaneous and the two minute values, is less than 5%. Following the analysis due to Gillis and Gilman, described in Chapter II, it was expected that the effect of end-rotation would be evident as a difference between γ_δ and γ_Γ. Further it was predicted that this difference would take the form such that $\gamma_\delta > \gamma_{true} > \gamma_\Gamma$, which is observed experimentally in Table 7. It is concluded that the effects of end-rotation account for a large portion of the difference observed between γ_δ and γ_F as was suggested in Chapter II. It is also noted that γ_F does not differ too greatly from the instantaneous value of γ_t and its inclusion in Table 6 which includes a comparison with previously published values should not involve any significant error.

The previous examination of the p.m.m. results using two methods of analysis produced two quite different values for the specific fracture energy. It was thought that a similar comparison for the cleavage experiments on glass might prove informative. Following the analysis due to Berry and described earlier, the value of n occurring in the generalized beam expression was extracted from the slope of a plot of $\log F/\delta$ versus Log L for the two long specimens. γ was then calculated as before from the plot of $F\delta/w_1$ versus L, whose slope was $2\gamma/n$, and the results included in Table 7. It is evident that the value of this constant n for glass is nearer to the ideal of n = 3 than was observed for p.m.m. ($n \simeq 2.6$) and seems likely that this can be correlated with the magnitude of end-rotation effects. As expected the

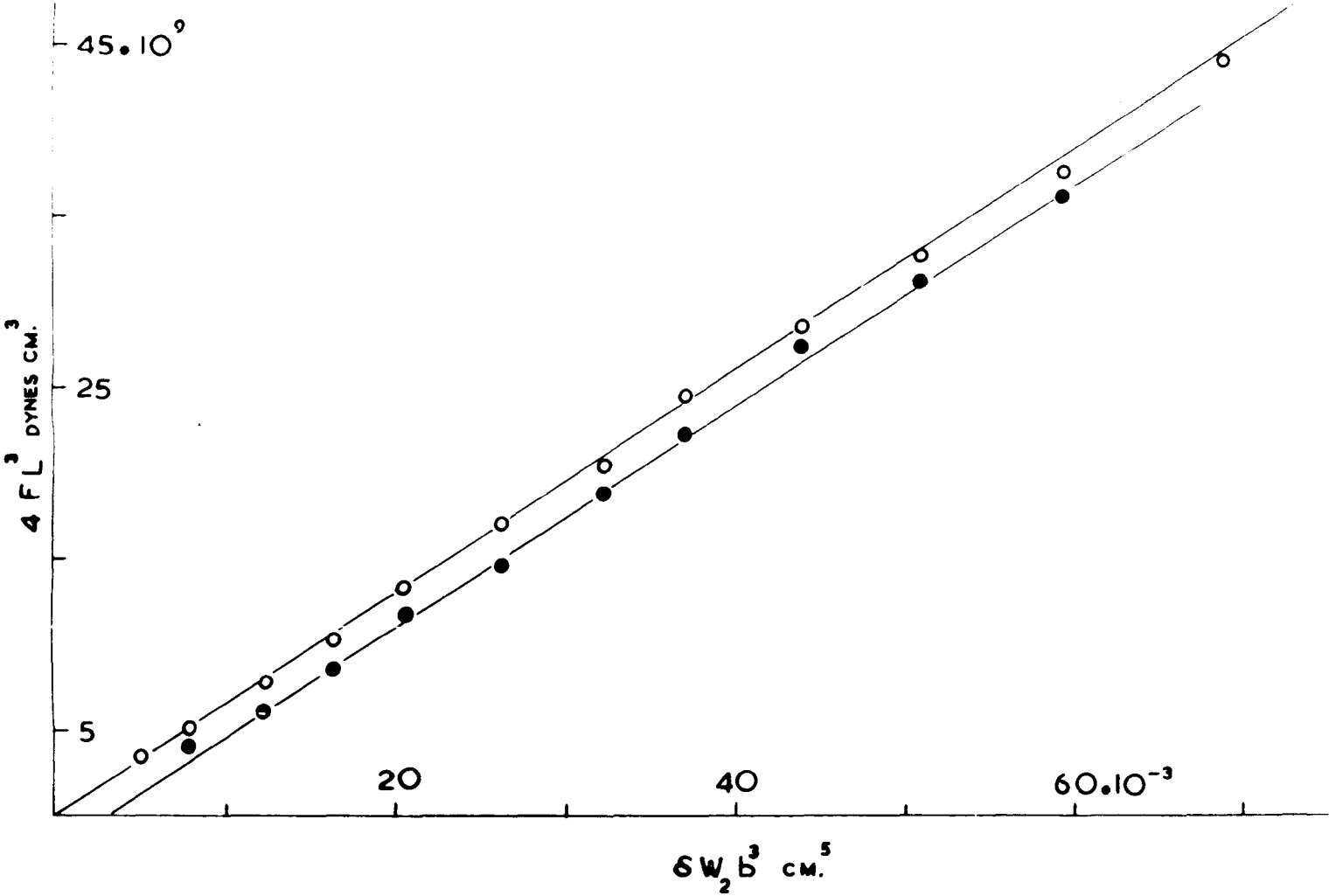

Fig. 27

"Young's modulus plot" from the experimental data recorded in a cleavage experiment at t = 0 and t = 2 mins.

narrow beam was a closer approximation to the simple cantilever than the broad beam. In general the usual cleavage tests were restricted to beams of less than 3cm width. As has been suggested, it is difficult to estimate the accuracy with which a value of n can be obtained from the log plot, but the 12% difference between γ and γ_t is perhaps not significant in view of the ±10% accuracy in the values of γ_δ and γ_F calculated from a reduced plot.

Another possible method of checking the extent of the simple beam approximations is by calculating Young's modulus from the experimental data recorded in a cleavage experiment. For a bending beam we may write:

$$\delta = \frac{FL^3}{3EI} \qquad \text{or} \qquad E = \frac{4FL^3}{\delta w_2 b^3} \qquad 4.7.1$$

when $I = \frac{w_2 b^3}{12}$

Fig. 27 illustrates the plot of $4FL^3$ versus $\delta w_2 b^3$ for experimental data taken at the instant of propagation and two minutes later. Two parallel lines resulted, both giving an effective E of 6.54×10^{11} dynes cm^{-2} which lies within 7% of the value determined in a separate bending experiment (Table 2). The evidence of Fig. 27 is accepted as showing that in cleavage experiments on glass the sides of the crack may be considered to act as simple cantilever beams without involving large errors in the calculated value of the specific fracture energy.

In summary then, unlike p.m.m. the cleavage fracture energy of glass does not seem subject to large deviations from the use of different analytical methods. The author's opinion is that this may be interpreted

as showing that the deviations from a simple cantilever system are small, an observation supported by the similarity of γ_o (semi-empirical analysis) and γ_t values. The values of γ_F (t = 0), which are chosen to eliminate effects due to prolonged crack growth, illustrate the variation of the fracture energy of soda-lime-silica glass with environment. A number of previously published values of γ exist, some of which are included in Table 6. The results of these experiments will be discussed and the values compared with the author's.

4.8 Fracture surface energy values

In 1920 Griffith published his theoretical criterion for fracture: in a brittle material the energy balance between the surface energy of the newly created surface and the elastic energy stored in the stress field around a crack was the controlling factor in the propagation of a crack. Using Inglis' solution for the local stresses around a slit crack in a flat isotropic plate of uniform thickness under a uniform applied tensile stress, Griffith derived two expressions for the critical stress for fracture.

$$\sigma = \sqrt{\frac{2ET}{\pi c(1-\nu)}} \qquad \text{for plain strain} \qquad 4.8.1$$

$$\sigma = \sqrt{\frac{2ET}{\pi c\nu}} \qquad \text{for plain stress} \qquad 4.8.2$$

where E is Young's modulus, ν is Poisson's ratio, T is the surface energy and 2c the length of the crack.

The experimental verification was carried out by measuring $\sigma\sqrt{c}$ for bulbs and tubes into which cracks of lengths ranging from 0.15" to 0.89" had been introduced. The specimens were subsequently annealed and the time of loading to fracture observed to vary from 30 seconds. to 5 minutes. According to Griffith's theory $\sigma\sqrt{c}$ should have a constant value $\sqrt{\frac{2ET}{\pi c\nu}}$, and the observed values had an average of 239 lbs.ins.$^{3/2}$. Griffith determined T, the surface energy, by the extrapolation to room temperature of measurements he carried out at high temperatures, using the angle of sag of a fibre of glass to calculate T. The extrapolated value of T was 0.0031 lbs per inch (543 ergs cm^{-2}), which yields a value of 266 lbs.ins$^{3/2}$ for the theoretical value of $\sigma c^{\frac{1}{2}}$. In a second paper (1924) Griffith corrected the original expression for the critical tensile stress to give

$$\sigma = \sqrt{\frac{2ET}{\pi c}} \quad \text{for plain stress} \qquad 4.8.3$$

The two expressions differ only in the presence of Poisson's ratio, but the comparison of the empirical and theoretical values of $\sigma\sqrt{c}$ was carried out using the original expression (Equation 4.8.2). Substitution of the experimental data obtained by Griffith, into the modified expression produces a theoretical value of $\sigma c^{\frac{1}{2}}$ of 133 lbs.ins$^{3/2}$ and shows a large discrepancy between the theoretical and experimental values. The value of $\sigma c^{\frac{1}{2}}$ predicted when the value of γ in air is used instead of the surface tension (i.e. ~4000 instead of 543 ergs cm^{-2}) is 358 lbs.ins$^{3/2}$. We may conclude that Griffith's experimental observation of $\sigma c^{\frac{1}{2}}$ can be explained as well by the use of a fracture energy of ~4000 ergs cm^{-2} as one of 543 ergs cm^{-2}.

A possible explanation of the low experimental value obtained by Griffith might be found in terms of the observation of the crack length. Observations of cracks in plates suggest that it is often extremely difficult to see the true extent of a crack in an unstressed state, a considerable portion of the crack length being less than a wavelength of visible light in width. In this respect it is interesting to note that when the strain is released on a partially cleaved specimen the crack length may appear to be reduced by several centimeters. It is improbable, however, that the discrepancy of a factor of 2 in $\sigma\sqrt{c}$ can be accounted for entirely in terms of an underestimation of the crack length since this would require c to have four times its apparent value. It is feasible that crack extension could occur to some extent in the long straining times before fracture (up to five minutes); indeed in view of the phenomenon of prolonged crack growth observed in the cleavage experiments on glass, it seems quite probable.

In 1958 Kies and Smith reported a measurement of the crack extension force (G_c) necessary for the onset of unstable fast fracture in glass. This followed directly the work of Irwin (1948) who suggested that the Griffith theory could be made generally applicable by substitution of 'the energy spent in a localized plastic strain' for 'surface energy' as a measure of resistance to crack extension. Orowan (1949) made a similar suggestion. The values of G_c were obtained from tensile tests on plates of glass which contained a central cut or slot as a starting crack.. The equation for G_c is given by

Irwin (1958) as

$$G_c = \frac{2A\sigma^2}{E} \tan \frac{\pi a}{2A} \qquad 4.8.4$$

where the width of the plate is 2A, the length of the crack 2a, and σ is the stress to fracture. The fracture energy as we have defined it is simply $G_c/2$ and the values obtained for "moist air" and air at 2% R.H. were 7×10^3 ergs cm^{-2} and 14×10^3 ergs cm^{-2} respectively. It is possible that the large differences between these values reflects not merely the effect of environment but also the difficulty of aligning the specimen to give the correct tensile stress free from bending.

Shand (1961) carried out a similar series of experiments, introducing small cracks into rods by means of a tungsten-carbide wedge and subsequently breaking them in four-point-bending. The mean value of the fracture energy in air was calculated to be 1.7×10^3 ergs cm^{-2}.

In view of the apparent discrepancy between the cleavage and tensile measurements it was decided to carry out the series of tensile tests on precracked specimens described in Chapter III. In these experiments the crack length was varied from 0.13 cm to 0.45 cm and values of the fracture energy were estimated from the Irwin-Orowan equation

$$\sigma = \sqrt{\frac{2E\gamma}{c}} \qquad 3.8.1$$

using the measured breaking stress and the corresponding initial crack depth. The rate of loading was such that fracture occurred after about five seconds. The mean value of the fracture energy was 2.5×10^3 ergs cm^{-2}; the standard deviation of the group of fifteen samples was 1.7×10^3 ergs cm^{-2}. The large scatter was mainly due to the difficulty involved

in aligning the araldite grips such that the specimen was uniformly stressed and not subjected to any bending. However γ obtained from these crude tests and the value obtained by cleavage are perhaps not significantly different. We may therefore tentatively suggest that the specific fracture energy of glass is a material constant which is independent of the particular stress distribution used in its measurement. It would also follow from this that an energy balance criterion for fracture is applicable to glass although the fracture energy of ~ 4000 ergs cm^{-2} is significantly higher than the surface energy.

An extensive study of the fracture energy of plate glass was carried out by Culf (1957) using a cone crack technique developed by Roesler (1956). Culf calculated the fracture energy from the depth of the cone crack produced on a block of glass under a loaded indenter. An expression relating the dimensions of the cone crack to the load on the indenter was derived:-

$$\gamma = \frac{wP^2 \sin a}{4\pi G R^3} \qquad 4.8.5$$

where P is the indenter force, G is the shear modulus and a is the angle of the cone of radius R.

The constant w was evaluated by a method of similarity; its value is determined by 'a' and Poisson's ratio ν, which are constant for a particular glass. During these experiments it was observed that the depth and radius of the crack increased with time. The values of the radius and depth after fifteen minutes of growth were selected arbitrarily

for the calculation of the fracture energies. The numerical values obtained by the cleavage technique reported in Chapter III are consistently lower than those reported by Culf, and show rather smaller changes with environment. Two important points will be discussed in connection with the cone crack technique. Auerbach (1902) observed that glass would withstand a much higher stress under a small ball than a large one. It was also noted that, once formed, the size of the crack relative to the diameter of the ball was much larger for the smaller ball. Preston (1926) verified this experimentally and further reported that using the same ball, different initial loads were required to produce the initial crack and different cone fracture sizes resulted. Culf reports that the term R^3/P^2 increases with increasing S/Δ, where S is the diameter of the crack and Δ the diameter of the indenter, eventually reaching a constant value. This is equivalent to saying that γ varies with Δ (the indenter size) since

$$\gamma = \frac{KP^2}{R^3}$$

where K is a constant. It is concluded in view of this variation with indenter size that the fracture energy values presented by Culf cannot be regarded as absolute. The relative values, in principle, may still illustrate the variation of fracture energy with environment. This brings us to the second feature of Culf's measurements which merits attention: the effect which prolonged crack growth has on the calculated values of fracture energy. Table 4 which illustrates the effect of crack growth

on cleavage fracture energies suggests that in environments where the initial growth rate is high, fifteen minutes can produce a considerable reduction in the calculated fracture energy. Culf uses crack lengths taken after fifteen minutes of growth which would tend to magnify the effect of some environments on γ. However, the ratios of the fracture energies taken after fifteen minutes of growth for the cleavage and cone crack experiments are to a first approximation the same (Table 8).

TABLE 8

Ratio of $\gamma_{15 \text{ minute}}$ values

Environments (compared)	Cleavage	Cone crack
Water : Liquid Paraffin	~0.49	0.45
Water : Air	~0.77	0.75

Weiderhorn (1966) used the double cantilever cleavage technique as modified by Westwood and Hitch (1963) to measure the fracture energy of a soda-lime-silica glass. This technique differs from that used here in that the load on the cantilever arms of the specimen (i.e. F) rather than the displacement, δ, was controlled. A crack was introduced into the soda-lime-silica microscope slide by cleavage "or otherwise" and the critical force necessary to move the crack measured. Using an Instron testing machine, two types of test were carried out: one method was to load the specimen rapidly enough so that the critical load was

reached before the crack could move very far; in the second method a constant load was applied to the specimen, and slow growth was observed at a load less than that required to cause rapid failure until the crack growth rate eventually increased catastrophically when a critical crack length was reached.

The slow growth observed by Wiederhorn is believed to correspond to the prolonged crack growth observed in this author's experiments under conditions of constant displacement, and the similarities and differences will be discussed in Chapter V.

Wiederhorn measured the fracture energy of a soda-lime-silica glass in five environments using a dozen specimens for each test. The fracture energy γ_o was calculated from the equation

$$\frac{1}{\gamma_A} = \frac{1}{\gamma_o} + (\alpha E/4\gamma_o G)(b/L_o)^2 \qquad 2.7.4$$

where the apparent fracture energy

$$\gamma_A = 6F^2_{crit} L_o^2/Ew^2b^3 \qquad 2.6.8$$

and a is an experimental constant.

A plot of $1/\gamma_A$ versus $(b/L_o)^2$ gave a straight line whose intercept with the ordinate was the reciprocal of the fracture energy, i.e. $1/\gamma_o$. Crack motion was observed under the microscope. The critical crack length L_o was taken to be the length at which the crack accelerated away and the critical load F_{crit} was the maximum before failure. Wiederhorn reports a standard error of the mean of 0.08×10^3 to 0.14×10^3 ergs cm^{-2} for the fracture energy values. This is rather

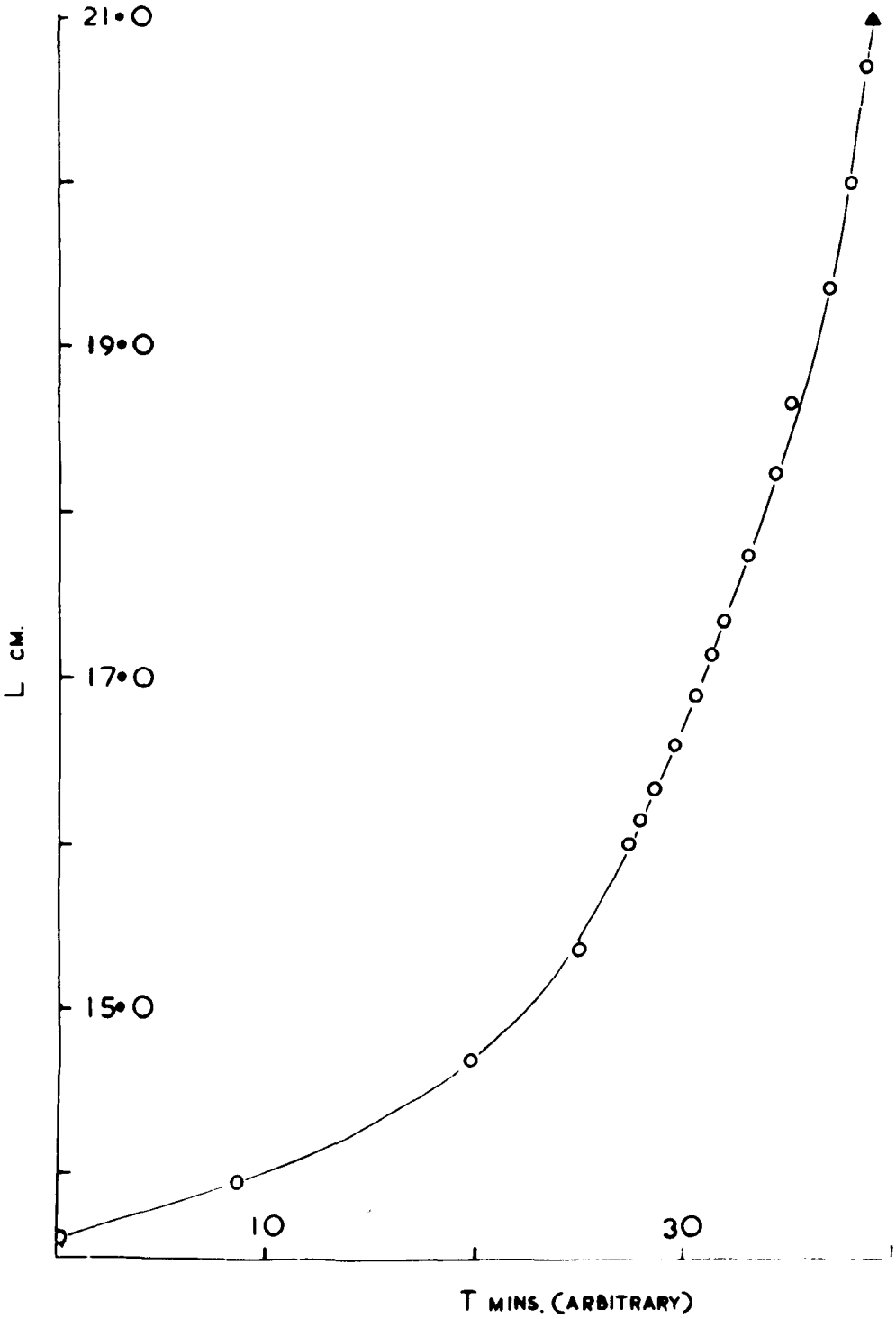

Fig. 28

Crack growth under constant load for "Float" glass cleaved in air

surprising in view of the difficulty of locating the critical length at which the crack accelerates away. This point might be illustrated by an examination of Fig. 28 which shows the crack length gradually accelerating to complete failure.

The equations derived by Westwood and Hitch and used by Wiederhorn are those which result from bending beam theory when account is taken of possible shear effects. Following the analysis of Gillis and Gilman we can calculate values of γ_t which correct the fracture energy values for effects associated with end rotation. From Table 7 we have seen that this correction is often sizeable. This correction is not attempted by Wiederhorn who measures only the cleavage force and not the deflection as well. We have examined the analyses possible for the cleavage system and considered that under the conditions described in Chapter III the particular analysis used does not make much difference. However, for the very short specimens used by Wiederhorn large end-rotation effects are likely since $L \simeq 2b$ only. No correction for, or even estimate of, the errors arising from end rotation is attempted and it is suggested that the results may be open to criticism on this score alone.

4.9 Summary and discussion

In the previous sections a number of experiments which have led to estimates of the fracture energy of glass have been discussed. It has been argued that Griffith's original experiments fail to support the notion that the fracture energy is simply the surface energy.

The variation in the published values of the fracture energy obtained from similar types of tensile tests makes it difficult to accept the technique as a satisfactory one. It is evident from the analyses of the cleavage technique which fit the observed data reasonably closely that this technique does not suffer from the ambiguities attributable to cone crack studies. However, the values of fracture energy published by Culf and Wiederhorn show similar environmental effects to those reported in Table 4 - namely, the drier the environment the higher the fracture energy. Two features which can be seen in Table 4 are perhaps surprising: HF solution which is known to be corrosive to glass has no greater effect on the fracture energy than water, and the second is that the fracture energy in a relatively poor vacuum is higher than that in liquid nitrogen which must surely be the drier of the two environments. The cleavage fracture energy values which do not include prolonged crack growth effects do not show the environmental effects to the extent reported by Culf. Although the few values obtained by Wiederhorn show a close correlation with those of the author it is interesting to note that the fracture energy of the three different glasses, soda-lime-silica, float glass and pyrex glass (Table 9) differ significantly, and this may represent to some extent the effect of composition. In view of the probable errors in Wiederhorn's values due to end-rotation effects, it is not possible to estimate the extent of the difference due to composition alone.

TABLE 9

Cleavage fracture energies of a borosilicate glass, soda-lime-silica and float plate

Environment	Borosilicate	Soda-lime-silica (Wiederhorn)	Float Plate
Air R.T.	4.7×10^3	2.58×10^3	4.0×10^3
Vacuum	6.0×10^3	4.06×10^3	4.75×10^3
Water	2.5×10^3	0.96×10^3	3.3×10^3

The high values of fracture energy are usually interpreted when they occur in plastics and crystals as being due to plastic deformation at the crack tip (Cottrell 1964, Clarke and Tattersall 1966).
In view of the brittleness usually attributed to glass, it would appear difficult to explain the high fracture energy in these terms.
Marsh (1964) however, has suggested that plastic flow has been observed in glass, for example in diamond pyramid hardness indentation.
He further suggested that crack propagation itself occurs by a process of flow rather than by a brittle process. It is important to note that the cleavage technique was used successfully by Westwood and Hitch (1963) to measure the surface energy of a number of crystals, illustrating that the technique itself is not responsible for the high γ values.

Strictly speaking, perhaps we should regard the cleavage technique for the measurement of fracture energies as inapplicable to those materials which exhibit prolonged crack growth. A prerequisite for the use of the energy balance criterion for fracture is the attainment of equilibrium. Until a study of the prolonged crack growth itself has been carried out no decision can be taken as to the conditions most appropriate to equilibrium. Preliminary tests have established that fracture energy values calculated from crack lengths after several months of growth approach the surface energy value. It is therefore important to determine the reasons and, if possible, the mechanism of this prolonged growth before interpretating or even accepting the values of the fracture energy calculated from data obtained in short time tests. The second part of this thesis comprises a detailed examination of the prolonged crack growth together with possible interpretations of the phenomenon.

Although a complete understanding of the fracture energy values is not possible at this stage, the agreement between the values obtained in the cleavage and tensile tests suggests that observed variations of fracture energy ought to be reflected in tensile strength tests under certain conditions: when the material is subject to a known flaw, or when no static fatigue is observed. The problem of finding strength results which correspond to these conditions is a major one. However, certain features of the variation of the tensile strengths are known. It has been established that the strength of all

glass is affected by water. Thomas (1960) demonstrated that his undamaged high strength fibres were weakened by wet storage in an unstressed state. From the fracture energy values we might surmise that this is due to a reduction in the strength of the glass itself, but from the tensile tests only the observation is ambiguous as it could equally well be associated with the formation of a flaw. Mechanically damaged rods when stored unstressed in liquid water become stronger (Mould 1960), and also exhibit delayed fracture when stressed in a moist atmosphere. It is the author's opinion that these phenomena can be directly related to the reduction of γ by water; the liquid water reducing the potency of unstressed flaws, but increasing that of the stressed ones by reducing γ. Static fatigue or delayed fracture, as it is sometimes described, has for many years complicated the measurement of the strength of glass. One generally accepted feature of the phenomenon is the factor of approximately four which is observed between the upper and lower fatigue limits. Reference to the Irwin-Orowan equation, viz

$$\sigma = \sqrt{\frac{2E\gamma}{\pi c}} \qquad 3.8.1$$

indicates that this could be explained in terms of a change by $\frac{1}{16}$ in γ. Calculations based on the preliminary experiments on prolonged crack growth indicated that the fall in γ covered almost exactly a range of sixteen times. It is evident that fracture energy observations may be used to a large extent to relate the previously inexplicable phenomenon observed in tensile tests by a single hypothesis.

Further correlations between the fracture energy values and the tensile strengths may be drawn with respect to temperature effects. Proctor et al. (1967) have established that direct thermal energy effects play little part in determining the strength of "flaw free" silica fibres. This is in accord with the results above which revealed that the fracture energy of float glass in silicone oil remained unchanged when the temperature was raised from 20°C to 200°C and that the fracture energy in liquid nitrogen was little different from any other dry environment. The effect of composition on the fracture energy has been observed and Table 10 illustrates a correlation between the fracture energies of pyrex and float plate and the tensile strengths of etched "flow free" X8 and pyrex glasses (Brearley et al. 1962).

TABLE 10

Correlation between cleavage fracture energies and tensile strengths

Environment	Soda-lime-silica glass		Borosilicate	
	Mean breaking stress kg mm^{-2}	γ ergs cm^{-2}	Mean breaking stress kg mm^{-2}	γ ergs cm^{-2}
Air	340	4.0	270	4.7
Liquid N_2	430	4.7	500	6.0

In conclusion, we may remark that a limited correlation of fracture energies and tensile strengths is possible, but that it seems likely that fracture energy measurements will prove far more instructive and less ambiguous than tensile strength measurements. In this chapter we have examined fracture in p.m.m. and suggested that the high values of fracture energy may be attributed to a fracture process which involves plastic work. Following the suggestion of Marsh (1964) the high fracture energies observed in soda-lime-silica and borosilicate glasses would lend support to the idea that in glass, plastic deformation at the crack tip gives rise to high fracture energies. As we shall see, this approach may be developed to explain a number of the features of cleavage fracture. Any evaluation of fracture energies or interpretation of the high observed values and their variation with environment can only be realistic if it includes the phenomenon of delayed fracture and its apparent equivalent in cleavage - prolonged crack growth.
The following chapters describe the series of experiments designed to examine this phenomenon of extended crack growth and include a discussion of possible interpretations.

CHAPTER V

THE PHENOMENON OF CLEAVAGE CRACK CREEP

5.1 Introduction

The fracture energy values obtained from the cleavage experiments described in Chapter III have been calculated under the assumption that a differential energy balance was satisfied. In fact this was observed not to be strictly true, and experimental data was collected at pseudoequilibrium positions which occurred between successive increments of the end deflection, when the crack had small but finite velocities. After each increment of strain the crack length increased continuously with time, the crack velocity falling as the crack grew. Also, as the crack length increased with time at constant deflection, the force on the loading pins decreased. These changes are illustrated in Chapter III (Figs. 16A,B). Slow crack growth before catastrophic failure was also observed when cleavage was carried out under a constant load, and it will be shown later that the two observations are manifestations of the same phenomenon.

In spite of some risk of confusion we shall for convenience use the word 'creep' throughout the remainder of this thesis to refer to this slow crack growth; this is not necessarily to imply that the processes involved either at the crack tip or in the cantilever arms are in any way similar to those responsible for the macroscopic delayed strains which are traditionally described as creep.

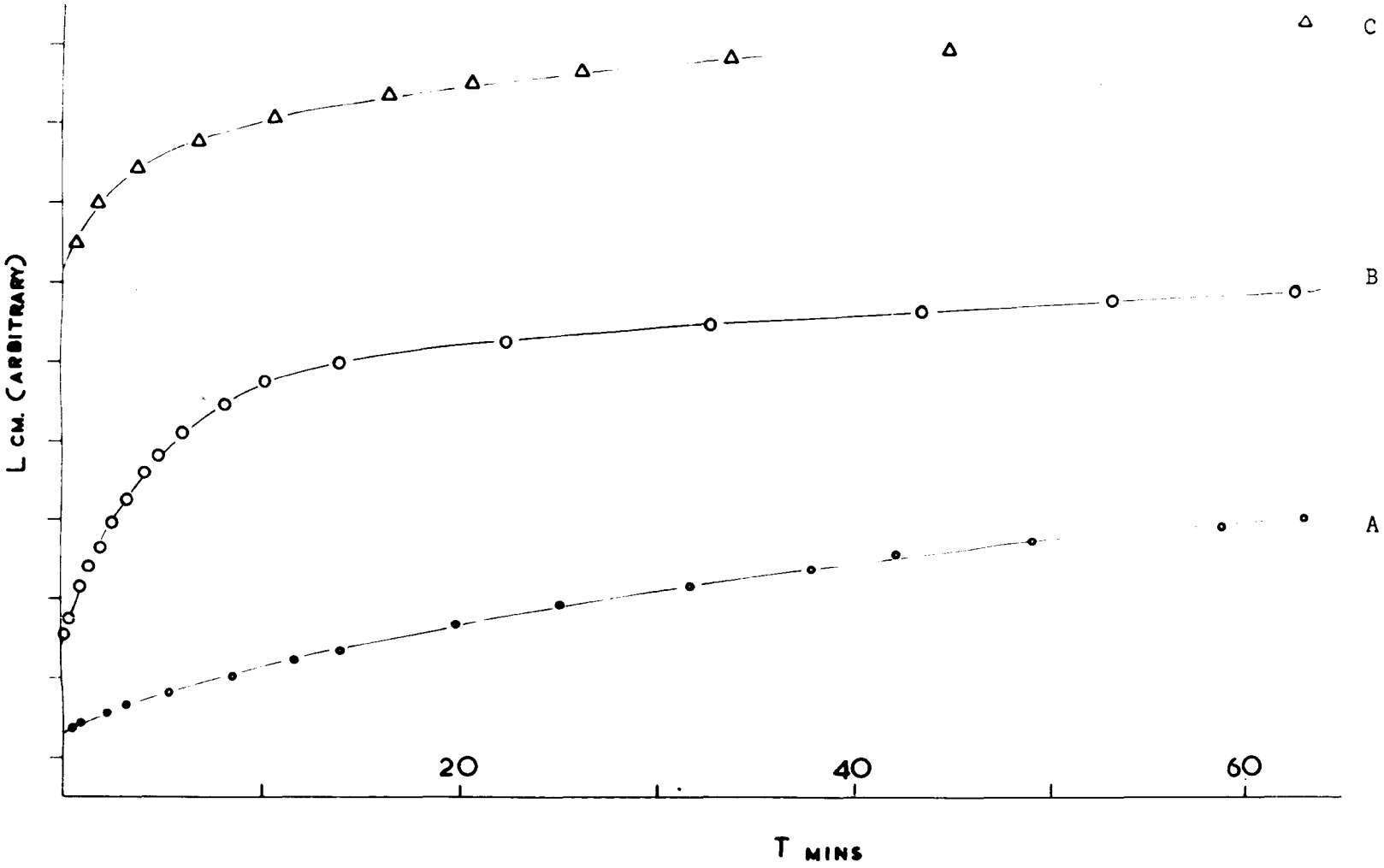

Fig. 29

Creep curves for similar specimens tested in: A - dry nitrogen
B - air
C - water

In this chapter it is intended to describe the first known attempt (apart from some limited experiments by Wiederhorn 1966) to study in detail the phenomenon of creep. Many of the experiments described were carried out to establish the general nature of the phenomenon rather than examining the quantitative details. In this respect the experiments and results should be regarded as preliminary and it is hoped that with the knowledge gained here it is now possible to design specific experiments which would perhaps produce more quantitative information. The results of specific experiments to determine particular characteristics of the phenomenon will be discussed. The possibility that the slow crack growth occurs through a slow rate-determining supply of energy from chemical reactions or other interactions at the tip will be examined, and we shall show that creep is most likely to be explicable in terms of a reduction of the fracture energy in time.

5.2 Experimental observations of the phenomenon of creep

The phenomenon of creep is clearly not restricted to glasses. Benbow and Roesler (1956) and Berry (1963) have observed slow growth of cleavage cracks in polystyrene and p.m.m. Benbow (1961) recorded creep (as defined) in polystyrene polymers of various molecular weights. Culf (1957) noted creep of cone cracks in blocks of glass and recorded a dependence on environment. Creep has also been observed in cleavage experiments on some epoxy resins, carried out in this laboratory (Griffith 1967); an interesting feature here was that this only

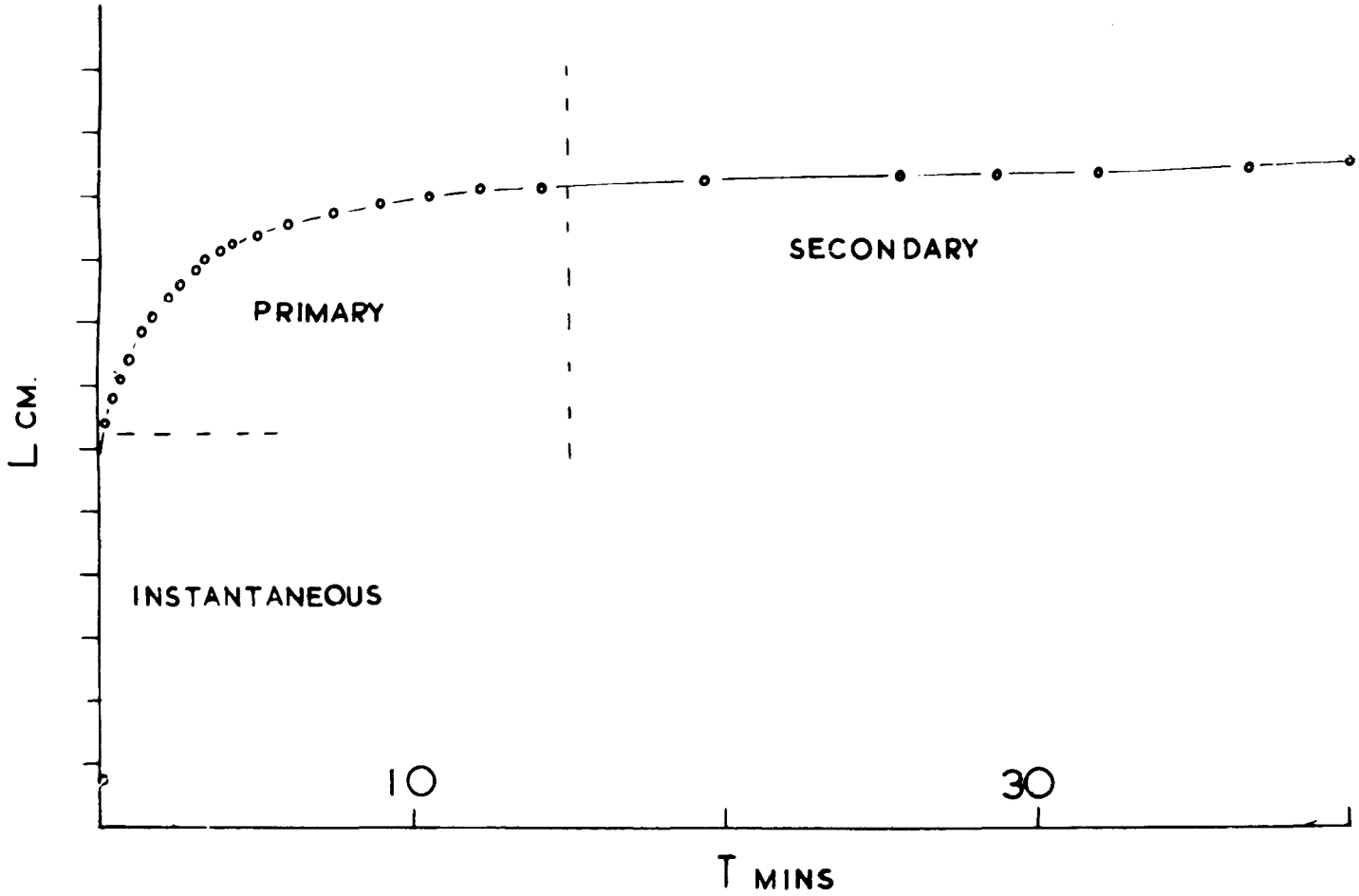

Fig. 30

Creep in air under constant deflection

occurred in the resins which had a small percentage of hardener (less than 10%) corresponding to fracture energies in the range $5 \times 10^2 \rightarrow 10^4$ ergs cm^{-2}. We might from these results correlate the appearance of this phenomenon with a particular range of fracture energies or hardness, and indeed we shall see later that a number of correlations between fracture energy and hardness are possible.

Originally creep was observed in glass and p.m.m. when cleavage was carried out in air. Under these conditions the rate of increase of the crack length seemed to decrease approximately exponentially with time. Preliminary experiments indicated that to a first approximation for a given specimen, the creep curve (L versus t) was independent of L_o and δ, but dependent on the beam dimensions and environment. The shape of the creep curve changed noticeably as the test environment was dried. This is illustrated in Fig. 29 which shows creep curves for similar specimens tested in water, air and dry nitrogen. Phenomenologically it seems possible to distinguish three stages of the crack growth in air (Fig. 30): the very rapid, almost "instantaneous", growth, a primary stage when the crack is moving relatively rapidly (~0.2 cm min^{-1}) and a secondary slow growth which corresponds to a rather slower (~0.02 cm min^{-1}) but very prolonged crack growth. Whether these stages involve fundamentally different processes cannot be concluded, but the division is very useful; we shall review the experimental evidence for such a division and then concentrate on the more prolonged stage of creep phenomenon.

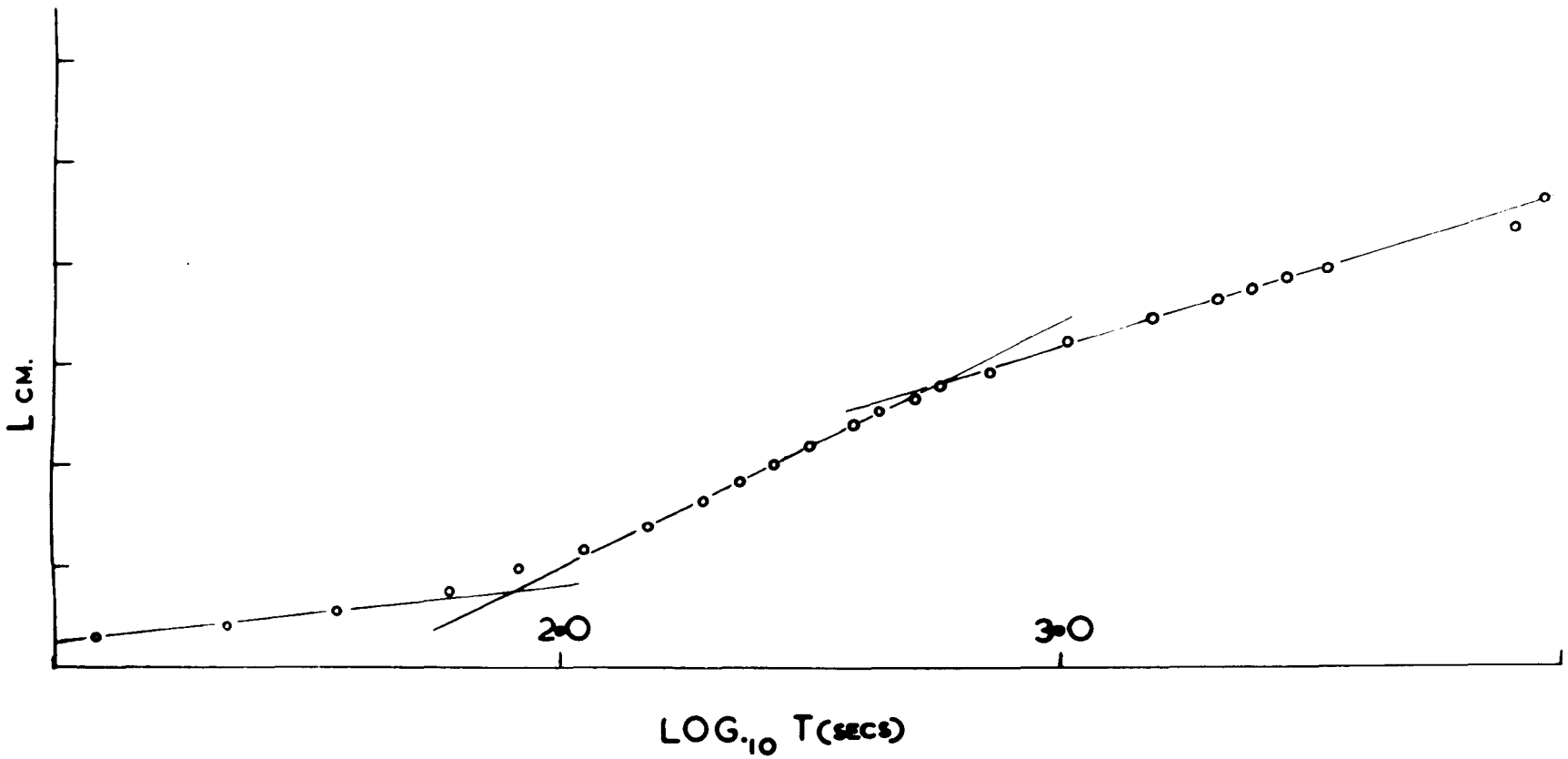

Fig. 31

Creep of a "Float" glass specimen cleaved in air

The creep curves in Fig. 29 indicate that in water the primary creep has almost disappeared and since we know that the fracture energy of glass is lower in water it appears that this portion of the creep has been condensed into the instantaneous stage almost entirely. In dry environments primary creep is not apparent and only the slower secondary process is observed ($v \simeq 0.05$ cm min^{-1}). The original subdivision of creep was carried out on the basis of rather tenuous evidence. The dependence of the primary creep on environment and in particular on water, together with the observation of creep in extreme environments, such as liquid nitrogen, suggested that more than one process was present. Two other pieces of evidence will be used to support this hypothesis, both involving the analysis of the basic crack length and time data. We have already implied that in appearance the creep curve (L versus t) is exponential, and to some extent this is confirmed by the L versus log t plots (Fig. 31). To a first approximation it would seem that three distinct regions are discernible which appear to correspond to the instantaneous, primary and secondary regions of the creep curve (Fig. 30). In view of the small crack lengths in each range, it was felt that this evidence could by no means be regarded as conclusive. However, when a series of tests was undertaken in which 'float' glass specimens were cleaved in various glycerol-water solutions and this data presented in the form of log t versus L plots (Fig. 32), it is observed that the second and third stages gradually merged to become a single straight line. The point of change over from the primary to the secondary creep occurred earlier as the water concentration

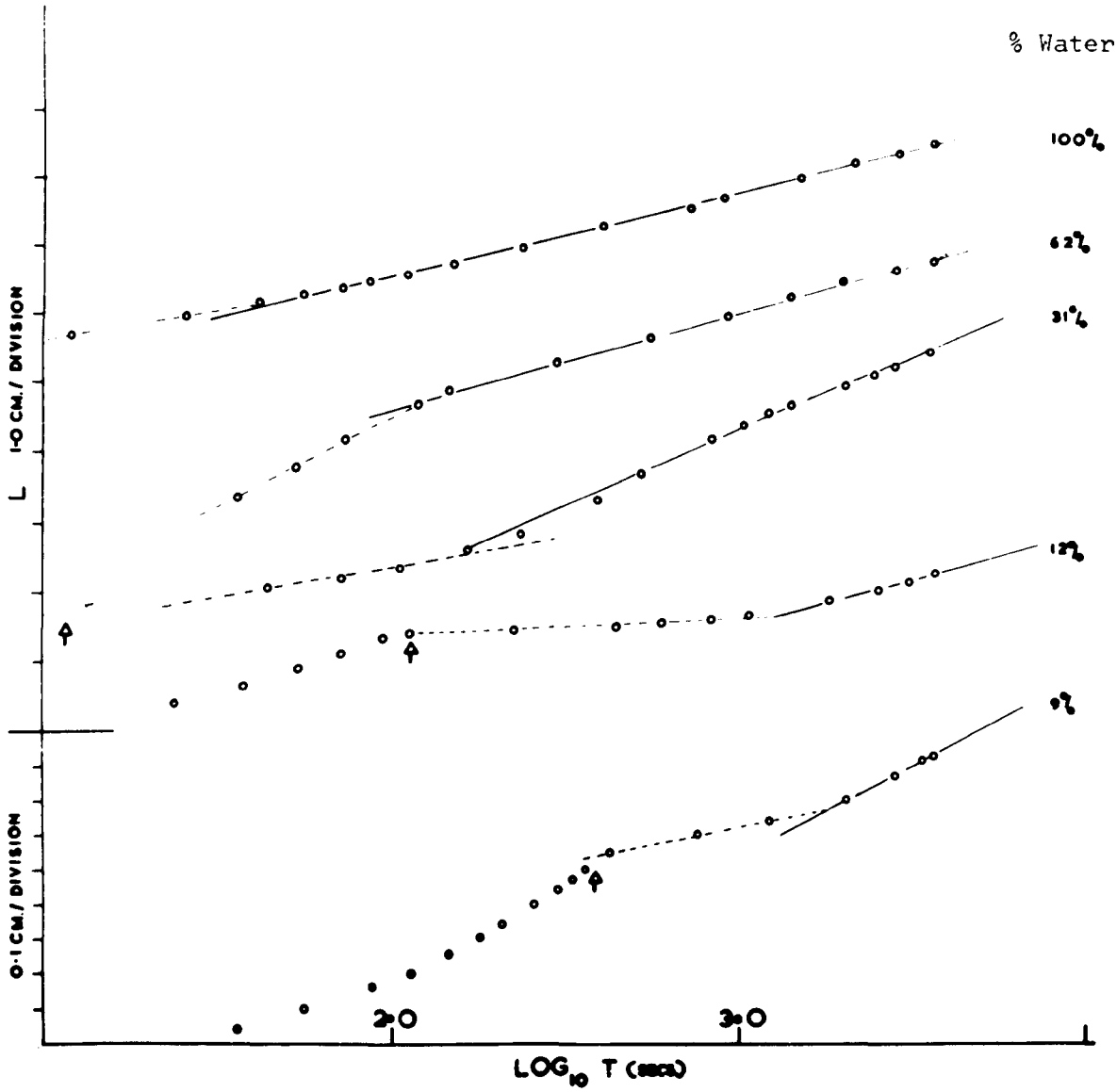

Fig. 32

Creep at constant crack displacement for glycerol/water solutions in similar specimens

increased. This adds considerably to the confidence with which we can suggest that the straight line sections do indeed reflect separate stages and it was concluded from these preliminary observations that two stages of creep occurred in glass: a primary process which was environment dependent and a secondary process which was substantially independent of environment.

The cleavage fracture surface of glass ("Float" and Pyrex plate) is remarkable only in the absence of morphological features. Unlike fracture surfaces which result from rupture in tension or bending, the cleavage surface appears optically smooth. The only regularly observed features are "rib markings" which appear at crack lengths which correspond to increases in the displacement of the grips. These rib marks are thought to mark inflections of the crack and in this respect are similar to Wallner lines (Murgatroyd 1942) which are also occasionally observed. The ribs take the shape of the crack front (Fig. 33) which for glass is concave to the unbroken portion, that is to say, crack propagation takes place with the sides leading. Although ribs are easily visible without the aid of a microscope, interferogram studies indicated that the rib mark is an inflection in the surface and not an abrupt step and that the total change in height was of the order of a wavelength. It is interesting to note that, unlike glass, the crack front in p.m.m. is convex to the unbroken. It is possible that the shape of the crack front may have some fundamental significance, but the nature of this does not seem obvious as yet. For pyrex glass the crack front is also concave but with a

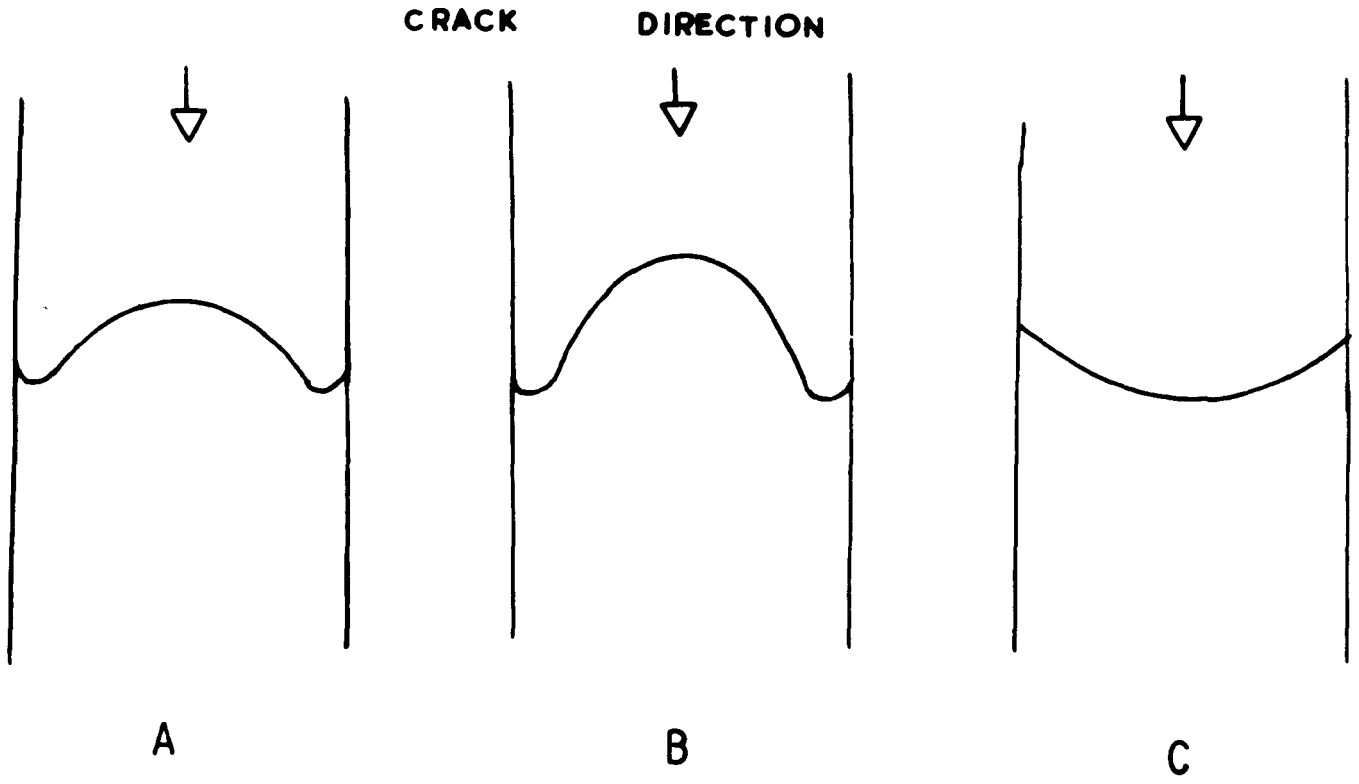

Fig. 33

Schematic representation of the cleavage crack fronts for:

A - "Float" glass B - Pyrex glass C - p.m.m.

greater curvature than for soda-lime-glass, and it was noted that in most environments the creep rate was greater in Pyrex.

The cleavage fracture morphology of p.m.m. is quite different from that of glass. Not only is the surface rougher, but it exhibits interference colours of great complexity; the interpretation of these colours has already been discussed in Chapter IV. A comprehensive examination of the fracture morphology has been carried out by Berry (1963) and the present author will not describe those of his own observations which only confirmed the conclusions drawn by Berry. One interesting feature of the morphology produced during creep provided evidence to suggest that more than one process may be involved in slow fractures in p.m.m. Several specimens were cleaved in an atmosphere of dry nitrogen and it was observed that for these cleavage surfaces the zones corresponding to secondary creep were noticeably rougher than the regions corresponding to the fast moving crack produced immediately after the displacement had been increased. Fig. 34 illustrates the onset of this rougher structure on a fracture surface. Although similar evidence does not exist in the cleavage fracture morphology of glass it would seem that there, too, more than one stage of creep is present.

5.3 Preliminary experiments and results

Creep experiments were essentially observations of the slow crack growth and the influence of the environment upon this growth. These experiments involved the introduction of a cleavage crack into a normal

Fig. 34

The onset of a second stage of creep in a p.m.m. specimen cleaved in dry nitrogen

specimen as described in Chapter III. Measurements were most frequently taken on cleavage cracks growing at a fixed separation of the cantilever arms (2δ), although a number of observations were made on specimens which had a constant load applied to the cantilever arms. Cleavage under constant deflection is a stable system, a point we have discussed in Chapter II, while cleavage under constant load might be regarded as similar to tensile fracture in that both lead to catastrophic failure. The advantages of the former technique are obvious, (in principle the limit of the creep process can be determined merely by waiting), but a comparison of the two different stressing situations proved to be useful. Once aware of the phenomenon of creep, we were posed with a number of problems as to the extent and rate of the process and the nature of the determining factors in both cases.

Extent of creep growth

The revelation that the crack growth was approximately exponential in time accentuated the difficulty of estimating the limit of the process. Long term experiments were initially subject to two restrictions: (a) if carried out on the cleavage machine they prevented its use for any other test, and (b) all experiments were initially restricted to a maximum duration of several months due to a proposed move from one laboratory to another. In order to remove the first complication two small cleavage systems (Fig. 35) were constructed and were used to strain the usual cleavage specimen so that creep could be observed for long periods of time. This apparatus was limited to creep observations in air.

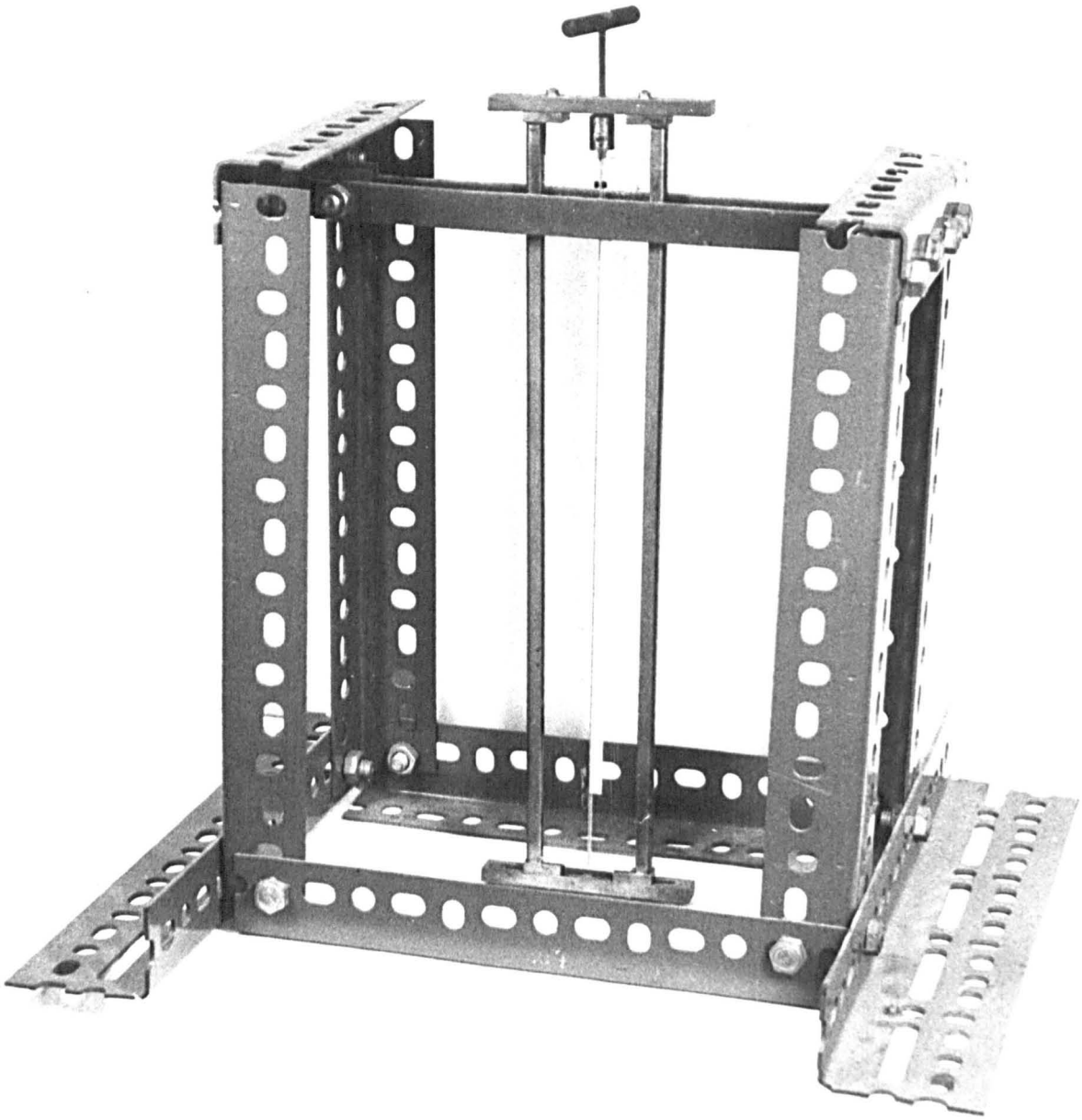

Fig. 35

Wedge type cleavage system as used in long term creep observations

Using this apparatus and also carrying out creep tests in the cleavage machine, it has been possible to obtain some preliminary information on the total extent of creep. Crack growth in soda-lime-silica glass in air was followed for 14 months, when the crack which was still growing had a velocity of approximately 10^{-6} cm min^{-1} compared with an initial velocity of approximately 1 cm min^{-1}. These results were, of course, not available because of the prolonged nature of the experiment until after the majority of the experiments, yet to be described, had been completed. Assuming that the initial crack length corresponded to a fracture energy of 4000 ergs cm^{-2} the position of the crack front after 14 months corresponds to a value of 340 ergs cm^{-2}, which is of the same order as the surface energy of glass. The actual value of the surface energy is in some doubt but appears to be between 200 - 500 ergs cm^{-2}, (Griffith 1920, 540 ergs cm^{-2}, Charles 1961, 175 ergs cm^{-2}). A similar calculation for the creep of a cleavage crack in soda-lime-silica glass in water showed that after three or four weeks the fracture energy appeared to be approximately 430 ergs cm^{-2}. If it is assumed that a similar fall is possible in all environments, given time, then for dry environments such as liquid nitrogen, we would still observe crack growth after ten years! Extensive examination of the secondary creep in many environments like liquid nitrogen or vacuum was not practicable and observations in these environments were limited often to periods as short as fifteen minutes.

These simple experiments indicated that extensive crack growth in cleavage occurs over very long periods of time, and the effective fracture energy falls to values of the order expected for the surface energy. The overall rate at which the growth proceeds depends on the environment.

Creep growth rates

Detailed analyses of some of the earlier experiments showed that the creep rates, as reflected in the slope of the L versus t plots, varied with the beam width. The possibility that a stress corrosion mechanism was responsible for part if not all of the creep growth argued for a more detailed examination of this dependence of creep rate on specimen size; in particular that the variation of creep rate with the magnitude of the stresses at the crack tip should be determined.

Following Gilman's analysis, Chapter II section 6, for the crack positions corresponding to a constant fracture energy γ we may write for the bending moment in the beam at the position of the crack tip (M_c)

$$M_c = \sqrt{6\gamma EIw_1} \qquad 2.6.8.$$

Thus in a given ideal cleavage specimen, whenever the crack just propagates from a true equilibrium position, the stresses around the tip will be the same since these will be determined by the local bending moment. However, even assuming that the stresses at the tip are uniquely determined by the bending moment, we note that they will vary with

specimen size since M_c is a function of I. If the stresses at the tip, σ_{tip}, are simply related to the maximum fibre stress, σ, then:-

$$\sigma_{tip} = \frac{KMb}{2I} \qquad 5.3.1$$

where K is a constant.

Substituting for M_c and I

$$\sigma_{tip} = K\left(\frac{18E\gamma w_1}{w_2 b}\right)^{\frac{1}{2}} \qquad 5.3.2$$

so that it might be expected that if creep rates were determined by the stress at the tip and that if this stress were simply related to the maximum fibre stress, then the creep rate would decrease with increasing beam width according to $b^{-\frac{1}{2}}$.

In order to establish the actual dependence of creep rate on beam width, a number of specimens with beam widths in range 1.0 to 4.0cm were cleaved in air and creep curves were recorded at intervals down the specimen for periods up to one hour. At this stage it was difficult to establish a simple empirical parameter which could be used to characterise creep in order to compare quantitatively the behaviour of different specimens, and so the increase in crack length over a given period of time was used. Two points were obvious from the results of these tests:- the greater the beam width the higher the creep rate, and contrary to the conclusions drawn from the initial experiments, it was observed that the creep rate increased with increasing L_o down the specimen. It was remarked in the earlier section that the creep curve in air was

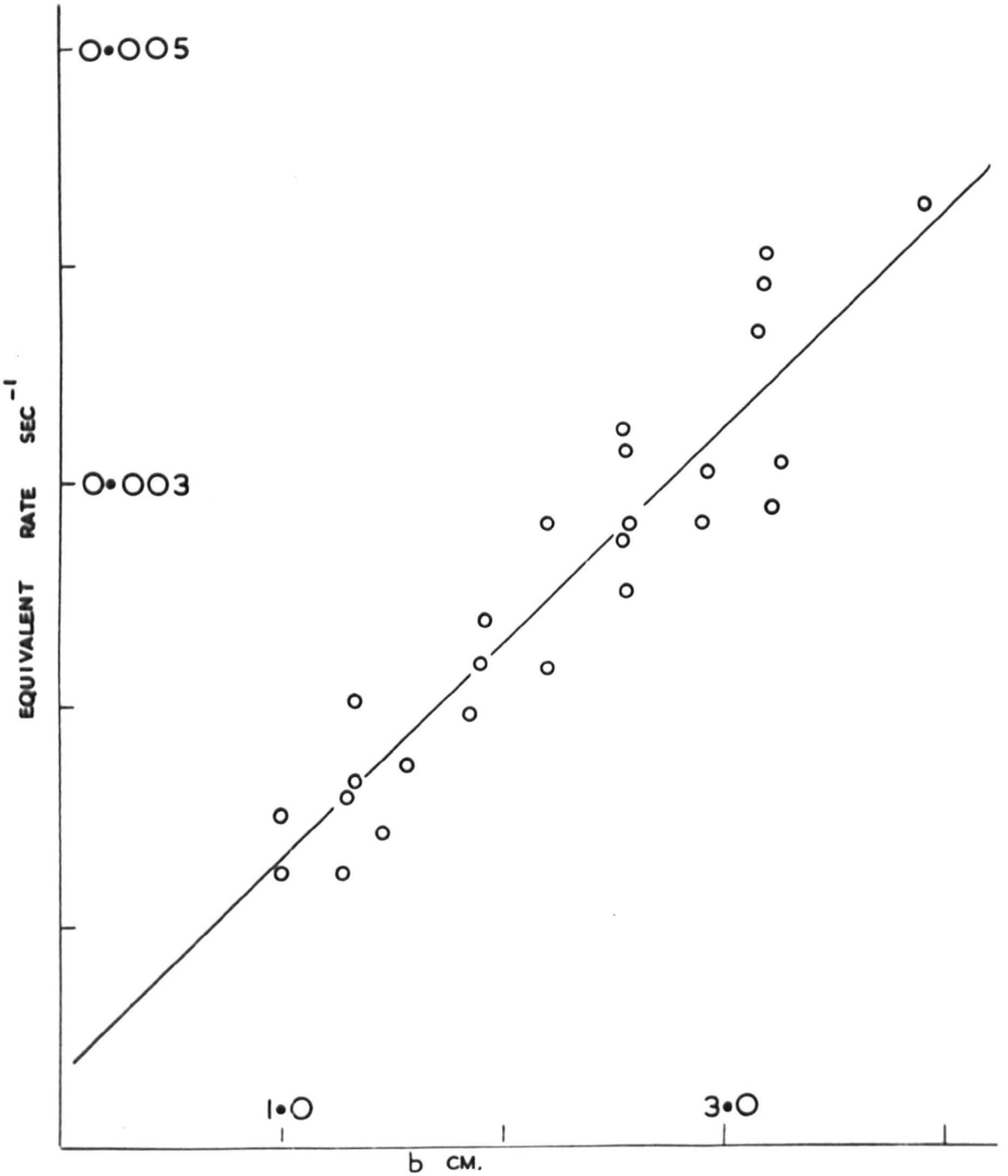

Fig. 36

The variation of 'equivalent creep rate' as a function of the specimen beam width, b

logarithmic in time; initial plots of L versus $\log_{10}$ t appeared to give straight lines over limited ranges of time. In order to establish clearly any variation with beam width this method of presentation has been adopted for the tests described above. To compare tests on different specimens an "equivalent rate" was extracted from the $\log_{10}$ t versus L plots. The "equivalent rate" for the section corresponding to the primary creep is defined as ΔL(cm) between $\log_{10}$ t(secs) at 2.0 and 3.0 divided by 90 which gives the equivalent of the average change in length per second. The equivalent rate is then plotted as the ordinate and the beam width as the abscissa in Fig. 36. The best straight line was determined by the method of least squares, and the slope found to be 9.77×10^{-4}cm with a standard error of 1.0×10^{-5}cm (1.03%). Quantitative use of this data is limited because of the insensitivity of the L versus $\log_{10}$ t plots which cover only small changes of L. From a similar analysis of the two other portions of the $\log_{10}$ t versus L plots, it was only possible to conclude that the section 0 - 2 minutes also showed a trend of increasing rate with increasing beam width, while the section from 15 - 60 minutes seemed independent of the value of beam width.

The observation that the creep rate increased with beam width, contrary to our initial expectation, was not too surprising in view of the sweeping assumption that the stresses at the tip are adequately represented by the maximum fibre stress. Gillis and Gilman (1964) remark that the restriction of anticlastic curvature at the crack tip

is also expected to be a function of the beam width and this must surely lead to an additional stress field around the tip of the crack. The problem of the dependence of the stress at the tip of the crack on the specimen dimensions is clearly a crucial one, and particularly difficult to handle experimentally as no theoretical solution appears to be available.

Indeed, as we shall see in Chapter VI, the argument that the stress at the tip is proportional to the maximum fibre stress, or even that the stress at the tip varies with beam width might not be correct. In developing a particular model to attempt a quantitative comparison with the experimental results a self consistency argument is used to determine the dependence of the crack tip stress on specimen size. We shall then imply that under the particular conditions defined by cleavage fracture, we would not expect a variation of stress with dimensions. However, for the present we will proceed under the assumption that a stress variation occurs with change in the specimen dimensions, but any interpretation based on the assumption will be regarded as tentative.

When new surfaces are exposed to the environment by fracture, they are very reactive as we have seen in Chapter I. The clean surfaces may react with the environment reducing the surface energy, and thus the fracture energy of which the surface energy is a part. The environment can also attack the highly stressed bonds at the tip of the crack which are vulnerable and if this happens the chemical energy of the reaction may contribute to the growth of the crack. It should be noted, however, that

even if a reaction is possible the rate may be limited by the rate at which molecules can get to the tip of the crack. The early indication that the creep rate might vary with the stress around the tip lent encouragement to the possibility of attributing the phenomenon to stress corrosion, and immediately suggested a second, perhaps more sensitive, test of the validity of this idea which would be to investigate the temperature dependence of the creep rate. It would be expected that stress corrosion would be a thermally activated process (Charles and Hillig 1961) and that the creep rates should therefore vary with the temperature.

Temperature effects

Because of the difficulty involved in obtaining uniform heating in a medium such as air, and because we have previously established that water has a marked effect on creep, in order to separate the effects due to the removal of water from the environment and those due to a temperature change, observations were made on specimens immersed in either a water or a silicone oil bath. Creep in water appears to include part of the primary creep which early experiments had indicated might be a stress corrosion phenomenon, while creep in silicone oil is entirely secondary creep and this we expected not to be a corrosion process. Creep observations were made on two similar specimens in each environment. The tests in water were carried out at room temperature, 20°C and at 80°C; in the latter case the temperature was maintained by the Ether control unit described in Chapter III which regulated a ½KW

heater immersed in the liquid. It was not possible to discern any difference between the creep rates at the two temperatures and it was concluded that either the primary creep process was not thermally activated or that the activation energy of the process was very high. For completeness, two specimens were cleaved in silicone oil (MS 550), one at 20°C and one at 200°C. Three creep observations were made on each specimen, in what was effectively an environment free from water. The results of these tests established that although the creep rate increased down the specimen, the average rate taken from the three observations was not significantly different between the two specimens (0.082 and 0.087 cm in 20 mins). The evidence for a non-thermally activated secondary creep is supported by the fact that crack growth in liquid nitrogen (-196°C) is not significantly different from growth in other dry media at room temperature.

These results suggest that neither the primary nor the secondary creep appears to be a thermally activated process, and although the evidence was not conclusive it was felt at that stage to be sufficiently reliable to favour the search for an alternative hypothesis which might account for the creep behaviour.

5.4 Possible energy sources for the creep process

We can at this stage usefully review some of the general a priori explanations which are possible. Suppose we make as an initial assumption that the energy required to extend the crack during creep remains at approximately 4000 ergs cm^{-2}, i.e. the fracture energy itself is not

changing with time directly. If this were true then increasingly large amounts of energy must be provided as the crack length increases by some source of energy other than the stored elastic strain energy in the cantilever walls of the crack. Earlier in the chapter a number of calculations of the fracture energy were carried out in which the crack length used was that observed after a considerable length of time. Two basic assumptions were involved in such calculations; the first was that the displacement δ at the top of the beam remained constant and the second was that the only source of energy was the stored strain energy i.e. ($\gamma dA = dU$). We will examine these two assumptions to establish whether or not they might be justified. The energy balance in cleavage may be written more fully as

$$\gamma dA + dU + Fd\delta + K.E + Q = 0 \qquad 5.4.1$$

where γdA is the fracture energy, dU the stored strain energy and Q an external energy source such as a heat of adsorption. As we have seen in Chapter II, for slow moving cracks the kinetic energy is small compared with the strain energy and may be neglected.

The term due to $Fd\delta$ represents work done by the movement of the cleavage force during creep, due to relaxation in the system etc. A closer examination of equation 5.4.1 above suggests that even if this movement is finite it cannot contribute to the fracture energy as calculated. Assuming that there are no external sources of energy, i.e. $Q = 0$, and neglecting the contribution due to the kinetic energy

we may write

$$\gamma dA + dU + F d\delta = 0 \qquad 5.4.2$$

and by expanding the expressions:-

$$\gamma w dL + \left(\frac{\partial U}{\partial \delta}\right)_L d\delta + \left(\frac{\partial U}{\partial L}\right)_\delta dL + F d\delta = 0 \qquad 5.4.3$$

but by definition,

$$\text{Force} = \frac{-\partial\ (\text{energy})}{\partial\ (\text{displacement})} \qquad 5.4.4$$

so that

$$\left(\frac{\partial U}{\partial \delta}\right)_L = -F \qquad 5.4.5$$

and equation 5.4.3 reduces to

$$\gamma w dL + \left(\frac{\partial U}{\partial L}\right)_\delta dL = 0 \qquad 5.4.6$$

This is saying that part of dU is due to the work done by the movement of the arms and it is not to be included twice in the energy balance. A way of checking the constancy of δ during creep can be derived directly from the simple bending beam formula and although, as we have seen, it cannot contribute to the energy balance it provides an estimate of the rigidity of the system. From simple bending beam formula neglecting shear

$$\delta = \frac{4FL^3}{Ew_2b^3} \qquad 4.7.1$$

which is the equation relating the end deflection of a beam of rectangular

cross-section to the load applied at the free end. For a constant deflection the equation becomes

$$F = \frac{K}{L^3} \qquad 5.4.7$$

where K is a constant. The experimental data from creep observations on "Float" glass cleaved in air, water, and HF solution were plotted in the form of F versus $^1/L^3$ and one of the straight line plots which resulted is shown in Fig. 37, giving a value of E of 6.5×10^{11} ergs cm^{-2}, and this evidence was taken as supporting the observations made above.

Having eliminated the energy term due to possible movement of the chucks, let us examine possible sources for the term Q in equation 5.4.1. The possibility of Q being a thermal energy contribution can be eliminated on two accounts. First the total energy required after prolonged creep is of the order of (4000 - 300) ergs cm^{-2}, if the energy required for fracture remains the same over the whole creep zone, which is absurdly large compared with kT. Secondly, it is impossible to reconcile such a theory with the evidence that little difference in the creep rate is observed between temperatures of 200°C, 20°C and -196°C.

It is possible that Q might be associated with a heat of adsorption or a heat of reaction of some species with the material at the tip of the crack. For a few chemical species heats of adsorption are as high as 100 Kcal $mole^{-1}$. Assuming that there are 10^{14} reaction sites per cm^2, which is about the number of sites on a close packed metal surface, a heat of adsorption of 100 Kcal would yield approximately 800 ergs cm^{-2}. Even in this extreme case the energy

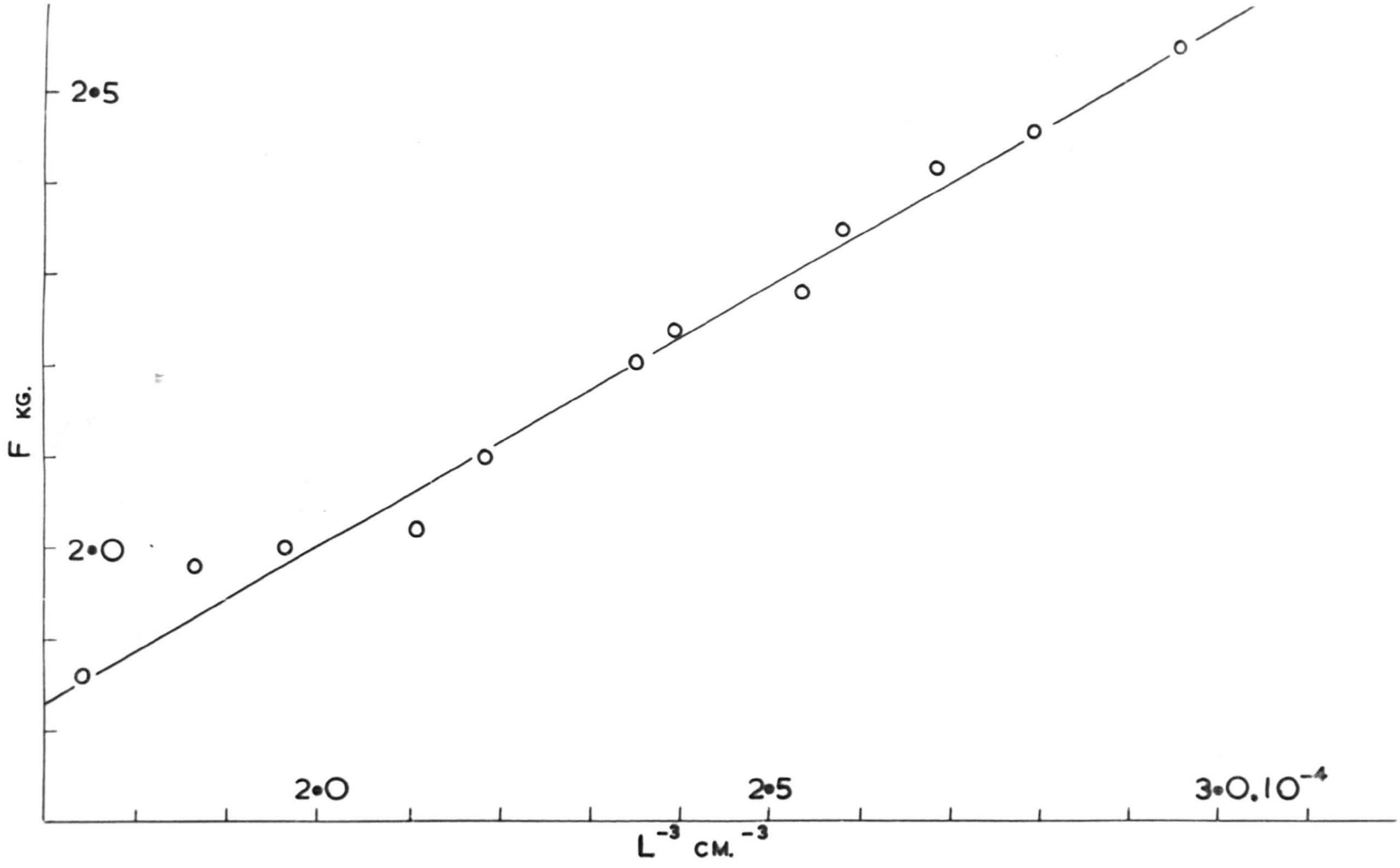

Fig. 37

Young's modulus determination from creep data from "Float" glass cleaved in water

available is not adequate to bridge the difference in energy between the beginning and end of the creep process, so that it would seem unlikely that adsorption could account for the creep process.

Modification of the material at the tip of the crack by an attacking species is essentially the process involved in stress corrosion. Although we have already tentatively eliminated this process especially as far as the secondary creep is concerned, a number of similarities between delayed fracture (static fatigue) and cleavage creep warranted examination. A correlation between creep and static fatigue can be drawn by an examination of the equations derived for the latter phenomenon and the empirical relationships used to describe creep. Two main approaches to static fatigue exist; the first is a flaw genesis hypothesis based on a statistical mechanics approach: non-equilibrium processes are determined by the difference between the rates at which bonds are broken and the rates at which bonds are formed. When bonds are stressed the rates are biased, and the overwhelming molecular activity is reflected in a probability function that is extremely stress and temperature dependent. These theories lead to equations similar to those derived from the pre-existing flaw theories - the second approach to static fatigue. Four of the resulting equations, two from each approach, relating the stress and time for delayed fracture are written as follows:

$\log t = A_1 + B_1 \log \sigma$ (Pre-existing flaws) Charles 1958 5.4.8

$\log t = A_2 + B_2 \log \sigma$ (Flaw-genesis) Poncelet 1948 5.4.9

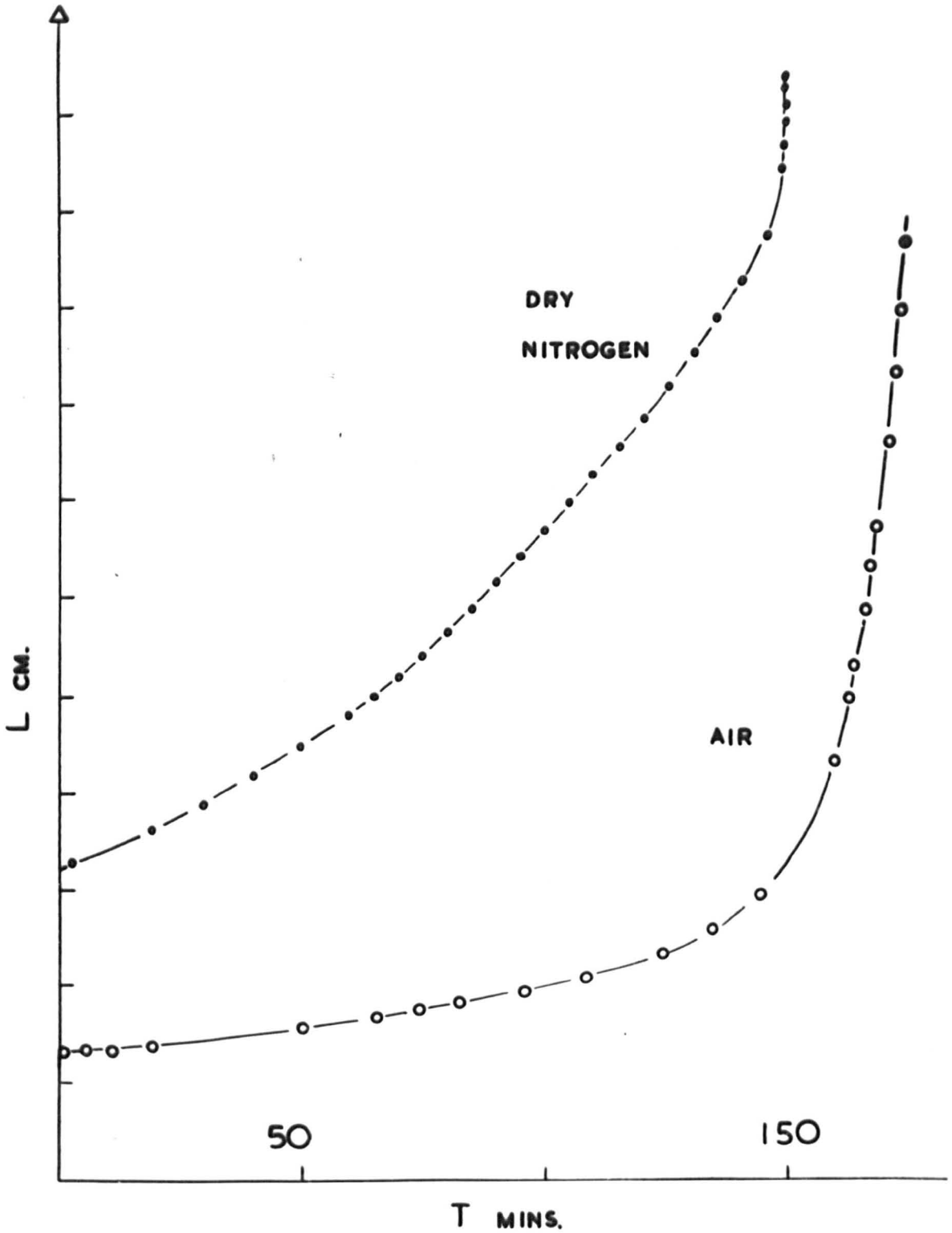

Fig. 38

Creep under constant load for "Float" glass cleaved in air and dry nitrogen

$\log t = A_3 + B_3/\sigma^2$ (Pre-existing flaws) Elliot 1958 5.4.10

$\log t = A_4 + B_4/\sigma$ (Flaw-genesis) Stuart & Anderson 1953 5.4.11

where A and B are constants.

For cleavage creep it is possible to write

$$\log t = A_5 + B_5/\sigma \qquad 5.4.12$$

If it is asuumed that the effect of beam dimensions is merely to change the stress at the tip of the crack. This similarity might indicate that static fatigue and cleavage creep are two occurrences of the same phenomenon. Wiederhorn (1966) has studied cleavage creep and proposed a stress corrosion mechanism. This proposal will be examined in some detail later in the chapter, after a few general points on stress corrosion, and a few pertinent features of cleavage tests have been discussed.

Gurney and Pearson (1949) claimed that water adsorbed on the glass surface, as well as atmospheric moisture, contributes to delayed fracture in glass. Gilman (1959) and Frank (1963) have proposed that the adsorption of water sets up an internal stress. Wang and Tooley (1958) have suggested a possible mechanism by which water may produce this stress and give rise to static fatigue in glass. It is suggested that the Na^+ network ions dissolve in the adsorbed water and are replaced by H^+ ions which attract water molecules into the spaces originally occupied by the alkali. The water molecule is too large and a state of internal stress is set up which breaks the Si network. This may be generalized into a suggestion that the water reacts with the bonds within a crack and forms

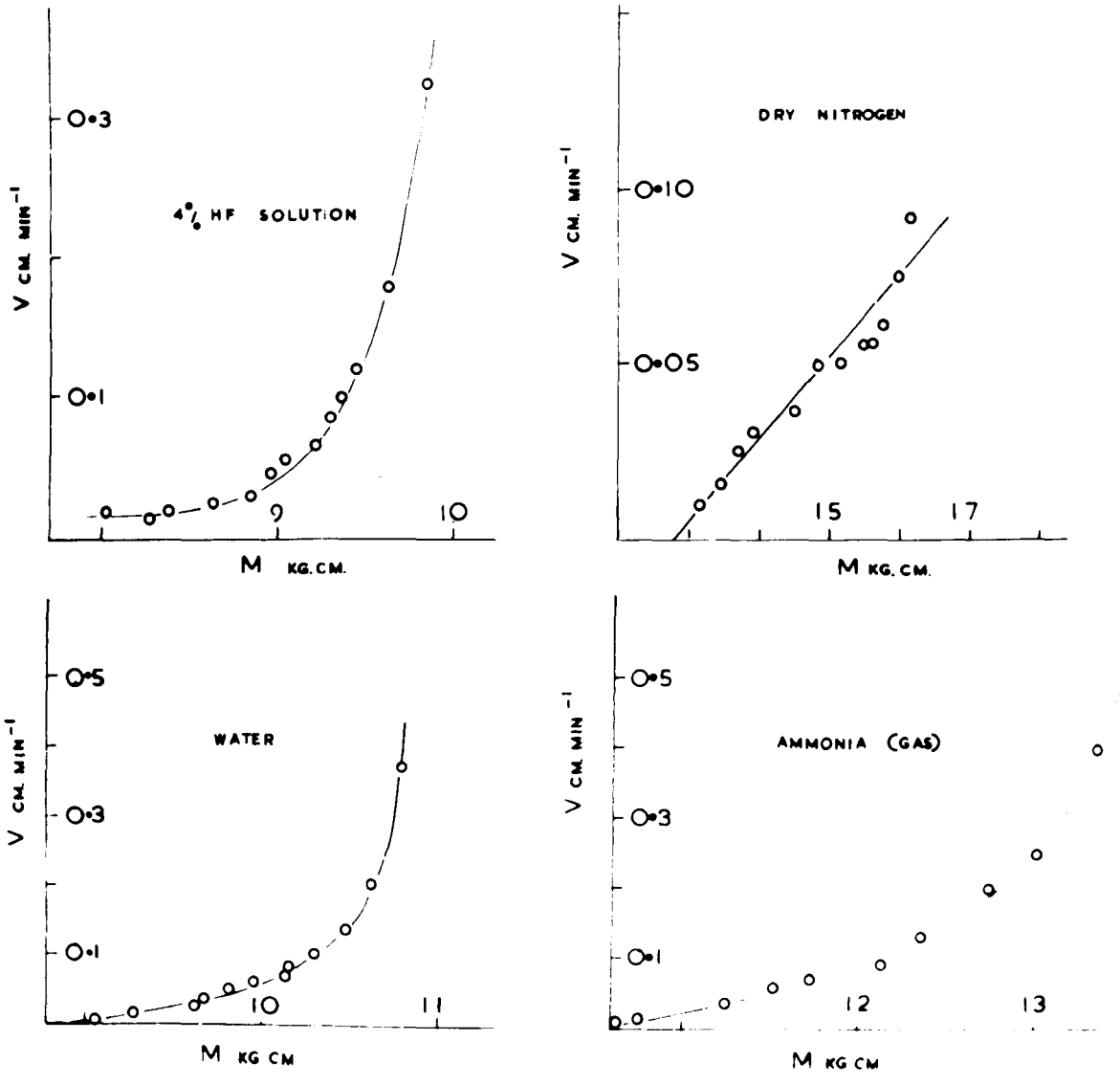

Fig. 39

Sample graphs showing relationship between the bending moment and the crack velocity during creep

reaction products which have a larger volume than the glass. These products act as a wedge stretching the bonds at the vertex of the crack and producing a self-sustaining process. For a crack subject to a tensile stress the process would accelerate as the increasing leverage allowed the instability to set in, but for cleavage under constant deflection, the rate is unaffected by the applied load and would be expected to remain constant. These theories fail to explain the occurrence of creep in environments in which the presence and mobility of water are greatly restricted, such as liquid nitrogen or in vacuum. It is also difficult to reconcile the absence of obvious thermal activation with such processes.

Failure to find an adequate source of energy, and one which is suitably behaved, forces us to question the assumption made earlier in this section - that the energy required to propagate the crack remains at ~4000 ergs cm^{-2} throughout the creep. In order to discuss alternative possibilities in experimental terms, it will be necessary to return to a discussion of the general problem of analysing the data collecting in a creep experiment.

5.5 A brief discussion of the analysis of creep data

It is an inherent property of the cleavage experiments described in Chapter III that the total changes of the crack length are restricted to a factor of approximately two. Observations of creep at constant deflection were often limited to a change of a few centimetres, say from L = 10 to L = 15 cm over a period of many hours. During these creep

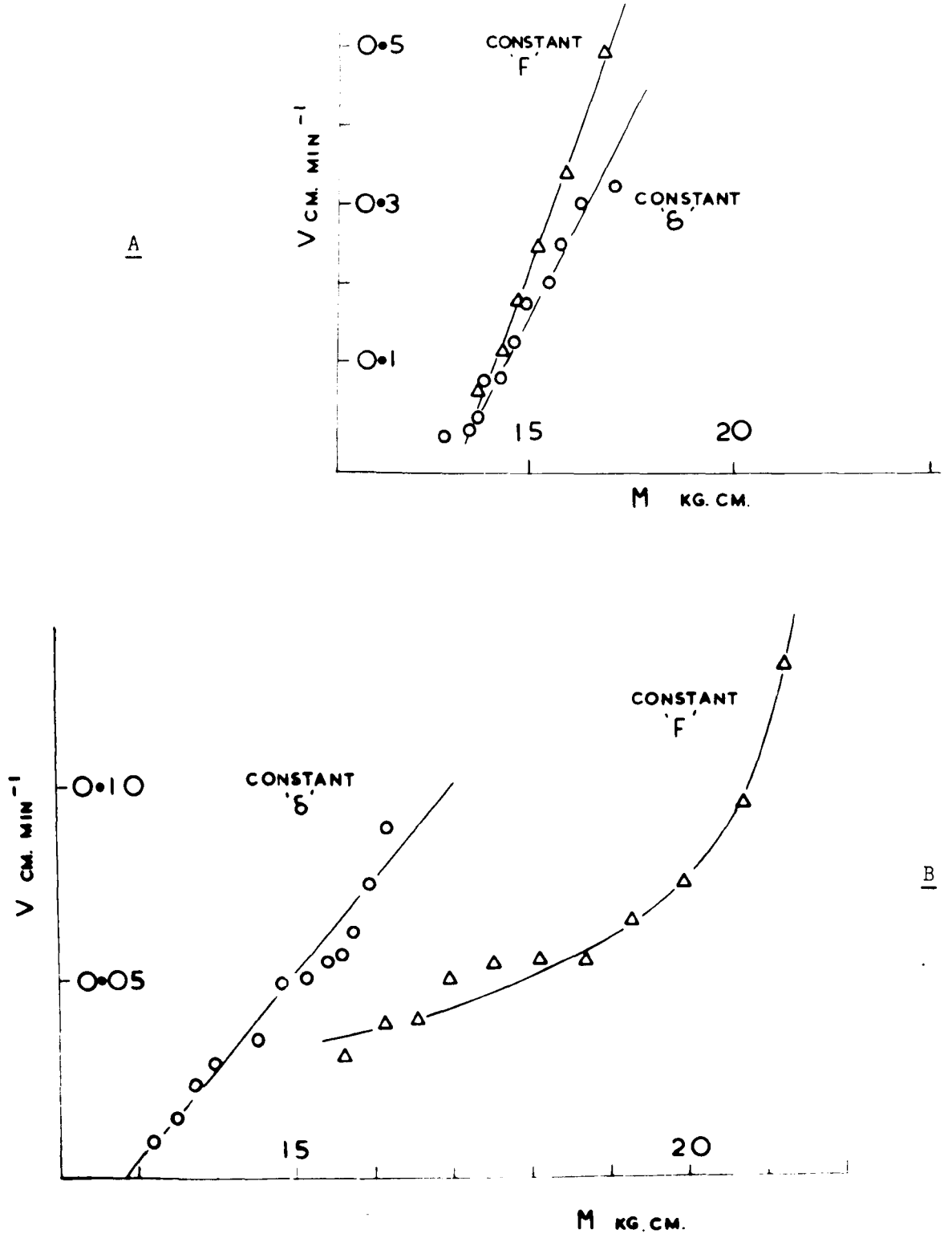

Fig. 40

Bending moment/velocity relationship for cleavage in (A) air and (B) dry nitrogen

experiments on soda-lime-silica and borosilicate glasses the variation of the cleavage force was recorded continuously. Wiederhorn, whose work will be examined later, carried out observations of the creep which occurred in cleavage under constant load, and concluded that the crack velocity was exponentially dependent on the load. A series of experiments was carried out to determine whether the two observations of creep were equivalent. Cleavage under constant load was achieved by supporting the specimen in one of the machine chucks as usual and then fastening the pin through the other half of the specimen to the load F by means of a wire which passed over a pulley. The load was increased until visible crack growth had occurred over a period of about an hour, and the growth was then recorded until the specimen failed. Creep curves from cleavage tests in air and dry nitrogen are illustrated in Fig. 38. Because in cleavage the force and crack length are not independent at constant deflection, it was considered that an examination of the effect of the bending moment (M = FL) on the crack velocity might be more informative than the effect of force alone. Sample graphs of M versus the crack velocity V for cleavage creep at constant deflection in water, HF, Ammonia, and dry nitrogen are shown in Fig. 39. From these graphs one might surmise that whereas in N_2 the crack velocity was directly proportional to M, in more corrosive environments it was related in a complicated manner. An interesting feature of the M versus V plots is illustrated by Fig. 40A from which is is deduced that in air creep observed either under a constant load or constant deflection appears to be equivalent. But this does not seem to be the case in dry nitrogen (Fig. 40B) and might be taken as

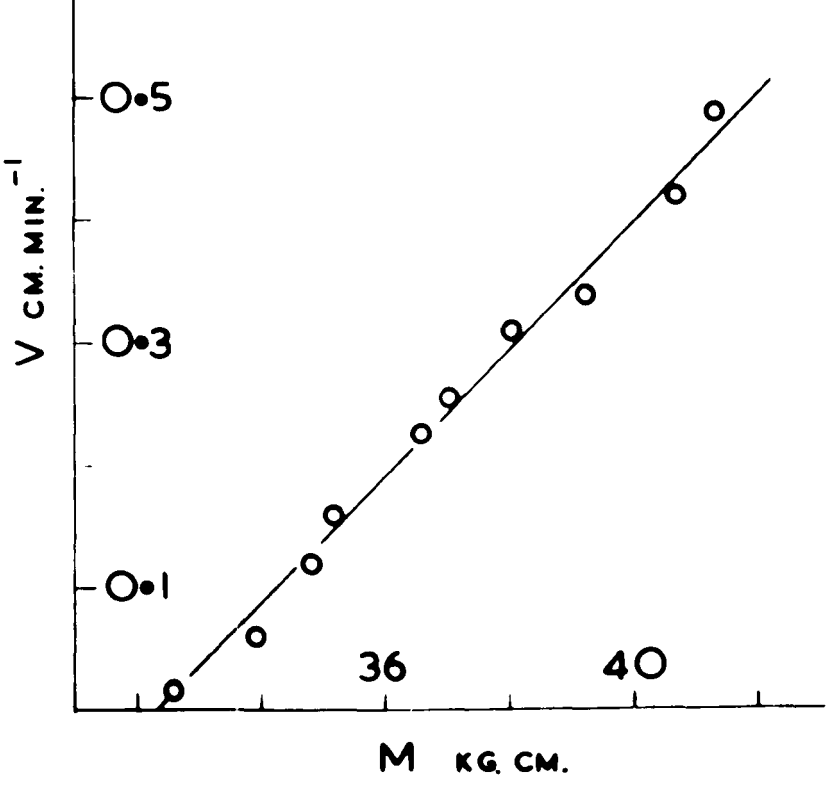

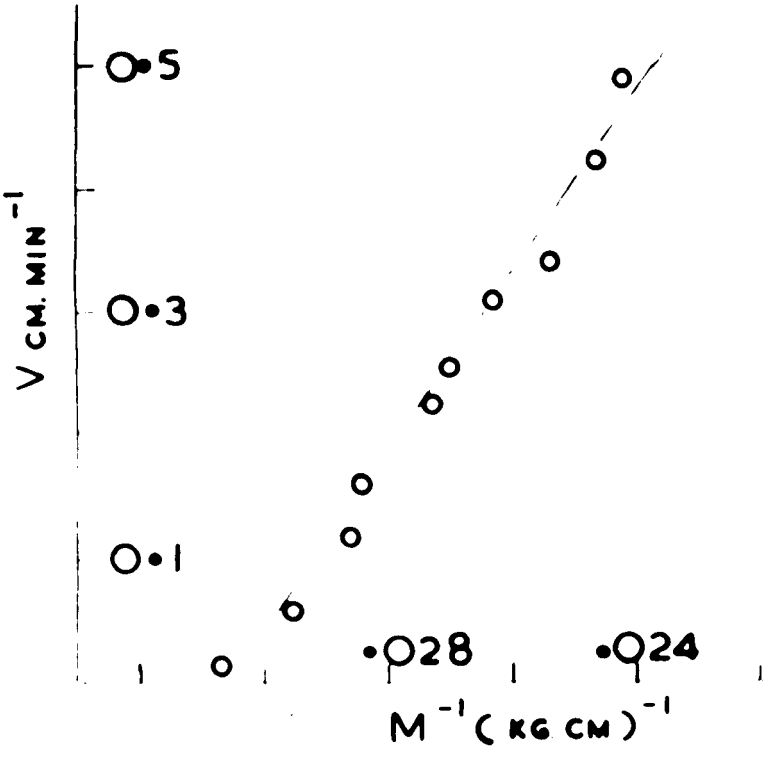

Fig. 41

A comparison of cleavage crack velocity data as different functions of the bending moment

an indication that different environments involve at least different rate determining processes. It is difficult to determine the actual relationship existing in any particular environment because of the small changes in M which occur compared with the high values of M involved. This may be succintly illustrated by a comparison of V versus M and V versus $^{1}/M$ and from an examination of Fig. 41 we must conclude that it is not possible to distinguish between them.

A final point which illustrates this difficulty of analysis of cleavage data will be considered. Early experiments and subsequent analysis indicated that a linear relationship between L and $\log_{10} t$ existed. A number of observations of creep in air over six decades of time were collected for specimens of different beam widths. When plotted in the form of $\log_{10} t$ versus L, straight lines resulted. Fig. 42 shows the experimental data from one such specimen presented as $L^{\frac{1}{2}}$, L, L^2 and L^4 as a function of $\log_{10} t$. It is obvious that there is little difference between any of the four ways of representing the experimental observations. This limitation is one which is inherent in the cleavage process and cannot be controlled; as a result interpretations should be subject to a high degree of caution.

We conclude that although given a particular hypothesis we might be able to test this to some extent, it is particularly difficult to proceed by induction from the experimental data to possible relationships and from there to mechanisms and models.

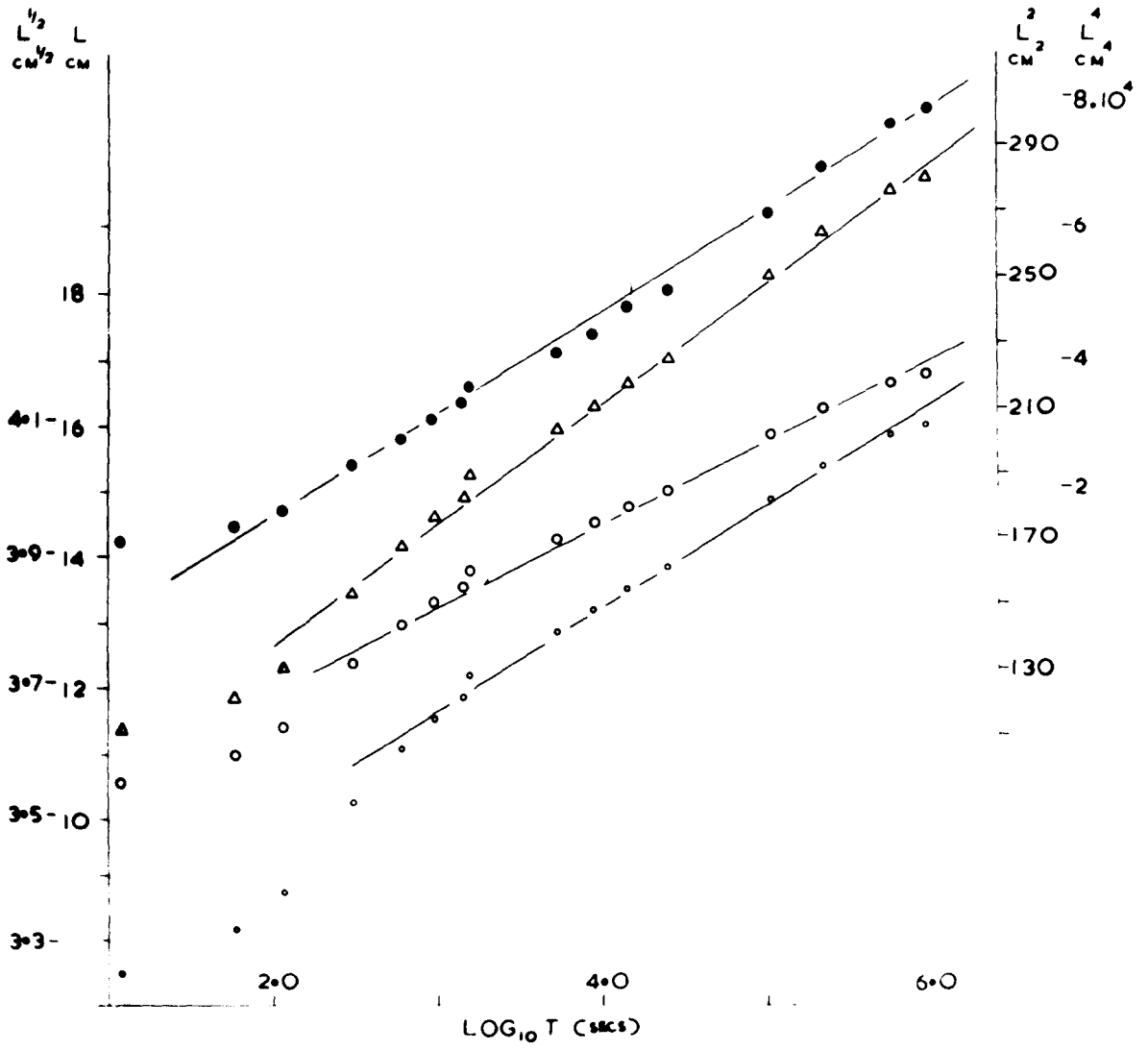

Fig. 42

Experimental cleavage data presented as various functions of crack length

c - $L^{\frac{1}{2}}$, o - L, Δ - L^2, ● - L^4

In the previous section we found that it was difficult to accept the assumption that the energy required to extend the crack stays constant during creep. A simple alternative is that the creep growth corresponds to a progressive decrease in the fracture energy with time. An examination of the previously described V versus M plots for air (Fig. 43) indicated that a systematic variation with beam width would account for the displacement of the lines, and by plotting M at V = 0 against various functions of b, it was established that M_o was related to b as $M_o = Kb^n$, where K was a constant and n was between 1.5 and 2.0. The equilibrium condition for cleavage, assuming a constant fracture energy, has been written as:

$$FL = \frac{\gamma^{\frac{1}{2}} E^{\frac{1}{2}}}{\sqrt{6}} (w_2 w_1)^{\frac{1}{2}} . b^{3/2} = K^1 b^{3/2}$$

where K^1 is a constant. Experimentally we have observed that $M_o \simeq Kb^{3/2}$. From this we conclude that if we extrapolate the creep process in air to zero velocity, we may represent this situation by an effective fracture energy (of ~160 ergs cm^{-2}) which is independent of the specimen size. This would support the hypothesis that the creep corresponds to a progressive decrease in γ with time.

If we assume that during creep γ is some function of time independent of L, δ, and F it should be possible to correlate all the creep curves. Since

$$\gamma = \frac{K^1 \delta^2}{L^4} \qquad 5.5.1$$

for a given specimen

$$d\gamma = -4\frac{K^1 \delta^2}{L^4}\left(\frac{1}{L}\right)dL \qquad 5.5.2$$

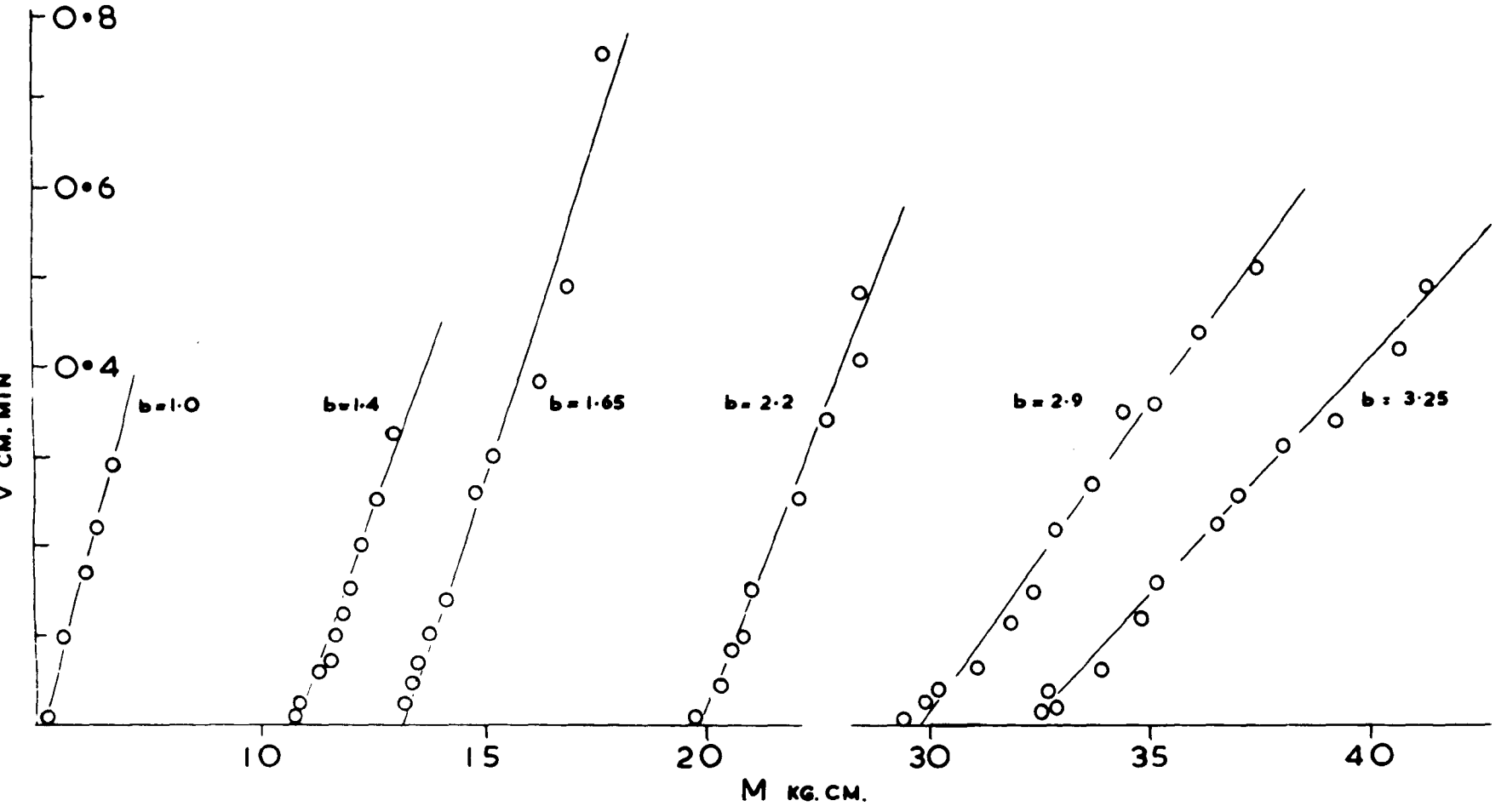

Fig. 43

"Float" glass creep data for specimens cleaved in air

and

$$\frac{d\gamma}{dt} = -4\frac{\gamma}{L}\frac{dL}{dt} \qquad 5.5.3$$

$$\frac{d\gamma}{\gamma} = -4\frac{dL}{L} \qquad 5.5.4$$

If γ is a simple function of time, then for any creep process $\frac{d\gamma}{\gamma}$ should be a function of time only and not beam dimensions. Experimentally it is observed that $^{dL}/L$ is not independent of δ, or beam width; thus from equation 5.5.4 above we must conclude that creep cannot simply be regarded as a progressive fall in the fracture energy. Also, whereas the sensitivity of expressions such as those involving M cannot be very great, we can measure L and so ΔL very accurately, so that this is a much more sensitive test of our hypothesis. In summary, we have examined possible explanations of the phenomenon of creep in terms of a gradual fall of the fracture energy in time, and concluded from simple observations that the crack length or apparent fracture energy, during creep is not simply determined by the time alone.

In Chapter IV it was mentioned that the high fracture energy might be interpreted in terms of plastic flow at the crack tip. If this is so then of course some mechanism is required which limits the flow and advances the fracture. Cottrell(1964) has expressed the fracture energy as

$$\gamma \simeq \sigma_y \alpha/2 \qquad 5.5.5$$

A simple possibility then is that the plastic extension is limited, and fracture occurs in preference to further flow when a critical

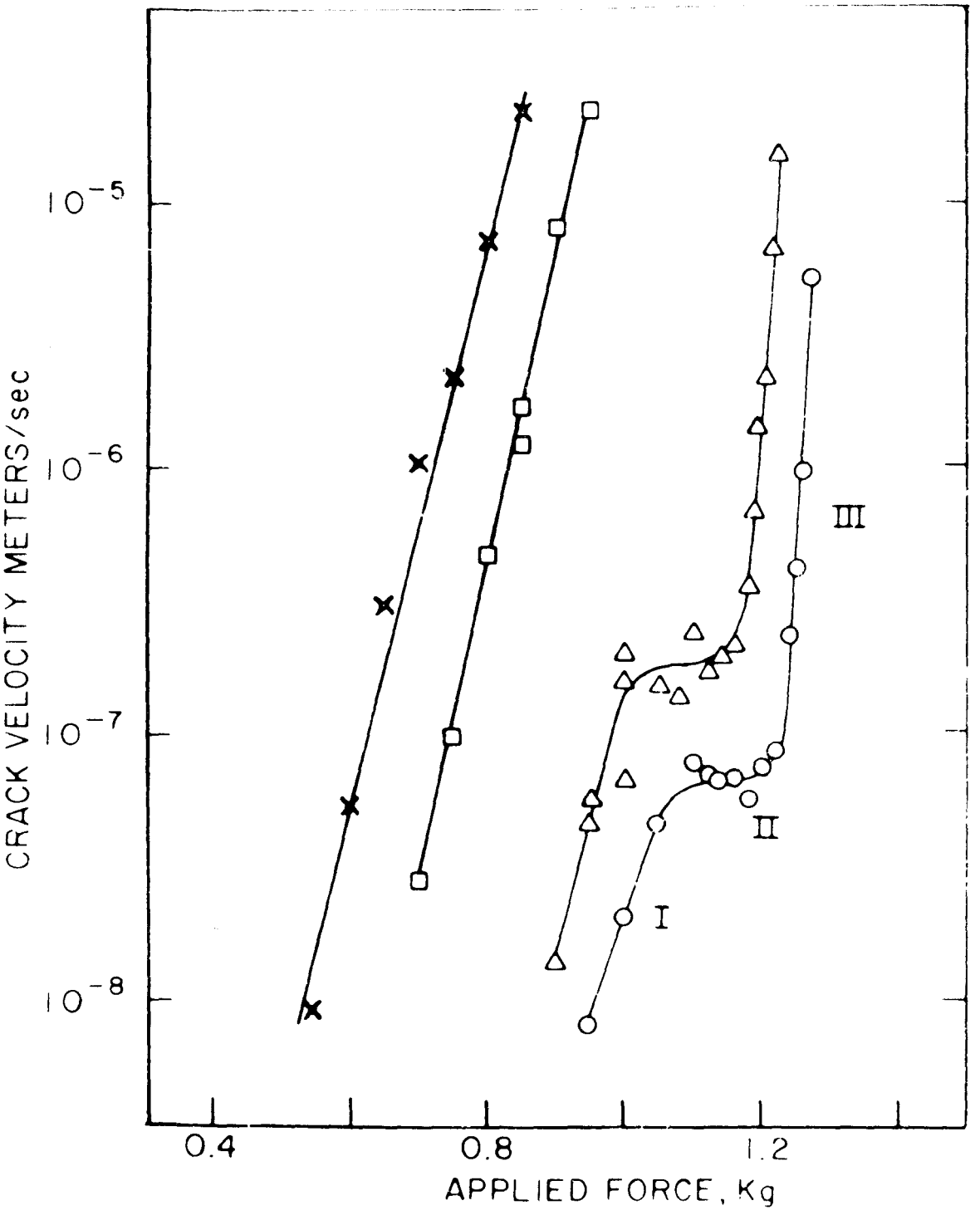

Fig. 44

Creep data (Wiederhorn 1966) for cleavage in water (X), moist air (□), nitrogen gas (Δ) and dry nitrogen gas (O)

extension is reached. Marsh (1964) has shown σ_y (the yield stress) to be a function of time and, in principle, it would seem that this might provide a correlation between creep and γ changing with time. But we see immediately that any model based on the hypothesis of a critical plastic extension will not fit the observations: it would imply that $\gamma = f(t)$ since $\sigma_y = f(t)$ and α_c = constant, and empirically γ is not a simple function of time. An alternative criterion for the termination of flow is the attainment of a critical plastic zone size, and we shall see in the next chapter that this is not in such obvious conflict with the experimental observations. Before we examine this model in detail, it would perhaps be useful to review the conclusions drawn from the early experiments to explore the nature of the creep process and also discuss in some detail the only previously published attempt to explain this slow crack growth.

5.6 Summary of observations on creep

We have established that some evidence exists which suggests that cleavage crack growth occurs in three stages. The instantaneous crack growth was used to calculate fracture energies and these exhibited a dependence on environment. A few observations have been made on the primary creep but the preliminary experiments indicated that it might be dependent on the stress and connected with the presence of water. The secondary process was not temperature activated and seemed insensitive to changes in beam dimensions. It was surmised that although

it appeared to correspond to an actual fall in fracture energy, this could not be represented simply as a function of time alone. Creep has been shown to be an extensive process lasting possibly years and influenced by the environment.

5.7 A discussion of the theory due to Wiederhorn

During the initial experiments to explore creep, some of which are described above, the report by Wiederhorn (1966) was published. In this report a limited description of the slow crack growth in short cleavage specimens subject to a constant cleavage force is described and explained in terms of the stress at the tip and the effect of water. Since this is the only attempt to account for the creep phenomenon, we shall examine the results and proposed interpretations in some detail. It will be convenient first to summarize briefly the aspects of creep reported by Wiederhorn and then to review his explanation before analysing these critically in the light of the studies carried out here.

Wiederhorn used the double cantilever cleavage technique as modified by Westwood and Hitch (1963) which is described in Chapter II. Testing pre-cracked microscope slides, he observed slow growth prior to catastrophic failure in cleavage under constant load. The crack growth curves he obtained for air and dry nitrogen are similar to those obtained in this work using "Float" plate glass (Fig. 38). By studying the load dependence of the velocity it was concluded by Wiederhorn that

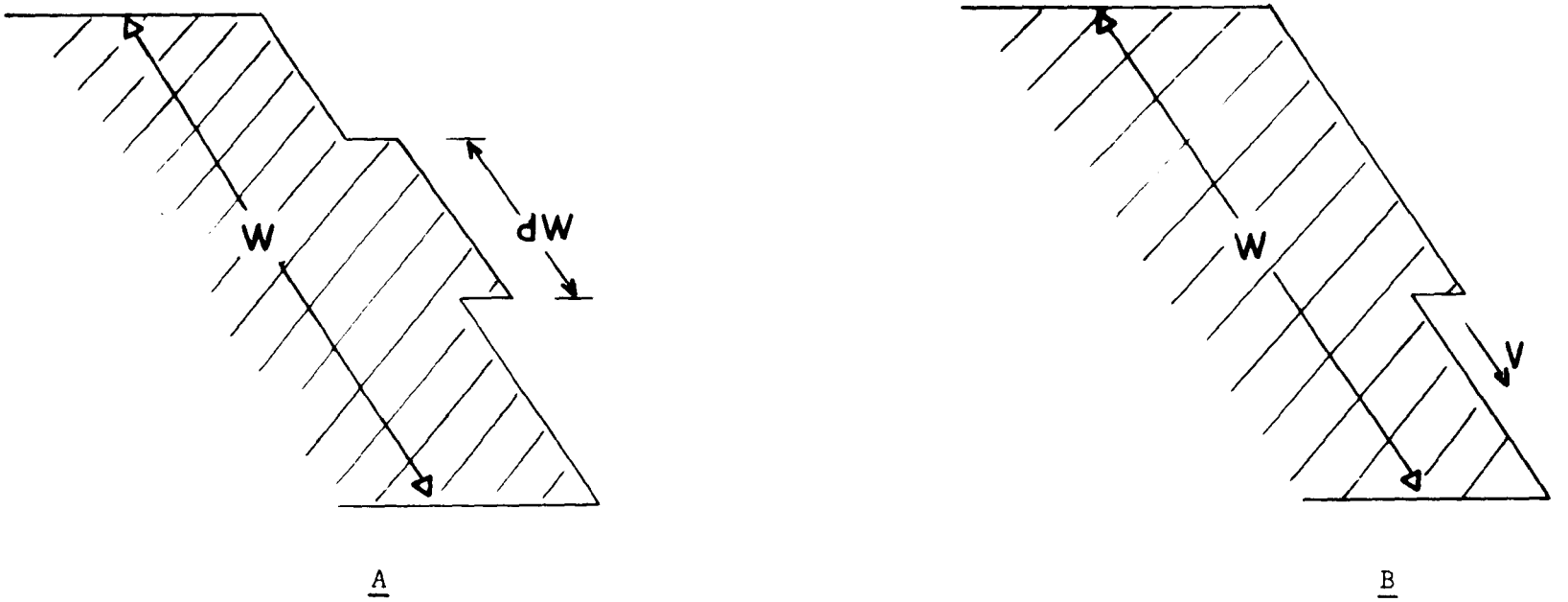

Fig. 45

Crack surface containing (A) a fluctuation and (B) a jog on its perimeter

an exponential variation was appropriate (Fig. 44). He argued that initially in all cases the velocity could be expressed as

$$V = V_o \exp \beta F \qquad 5.7.1$$

which is similar to the equation forthe velocity of corrosion normal to an interface due to Charles and Hillig (1961)

$$V = V_o \exp(V^*_\sigma - \Gamma V_m/\rho)/RT \qquad 5.7.2$$

By defining an effective stress at the tip σ_o as

$$\sigma_o = \sigma - \Gamma V_m/V^*_\rho \qquad 5.7.3$$

equation 5.7.2 reduces to

$$V = V_o \exp \sigma_o V^*/RT \qquad 5.7.4$$

which, argues Wiederhorn, is of the same form as equation 5.7.1, and if σ_o is proportional to F then β is proportional to the activation volume of the reaction (V^*). Since the initial slopes (Fig. 44) are similar, the first sections of all these curves are assumed to be due to water, and the displacement along the F axis to reflect the effect of varying the water concentration at the tip. The second stage of growth in nitrogen (Fig. 44) is explained by Wiederhorn as a transport controlled process, i.e. the rate of transport to the crack tip is slower than the thermally activated process, so that the crack velocity in this region would be expected to be stress independent.

The final creep regions (Fig. 44) have different slopes from the initial regions and therefore are assumed to have different activation volumes. Wiederhorn concluded that a different mechanism was involved,

which was independent of water, and followed a fluctuation theory proposed by Hillig (1962). In deriving an expression for crack motion under tensile stress, Hillig assumed that the fluctuation at the stressed crack tip was sufficiently large to cause the remaining line of bonds to be at the critical stress σ_c and so break. The crack velocity was then determined by the frequency of the fluctuations. Using the crack velocity in dry nitrogen and the distance travelled before catastrophic failure, Wiederhorn showed that Hillig's theory failed to predict the observed high crack velocity for the low stresses used in the cleavage experiments, and concluded that Hillig's theory cannot be used to explain the experimental observations in this region of crack growth.

Consequently Wiederhorn suggested that the existence of another type of fluctuation (a jog of one interatomic spacing (Fig 45)) on the crack front would more successfully explain his experimental observations. The value of the predicted crack velocity using this theory agreed with that observed for the stress applicable, and it was subsequently concluded that the experimental results of this final region of crack growth could be explained in terms of crack propagation controlled by the motion of jogs.

Two criticisms of Wiederhorn's interpretations must be made, one of which arises directly from the experiments described in Chapter III. We recall the insensitivity of the M versus velocity plots and note that Wiederhorn based his hypothesis on logarithimic plots of velocities obtained from variations of crack length of approximately 0.8cm in air

and 0.03cm (which is a 1% change in length) in dry nitrogen. It must also be emphasized that in our cleavage experiments a rapid variation of velocity with M was noted, but that for most environments the velocity was not uniquely determined by M. In general terms, it would appear that the idea of stress corrosion as an explanation of the primary creep is acceptable. The apparent lack of thermal activation may be explicable in terms of a transport limited process. Wiederhorn supposes that a number of stages are possible in the creep process, one environment dependent and the more prolonged stage explicable in terms of statistical fluctuations at the tip of the crack. It is assumed in this approach that the fracture energy remains constant at its high value throughout the creep process.

It is perhaps not surprising that by assuming the presence of a jog, Wiederhorn can predict a sufficiently high crack velocity for stresses below the critical stress ($\sigma < \sigma_c$) which agrees with the experimentally observed value. What is surprising is the assumption. In effect, Hillig calculates the frequency of formation of a jog, which once formed propagates across the crack front at a velocity high compared to the rate of formation. Unless the material has some intrinsic property which prevents the jog, once formed, from disappearing (a point not discussed by Wiederhorn), the problem remains essentially that of Hillig: the formation of a jog. Thus Wiederhorn's assumption is one in which the problem is avoided rather than solved. We conclude that, following Hillig's approach, crack propagation in dry nitrogen or

liquid nitrogen cannot be explained in terms of statistical fluctuations. Apart from the absence of thermal activation, to a first approximation the creep rates are the same in liquid nitrogen and silicone oil at 200°C, the extent of the creep process would rule out any statistical fluctuation theory. Such theories predict that measurable crack velocities are feasible within a few percent of the critical stress for catastrophic growth, σ_c, but the extensive growth observed here would lower the applied stress to such a level that crack growth by statistical fluctuations would be quite impossible at the rates observed.

Despite the high value of the fracture energy, Wiederhorn attributed the slow stage of crack growth to stress corrosion or statistical fluctuations at the crack tip. Wiederhorn argues that the possibility of plastic flow contributing to the high fracture energy is eliminated on the grounds that if it occurred at the tip of the crack, the two fracture surfaces would not match. Berry (1962) established by an extensive study of the topology of the fracture surfaces of p.m.m. that the two fracture surfaces were identical. As we have observed in Chapter IV, plastic flow is known to take place in fracture of p.m.m. and we must conclude that Wiederhorn's observations are quite unfounded.

Finally we note that, as in Chapter IV, it was concluded that the evaluation and interpretation of fracture energies required an understanding of creep, so we suggest the converse is also true. It seems necessary to examine both features of the cleavage fracture process which have every indication of being intimately related.

The high value of fracture energy and the existence of a creep process which occurs in a wide range of environments to such an extent seems explicable only in terms of a progressive fall of the fracture energy with time. In the next chapter the theories based on an explanation of the high values of γ and the creep as a time-dependent plastic flow phenomenon will be examined and the experimental data re-assessed in view of these theories.

CHAPTER VI

THE APPLICATION OF A CRITICAL PLASTIC ZONE SIZE THEORY OF FRACTURE

6.1 Introduction

In this final chapter the evidence for plastic flow will be reviewed, and we shall examine a possible plastic flow theory of fracture propagation. The examination and subsequent development of this theory was the result of many discussions held with Dr. D.G. Holloway. The experimental observations impose a number of restrictions upon possible fracture theories but it will be shown that a critical plastic zone size hypothesis for fracture in glass is not incompatible with the present experimental results. The phenomenon of creep and the observed cleavage fracture energies will be reviewed and interpreted in terms of this hypothesis. Finally, a number of suggestions for further experiments are included.

6.2 Plastic flow in glass

The high fracture energy of p.m.m. was shown in Chapter IV to be explicable in terms of a fracture process involving plastic flow. A number of authors have suggested that the phenomenon of plastic flow may be observed at room temperature in glass. The idea that plastic flow at the tip of the crack in glass might account for the high fracture energy was discussed briefly in Chapter IV. It is therefore of some importance to establish whether or not glass may behave in a plastic manner at room

temperature. The evidence for plastic flow in glass will be reviewed, and although the most substantial evidence has been supplied by diamond pyramid indentation experiments, we shall first briefly discuss the supplementary evidence.

When a hard point is drawn across the surface of glass the smooth furrows which result appear to be formed by plastic flow (Gehloff and Thomas 1926); when two furrows intersect the first groove seems to be filled by material displaced by the formation of the second. Taylor (1950) has described this effect in some detail and Bruche and Schimmel (1954) and Bruche and Poppa (1956) drew similar conclusions from electron microscope studies of the phenomenon.

Also it has been observed that residual stresses exist at the tip of a crack in glass after the load has been removed. Dalladay and Twyman (1921) and Holland and Turner (1937) explained the observed stresses in terms of a wedging effect produced by debris in the crack but Marsh (1963) demonstrated the existence of these stresses even in the absence of debris. Residual stresses would be expected if the material near the tip had been deformed plastically, i.e. permanently.

The equation for the stress at the tip of a crack in an elastic continuum under uniform tensile stress may be written according to Inglis (1913) as:

$$\sigma_{tip} = \frac{2\sigma c^{\frac{1}{2}}}{\rho^{\frac{1}{2}}} \qquad 6.2.1$$

where σ is the applied stress, c the crack length and ρ the radius of curvature of the tip. If this equation is applied to an atomic solid

then we would expect the radius of an elastic crack to be limited to a minimum of an atomic bond length. The concept of stress cannot be used meaningfully over distances shorter than the bond length but even if we take ρ as approximately the size of an SiO_4 tetrahedron, 2×10^{-8}" (~ 5Å) and using a value of 350 lbs.ins$^{3/2}$ for $\sigma c^{\frac{1}{2}}$ corresponding to the measured values of γ (Chapter IV), then the calculated stress across the Si-O bond has a value approaching 0.6E. This is absurdly large: it implies that the local stresses are very much greater than the theoretical values expected to correspond to the maximum in the interatomic stress-strain curve. A more physically feasible value of the stress can be obtained if a blunt crack with ρ ~ 40 - 50Å is postulated.

Brittle theory also fails to account for the crack velocities observed during fracture. Schardin and Struth (1937) observed that the velocity of a crack in glass increases with increased stress and tends to a limiting value determined by the elastic energy released and the kinetic energy of the crack. Mott (1948) and Roberts and Wells (1954) developed a theory for a brittle solid which leads to an expression for the limiting velocity, V_m, as:

$$V_m = 0.38\left(\frac{E}{d}\right)^{\frac{1}{2}} \qquad 6.2.2$$

where d is the density of the material.

Gilman, Knudsen and Walsh (1958) showed that for a brittle material such as LiF the theory agreed with the experimental results. It is also to be noted that for LiF the fracture energy is the surface energy. Schardin (1959) measured the terminal velocity of a large number of glasses

using multiple spark camera techniques and concluded that the observed values did not correspond with those predicted by brittle fracture theory. Dimmick (1951) showed that the high fracture velocities on glass were almost athermal,

$$\frac{1}{V_m} \, d \, \frac{V_m}{dT} \simeq 10^{-4}/^{\circ}K$$

and Schardin (1959) was able to correlate terminal velocities with micro-hardness estimates for a number of silicate glasses. Since it seems that both fracture and the creep observed in cleavage tests appear to be athermal, we might expect the correlation to be extended and creep associated with a plastic process, as indicated by micro-hardness tests.

Micro-indentation experiments

Perhaps the strongest evidence for plastic flow in glass is the micro indentation which it is possible to produce when a diamond is pressed into the surface. Tabor (1951) has established a theoretical basis for the well known correlation between the size of the indentation and the flow stress for metals. In principle it would seem possible to extend this correlation to glasses. Experiments relating indentation measurements to other properties of glass have been carried out, and an attempt to relate the indentation size to flow stress has been made.

That micro indentations are possible in glass would seem evidence in itself that plastic deformation can occur. Several authors (Ainsworth 1954, Douglas 1958, Keshishyan and Epel'baum 1959) have shown that indentation hardness can be related to the structure of glass indicating

that indentation hardness is a material property which is sensitive to changes in the structure, as would be expected of a flow stress. Westbrook (1960) carried out a series of experiments in vacuo on a number of simple glasses and observed a monotonic decrease in hardness as the temperature was increased. Irregularities in the fall at high temperatures were related to the structure or the thermal history of the glass. The diamond pyramid hardness number for a typical soda-lime-silica glass was observed to change by approximately a factor of two between -200°C and +200°C.

Marsh (1963) examined micro hardness indentations in glass produced by a heavily loaded diamond. An important feature of the results of these experiments was that in air the size of the indentation increased with the time of loading, thus implying that the flow stress varies with the time for which a load is applied.

Hill (1950) and Tabor (1951) assumed that the diamond pyramid indenter could be treated as a flat rigid die penetrating a plastic material and predicted a relationship between the Vickers hardness number P* and the tensile yield stress σ_y for a fully work hardened material, of the form: $\frac{P}{\sigma_y} \simeq 3$. Tabor (1948) had already found that results obtained with work hardened materials were in agreement with this prediction.

---

* $$P = \frac{2F \sin \frac{\theta}{2}}{d^2} \text{ Kgm/mm}^2$$

where F is the applied load in Kgm, d is the average diagonal length in mm., and θ is the tetrahedral < of the diamond.

However, the application of this theory to glass predicts flow stresses which are below the brittle fracture stresses observed experimentally, and no signs of flow appear before fracture. Marsh (1964) argues that this failure of indentation theory to apply to highly elastic materials such as glass is due to a change in the mode of deformation under the indenter. Samuels and Mulhearn (1957) and Mulhearn (1959), from an examination of equal strain contours, showed that material under the indenter is often displaced radially outwards rather than towards the surface as in the rigid die theory. This new mode of deformation is analogous to the expansion of a spherical cavity under an internal pressure. From an expression derived by Hill (1950), Marsh develops an equation relating the quantity P/σ_y to σ_y/E and Poisson's ratio ν.

$$\frac{P}{\sigma_y} = C + KB\text{In}Z \qquad 6.2.3$$

where C and K are constants and B and Z functions of σ_y/E. This theory predicts a lower P/σ_y for high σ_y/E, and at low σ_y/E ratios provides a high value of P/σ_y so that Tabor's relation is applicable. The new hardness theory was applied to a wide range of fully work hardened materials of various σ_y/E ratios. The experimental agreement suggested that the theory might be applied to glasses as most of them lie within the range of σ_y/E values covered. The values predicted on this basis were of the order of 0.05E. Marsh concluded that glasses flow plastically at clearly defined flow stresses which are less than the theoretical cohesive strength of glass so that flow is expected to play a significant part in the fracture process.

The method of obtaining yield stresses from indentation measurements proposed by Marsh is consistent with other observations of deformation in glass. Schlapp (1965) carried out a series of experiments on fibres subjected to high torsional stress. X8 fibres were strained to 3.1% strain for 170 hours and showed no permanent deformation. This places a lower limit of 200 $Kgm.mm^{-2}$ on the flow stress. From indentation hardness measurements the flat rigid die hypothesis predicted a flow stress of 180 $Kgm.mm^{-2}$ corresponding to 2.7% strain. Marsh's theory leads to a value for the flow stress of ~300 $Kgm.mm^{-2}$ (5% strain) which is consistent with the results of these torsion experiments.

Before we examine possible plastic flow theories of fracture we shall review a paper by Westbrook and Jorgensen (1965) who examined the phenomenon of indentation creep, i.e. the gradual increase in indentation size with time at constant load, in a wide range of materials. The authors suggest that the results of their experiments indicated that this creep was due to the presence of two types of water.

Indentation creep had previously been observed by Hargreaves (1928). Correlations have been established for metals between the time dependence of indentation creep over short periods and the delayed strain observed in conventional tests which involved many hundreds of hours. Westbrook and Jorgensen examined indentation creep in a wide range of materials: metals, oxides, alkali halides, covalent and metallic compounds. Indentations were carried out on single crystals of greater than 99.9% purity. Using a Vickers pyramidal indenter, times of loading were varied

between 2 and 200 seconds, and the load dependence was examined up to 200 gm., although cracking could generally be observed for loads greater than 100 gm. Three types of test were undertaken: in air, under toluene after a desorption treatment, and finally after swabbing with water. Indentation creep was observed in all but two materials, both metallic, when water was present but was not observed in a dry environment Indentation creep could, however, be produced in dry materials under toluene by bubbling a moist gas through the toluene across the surface of the material under test.

An examination of the load dependence of the hardness number revealed that for small loads, and therefore shallow impressions, the hardness in air was significantly lower than that measured under toluene, but gradually increased with depth until the values for air and toluene were approximately equal for depths greater than about 1.5μ (1.5×10^{-4} Å). Temperature tests indicated that indentation creep was marked at subnormal temperatures but disappeared at about 60°C. It was suggested that not only does increasing the temperature desorb the water, but that this desorption process is a predominant one, and not the mobility of the water molecules. Desorption at temperatures ranging from 25°C to 400°C showed that although indentation creep was removed by desorption at 50°C, a temperature of 200°C was required to eliminate the effect of water on the hardness level. Westbrook and Jorgensen suppose that this implies the presence of two types of water: strongly bound water, and a more mobile species whose proportion increases as the total amount of water present increases.

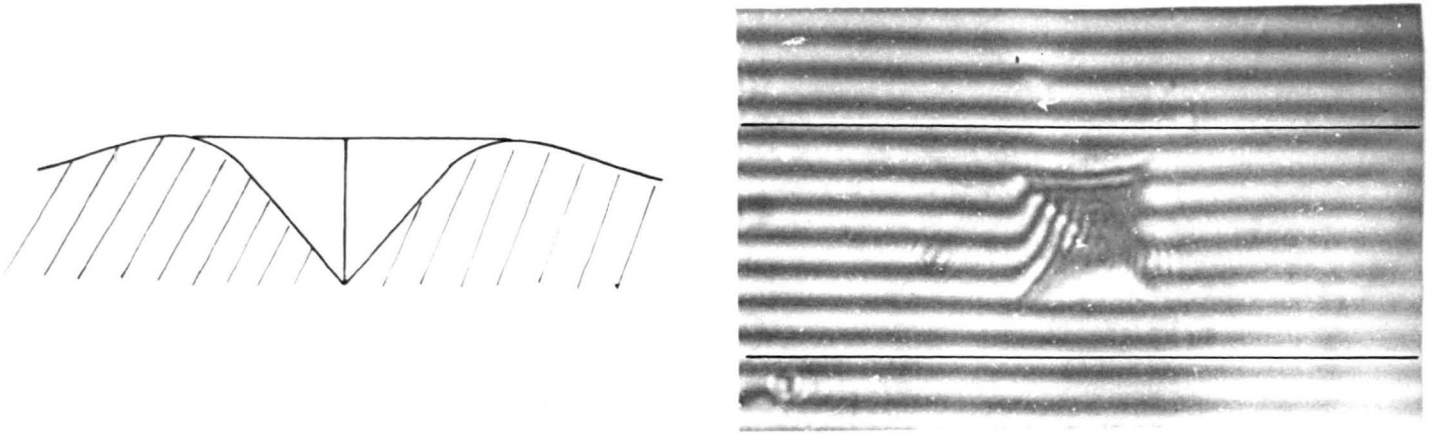

Fig. 46A

Vicker diamond indentation in 'Float' plate glass, showing schematic representation of "shoulders" and interference fringes on typical indentation. Note fringe spacing changes.

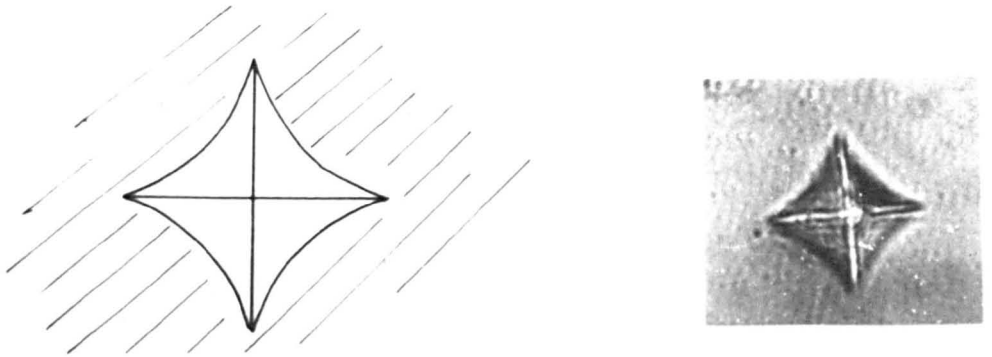

Fig. 46B

Schematic diagram and photograph of an indentation illustrating "bowing"

The use of diamond pyramid indentation measurements to produce a value for the yield stress in glass is subject to a number of difficulties. In a series of preliminary experiments carried out in conjunction with the present cleavage studies, it was observed that careful examination of the impression often revealed cracking at points on the perimeter of the impression even after very light loading (~ 10 gm). Even when cracks were not visible on the specimen they could invariably be seen after a light etch in very weak HF solution. The visibility of the cracks increased with time without etching and they appear to extend under and parallel to the surface. By striking interference fringes across the impression it may be shown that there are "shoulders" (Fig. 46A) to the impression which, although slight, extend over large distances compared with the size of the impression; the fringes only become parallel some distance from the impression. Marsh (1963) in deciding that a different mode of deformation took place in glass from that in metals, considered the disappearance of "shoulders" to contribute significant evidence. The effect of cracking on the measured flow stress may not be significant. It has been observed (Marsh 1963) that the bowing of the sides of the impression (Fig. 46B) is an elastic effect of unloading. It is possible that this might produce cracking; that is, the cracks are formed during unloading, and if so the cracking is unlikely to have a major effect on the hardness figures although it may affect the size of the impression slightly.

In summary, it is apparent that plastic deformation under certain circumstances may be observed in glass. Diamond pyramid indentations constitute the most significant piece of evidence. Although nothing is

known of the mechanism involved in the formation of the indentation, which may involve compaction and/or other mechanisms, it is clearly identifiable as a manifestation of a flow phenomenon. Assuming that indentations are due to flow and if fracture involves a flow process, then the high fracture energies are explicable in principle in terms of an irreversible work process. It is highly significant that the time dependence of hardness can be identified with static fatigue. Marsh (1964) suggested that fracture occurs at the flow stress and so the fall of the breaking stress in time observed in delayed fracture is related to the decreasing flow stress, and we would suggest with the observed fall of the fracture energy associated with creep. In attempting a correlation between fracture and flow, it is interesting to note that the time dependence of both processes appears, at least in part, to be due to the influence of water. Phenomenologically it seems possible to separate two effects due to water: an instantaneous reduction in the value of fracture energy (Chapter IV) or hardness (Westbrook and Jorgensen 1965) as well as an effect in terms of creep. It was felt that this provides further evidence to justify the search for quantitative correlations between fracture and flow. Finally, from the indentation experiments described above, we note that Westbrook's experiments (1960) indicated that the hardness of a typical soda-lime-silica glass changed by a factor of two in going from $+200^{\circ}C$ to $-200^{\circ}C$. A corresponding change was not observed in the fracture energy γ (Chapter IV). This might suggest that a simple direct correlation between flow stress, as measured by diamond pyramid hardness, and fracture

energy is not possible. However, Westbrook did not examine the effect of temperature on the indentation creep rate, so that the change in hardness observed could be due in part or entirely to a change in creep rate, and the results of Westbrook's experiments do not necessarily imply that the instantaneous flow stress varies with temperature. The correlations which do exist, however, were sufficient to prompt us to examine possible flow theories of fracture.

6.3 Plastic flow theories of fracture

The interpretation of the work of fracture as the energy of a process involving plastic work is not a new one; in Chapter I we discussed an interpretation due to Cottrell (1964). Suppose that plastic flow occurs in the material just ahead of the crack so that as the crack propagates the material in the tip will flow in turn - a small zone of plastic flow advances in front of the crack. It is expected that the work done on the plastic zone would be $\sim \sigma_y \alpha$ per unit area, where σ_y is the flow stress and α the plastic extension in the zone. The main problem with a flow process of fracture is obvious. From normal elastic plastic theory we expect that once flow starts at a crack or a notch, the plastically deformed zone will continue to expand until the whole cross-section of the specimen becomes plastic and then separates when there has been a 100% reduction in area at the neck. It is necessary to postulate a mechanism to terminate the plastic flow by fracture. Fracture criteria have been suggested which involve either critical stresses or critical strains. In the absence of

work hardening, the flow stress is normally constant and so within a plastic zone the stress is predetermined, and it would seem necessary to postulate a critical strain criterion for fracture. Cottrell (1964) proposed a critical strain criterion as being generally applicable to fracture and Wells (1963) showed that a critical crack opening displacement (which is equivalent to a critical value of plastic extension) was uniquely responsible for the initiation of brittle fracture in mild steel.

Any criterion which we adopt to describe fracture in glass must satisfy the general experimental observations. It has been clearly established that γ_o for a given environment is a constant independent of specimen dimensions or crack lengths. However, the fracture energy calculated at any given time during creep, γ_T, has been shown to depend both on the specimen size and the initial crack length. It is these two conditions in particular which allow us to discriminate between the two possible elementary flow criteria for fracture in glass.

The adoption of a critical extension α_c as a criterion for fracture has been shown (Chapter V) to be inconsistent with the conditions described above. The theory equates the fracture energy γ to $\sigma_y \alpha_c/2$ and creep is then associated with a change in σ_y with time. This predicts that the fracture energy during creep should be a function of time only, independent of the specimen and crack dimensions, which is not in accord with the experimental observations (Chapter V).

6.4 A critical plastic zone size criterion

As a critical extension criterion for termination of plastic flow ahead of the crack was found to be incompatible with experiment, it was necessary to examine other likely criteria. McLintock (1958) used a critical plastic zone size, R_c, as a criterion for fracture in some ductile metal alloys. Marsh (1964) has suggested that this criterion might be applied to fracture in glass. A number of suggestions have been made to the effect that glasses may consist of hard ordered regions about 20 - 100Å in size, separated by softer disordered regions. Tilton (1957, 1960) postulated the vitron concept of pentagonal ring structures for glass, the units of substructure being approximately 20Å in size. This is in accord with the neutron diffraction experiments of Milligan, Levy and Peterson (1951) and the electron microscopy observations of Warshaw (1960), Zarzycki and Mezard (1962). It is imagined that plastic flow takes place ahead of the crack involving movement of the substructure until large and incompatible strains are set up in the softer material which lead to fracture. Such a theory would require that the plastic zone size was of the same order as the units of substructure, say 50 - 1000Å.

We will adopt a critical plastic zone size as our criterion for fracture, and since the plastic zone size, R, is directly related to the extension α we may again express the fracture energy as: $\gamma = \sigma_y \alpha'/2$. The important distinction between this hypothesis and the critical extension hypothesis is that the extension at fracture, α', is determined both by the critical plastic zone size R_c and the yield stress σ_y. A qualitative

examination of the expression for γ reveals that we might expect, in terms of our model, two different kinds of effect on γ: a change in R_c with environment, and a change in the yield stress σ_y with time or environment. Creep is then explicable as a fall in the yield stress in time or as a reduction of R_c which may not be instantaneous in environments where the reactant is scarce.

Apart from the primary problems there are a number of subsidiary problems associated with the formulation and development of this hypothesis. The stresses at the tip of a cleavage crack are not calculable so that in developing this model we have been forced to use a self consistency argument to determine the dependence of the stresses at the tip on specimen size. We shall develop the critical plastic zone size hypothesis utilising an analysis due to Wells (1963) for plastic zone relationships, and applying this to cleavage fracture. By including the results of Marsh (1963) on the variation of the flow stress of glass with time, an expression for the crack growth in cleavage creep is derived. Finally a quantitative comparison with the experimental results is attempted.

The criterion for termination of plastic flow ahead of the crack is taken to be the attainment of a critical zone size, R_c. In order to develop an expression for the plastic zone size it is necessary to make a number of assumptions about the values of the stresses at the crack tip. By analogy with Inglis' expression for the stress at a crack tip under a tensile applied load, we suppose that the maximum stress at the crack tip normal to the plane of the crack is $\beta/\rho^{\frac{1}{2}}$ where ρ is the radius of the tip. We expect β to depend on the cleavage force F, the crack

length L_o and the beam dimensions. Applying the analysis due to Neuber (1937) for the stresses around the tip of a crack in an elastic-plastic material under uniform tension, the expression for the average stress across a plastic zone may be written:

$$\bar{\sigma} = \frac{1}{R}\int_{o}^{R} \sigma dR \qquad 6.4.1$$

and by analogy for the plastic zone at the tip of a cleavage crack

$$R\sigma_y = \int_{o}^{R} \beta g(r)dr \qquad 6.4.2$$

where $\beta g(r)$ is the normal stress at a point on the plane of the crack a distance r from the effective crack tip (L + R) into the material. Guernsey and Gilman (1959) from their photoelastic studies of the stress distribution around a cleavage crack concluded that at some distance from the tip the distribution was the same as for a crack under tension. Irwin (1957) developed an expression for the stress distribution around a notch under tension:-

$$\sigma(r) = \frac{k}{\sqrt{r}} \qquad 6.4.3$$

where $k = \frac{\sigma c^{\frac{1}{2}}}{\sqrt{2}}$ and c is the crack or notch length.

Thus the tensile and cleavage distributions to a first approximation are similar and it follows that

$$g(r) \propto \frac{1}{\sqrt{r}} \qquad 6.4.4$$

and

$$R\sigma_y = \int_0^R n \frac{\beta}{\sqrt{r}}\, dr \qquad 6.4.5$$

where n is a constant.

Integrating

$$R\sigma_y = 2n\beta R^{\frac{1}{2}} \qquad 6.4.6$$

or

$$R = \frac{4\beta^2 n^2}{\sigma_y^2} \qquad 6.4.7$$

Since $\sigma(r)$ seems to vary in the same way in the two stress situations, cleavage and tensile, we might expect the expressions for the plastic extension, α, in the zone, and for the zone size, 2R, to be similar. From Wells (1963) for the tensile case

$$\alpha = \frac{4\sigma^2 c}{E\sigma_y} \qquad 6.4.8$$

and

$$R = \frac{\sigma^2 c}{2\sigma_y^2} \qquad 6.4.9$$

where σ is the applied stress, c the crack depth and σ_y the yield stress. Combining the two expressions, we may write

$$\alpha = \frac{8R\sigma_y}{E} \qquad \text{for tension} \qquad 6.4.10$$

In view of the similarity of the forms of the equations, we shall assume that for the cleavage case the equation may be expressed as

$$\alpha \propto \frac{8R\sigma_y}{E} \qquad \text{or} \qquad \alpha = \phi.\frac{8R\sigma_y}{E} \qquad 6.4.11$$

where ϕ is a numerical constant. Although no doubt the cleavage and tensile cases are not exactly equivalent, in the subsequent calculations we shall assume that $\phi \approx 1$. We are then, of course, restricted to

calculations in terms of orders of magnitude rather than accurate evaluations.

Now $$\gamma_o = \tfrac{1}{2}.\alpha'\sigma_y \qquad 6.4.12$$

where α' is the plastic extension corresponding to the critical zone size given by the fracture criterion we have adopted, $R = R_c$.

Unlike the tensile case, in cleavage the stresses at the tip are not calculable, and we do not know how β in equation 6.4.7 above, varies with the cleavage parameters. In order to evaluate β and derive an expression for R_c we suppose that

$$\beta \propto F.f \text{ (beam dimensions)}$$

and by using a self consistency argument determine the possible form of f.

Thus $$R = \frac{F^2 f^2 (\text{beam dimensions})}{2\sigma_y^{\,2}}$$

and $$R_c = \frac{F_c^{\,2}(f)^2}{2\sigma_y^{\,2}} \qquad 6.4.13$$

if $F = F_c$ the critical force to extend the crack.

Now $$\gamma = \frac{F_c^{\,2} L_o^{\,2}}{2EI} \qquad 6.4.14$$

which we have determined experimentally to be a constant independent of beam dimensions, and

$$F_c^{\,2} = \frac{2\sigma_y^{\,2} R_c}{(f)^2} \qquad \text{from equation 6.4.13}$$

Combining these expressions,

$$\gamma_o = \frac{2L_o^{\,2} R_c \sigma_y^{\,2}}{2EI\,(f)^2} = \text{constant} \qquad 6.4.15$$

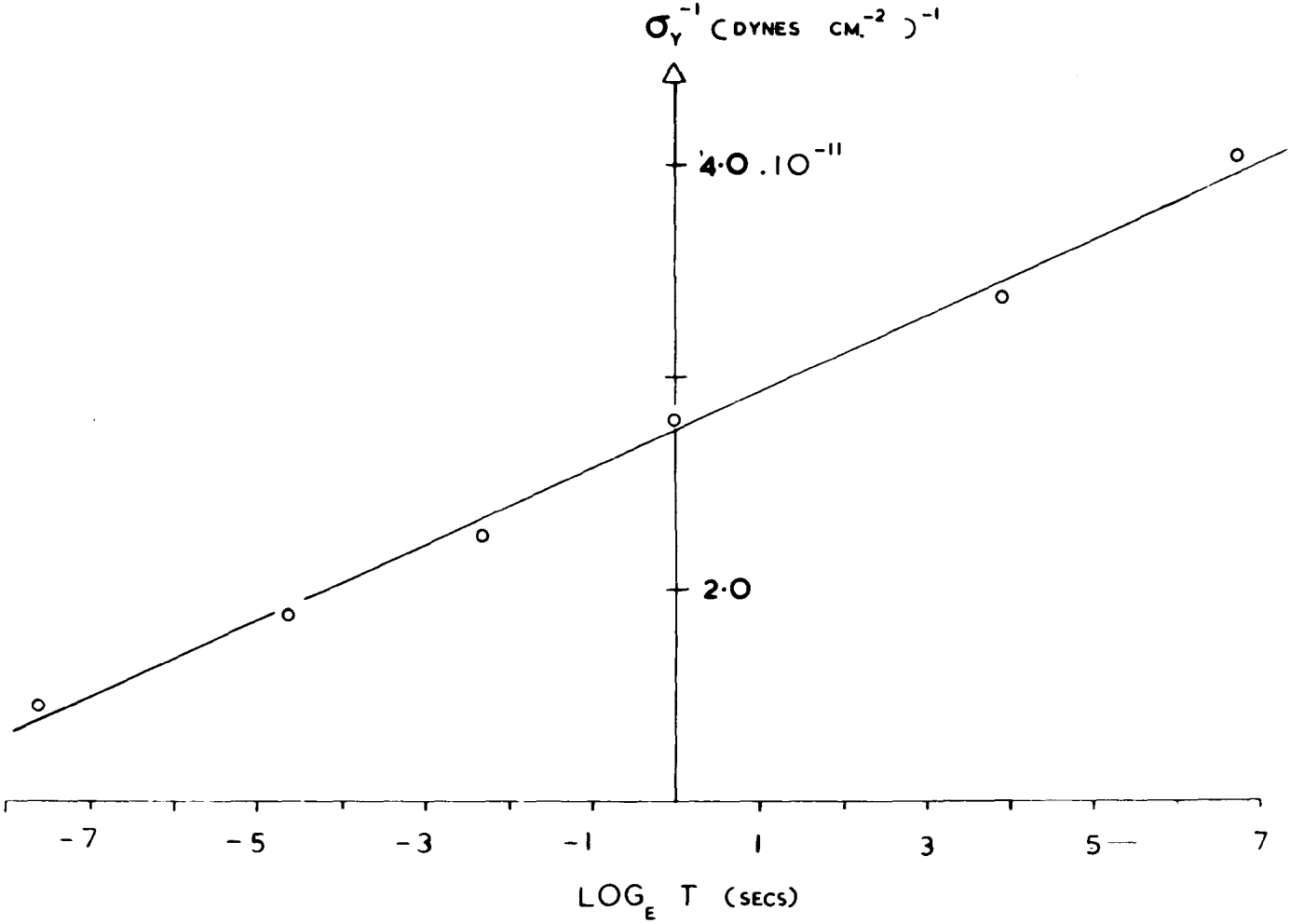

Fig. 47

The variation of yield stress with time. Replot of data obtained by Marsh (1964)

In this expression σ_y is a constant (at t = 0) and R_c and E are assumed constant, so that it must follow that

$$\frac{L_o^2}{I(f)^2} \text{ is a constant } = A \qquad 6.4.16$$

Rearranging

$$(f)^2 = \frac{L_o^2}{IA} \qquad 6.4.17$$

Whence

$$R = \frac{F^2L^2}{2\sigma_y^2 IA} \qquad 6.4.18$$

We have assumed a critical plastic zone size to be the appropriate criterion for cleavage fracture and have derived an expression relating the plastic zone size to the cleavage parameters. In order to examine the relationship between these parameters and time, predicted by our hypothesis we assume that the crack velocity is determined by the rate at which the zone ahead of the crack reaches its critical value,

i.e.

$$\frac{dL}{dt} = \frac{R_c}{T_c} \qquad 6.4.19$$

where T_c is the time interval taken for the zone ahead of a crack of length L to reach the critical size, R_c. The flow stresses reported by Marsh (1964) are shown in Fig. 47, replotted in a logarithmic form. From this figure we deduce that the yield stress of soda-lime-silica glass is related to time by the equation:

$$1/\sigma_y = k \log_c t + c \qquad 6.4.20$$

Substituting the expression for σ_y in equation 6.4.18 above, gives:

$$R = \frac{F^2L^2}{2IA}(k\ln t + c)^2 \qquad 6.4.21$$

and by writing

$$c = k\ln B \qquad 6.4.22$$

$$R = \frac{F^2L^2}{2IA}(k\ln Bt)^2 \qquad 6.4.23$$

Rearranging

$$\ln Bt = \frac{\sqrt{2}I^{\frac{1}{2}}A^{\frac{1}{2}}R^{\frac{1}{2}}}{FLk} \qquad 6.4.24$$

Thus,

$$t_c = \frac{1}{B}\exp\left(\frac{\sqrt{2}I^{\frac{1}{2}}A^{\frac{1}{2}}R_c^{\frac{1}{2}}}{FLk}\right. \qquad 6.4.25$$

And if

$$\frac{dL}{dt} = \frac{R_c}{t_c} \qquad 6.4.19$$

then the crack velocity, V, is given by

$$V = BR_c \exp -\left(\frac{\sqrt{2}I^{\frac{1}{2}}A^{\frac{1}{2}}R_c^{\frac{1}{2}}}{FLk}\right) \qquad 6.4.26$$

We note that this expression satisfies the requirements mentioned earlier: a constant γ_o is a condition already inserted into the derivation of equation 6.4.26, but the expression does predict a creep rate and thus total creep growth dependent on the value of L_o and the beam dimensions.

6.5 Experimental examination of the critical plastic zone size hypothesis

We have derived an expression relating the velocity of the cleavage crack to the time of propagation and the cleavage parameters. The crack length can only be obtained from this expression as a definite integral. As the predictions of the hypothesis can be evaluated from the original velocity equation, and the velocity is extracted from crack length - time curves originally, there seemed little to be gained in attempting this

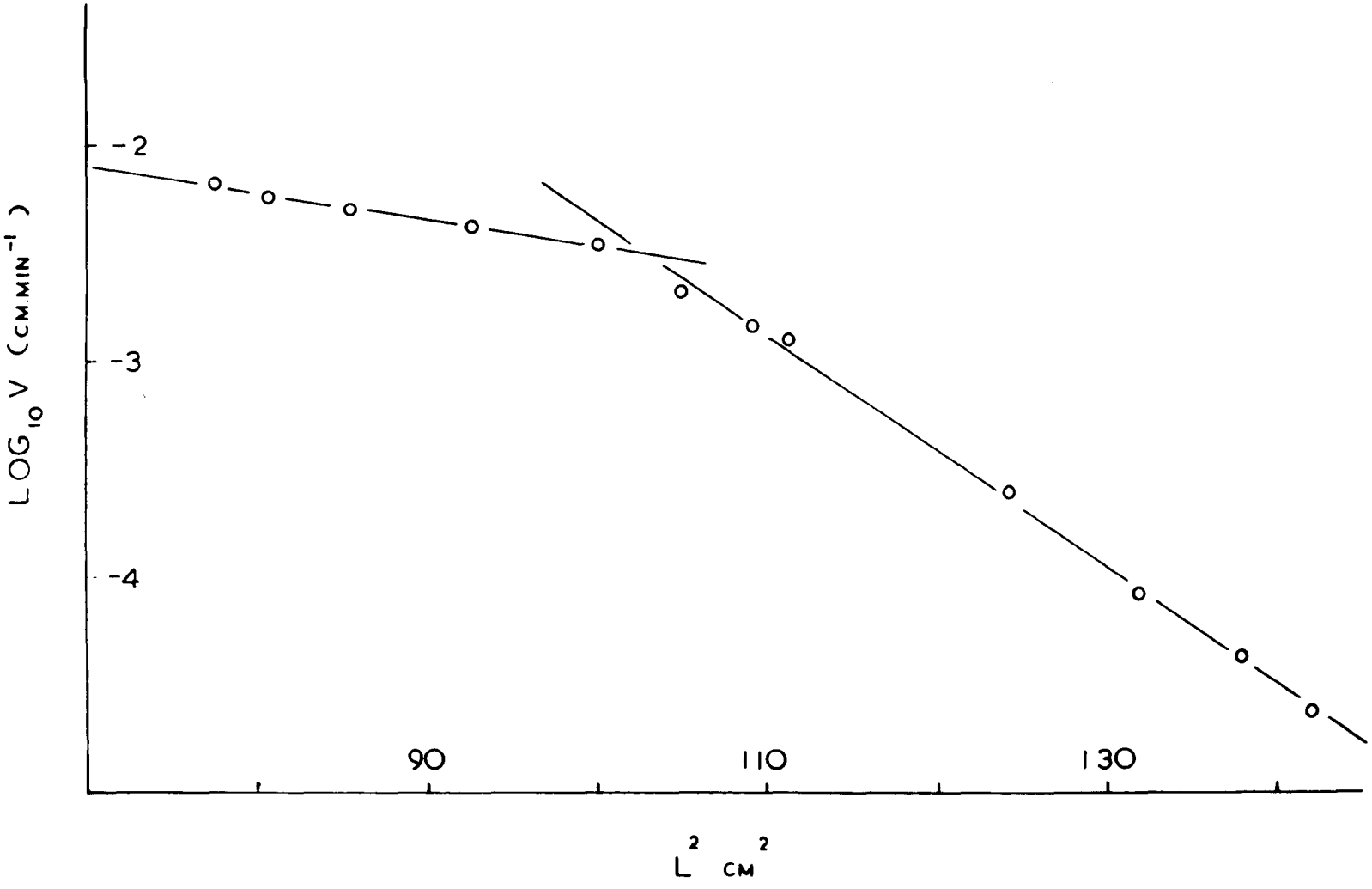

Fig. 48A

Creep data for typical 'Float' glass specimen cleaved in air at constant deflection (0-60mins)

integration, so that the quantitative examination of the hypothesis will be restricted to velocity relationships. Unfortunately we are limited to a small range of crack lengths even though it is possible to record changes of several orders of magnitude in the crack velocity and so our interpretations are once again subject to the difficulties, previously described, which are inherent in the cleavage creep.

From equation 6.4.26 we have

$$\log_c V = \log_c BR_c - \frac{\sqrt{2}I^{\frac{1}{2}}A^{\frac{1}{2}}R_c^{\frac{1}{2}}}{K} \cdot \frac{1}{FL} \qquad 6.5.1$$

Now FL = M, the bending moment at the crack tip, so that a plot of log V versus M^{-1} should give a straight line of intercept log BR_c and slope $(\frac{\sqrt{2}I^{\frac{1}{2}}A^{\frac{1}{2}}R_c^{\frac{1}{2}}}{K})$. It is expected that this relationship should hold both for conditions in which the crack displacement (2δ) is constant, and for those in which the cleavage force is constant.

At constant Force

$$\log V = \log BR_c - \frac{\sqrt{2}A^{\frac{1}{2}}I^{\frac{1}{2}}R_c^{\frac{1}{2}}}{KF} \cdot \frac{1}{L} \qquad 6.5.1$$

$$= \log BR_c - \overline{K}_f \cdot \frac{1}{L} \qquad 6.5.2$$

while at constant displacement,

$$\log V = \log(BR_c) - \frac{\sqrt{2}A^{\frac{1}{2}}R_c^{\frac{1}{2}}}{3KEI^{\frac{1}{2}}\delta} \cdot L^2 \qquad 6.5.3$$

$$= \log(BR_c) - \overline{K}_\delta \cdot L^2 \qquad 6.5.4$$

where $\overline{K}_f$ and $\overline{K}_\delta$ are expected to be independent of time and crack length.

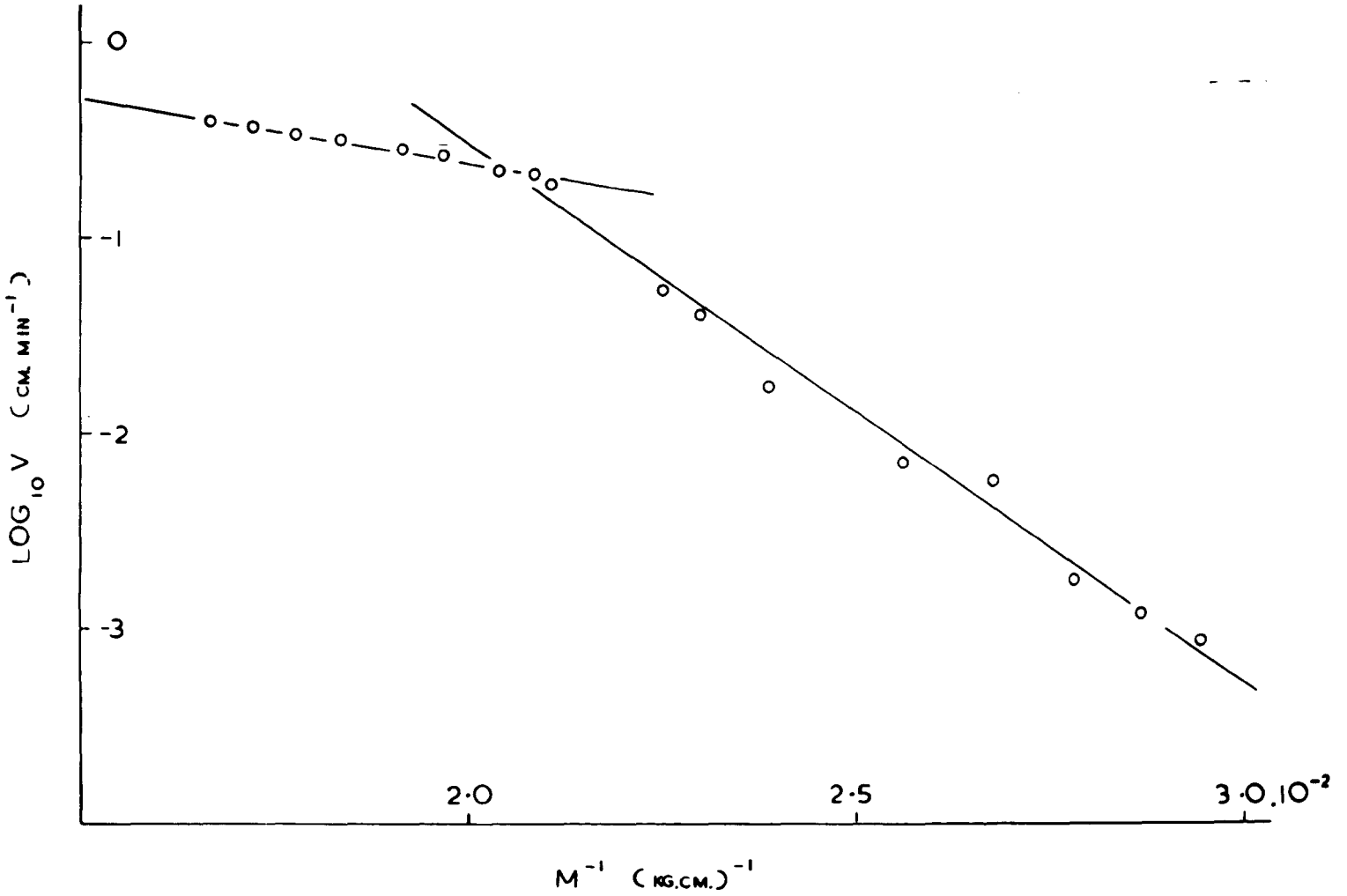

Fig. 48B

Creep for typical 'Float' glass specimen cleaved in air under constant load

From equation 6.4.26 we can predict that the crack velocity will increase as the crack extends under a constant cleavage force, but when the crack displacement is fixed the crack velocity will fall as the crack length increases; both effects are, in fact, experimentally observed features of cleavage creep. Figs. 48A and B establish the equivalence of creep in air under conditions of constant force and constant deflection. Equations 6.5.1 and 6.5.3 predict that the ratio of the slopes of these plots, $S_F : S_\delta$ is equal to $\overline{K}_F : K_\delta = \frac{3EI\delta}{F}$ for a particular specimen. This prediction, however, involves two rather basic assumptions. First we have assumed that the constant A, which is related to the stress distribution around the tip, and the critical plastic zone size R_c, are the same under the different conditions. Secondly we have assumed that our hypothesis accurately describes the creep process.

The value of the constant ($3EI\delta/F$) calculated from cleavage data gathered from the same specimen was 9.0×10^9 units and experimentally the ratio of $S_f : S_\delta$ was observed to be 8.4×10^9 units, showing reasonable agreement and justifying our assumptions.

The effect of environment on the cleavage creep is illustrated in Figs. 49 and 50, which show that a single relationship appears to hold in water, but that two lines are obtained in dry nitrogen as was observed in air.

Equation 6.5.3 predicts that $\overline{K}_\delta$ obtained from a plot of Log V versus L^2 should vary as $1/b^{3/2}\delta$. Table 11 shows a selection of values of $\overline{K}_\delta Xb^{3/2}\delta$ calculated for specimens of 'Float glass' for creep at constant δ over the range of approximately 6 - 60 minutes.

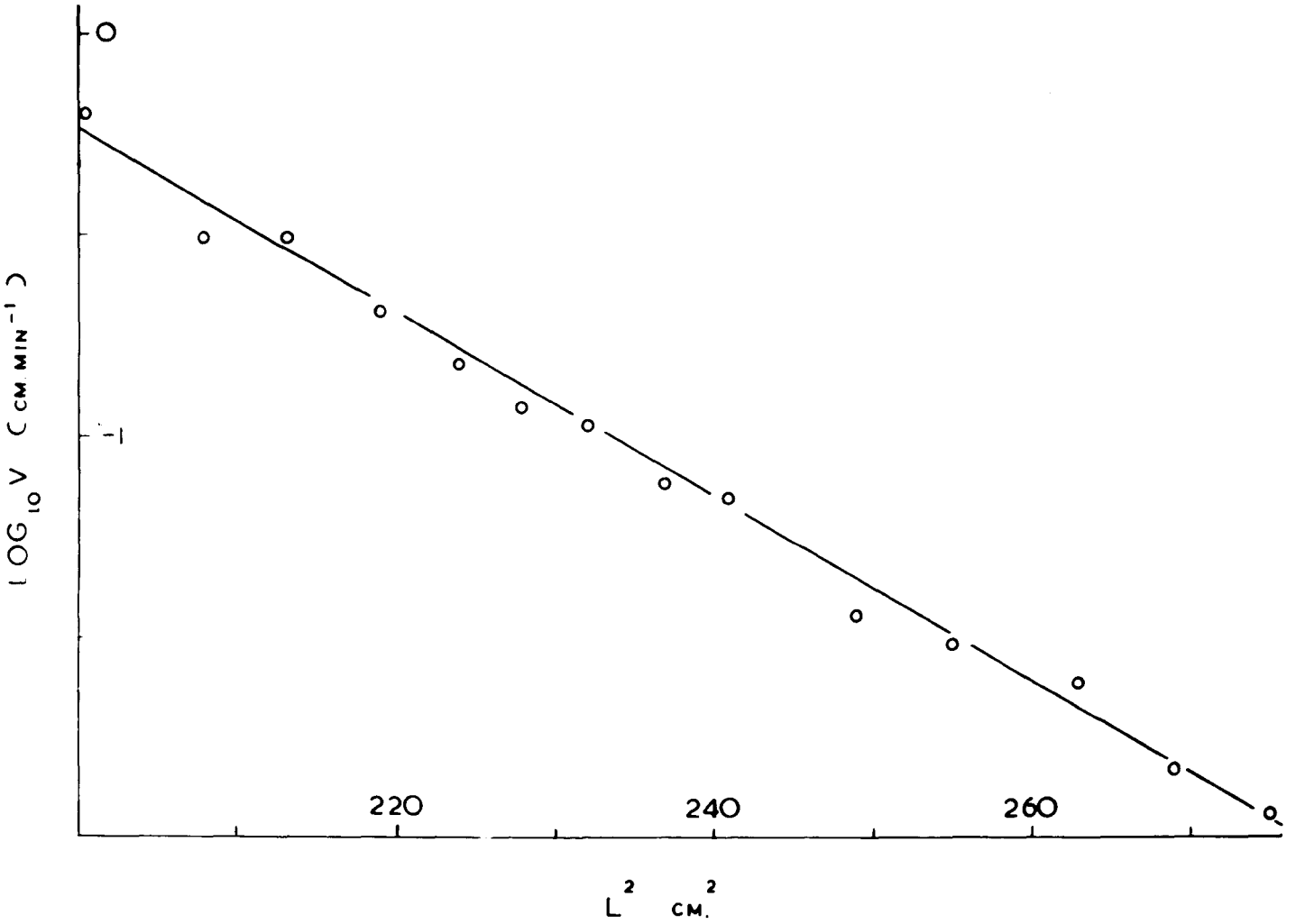

Fig. 49

An example of cleavage creep for 'Float' glass in water (0 - 60mins)

TABLE 11

$\overline{K}_\delta$ values for 'Float' glass

$\overline{K}_\delta$	b.cm	$\overline{K}_\delta \times b^{3/2}\delta$
	Air	
0.0084	3.90	0.259
0.0304	2.82	0.252
0.0330	1.45	0.264
0.0390	2.20	0.254
0.0192	2.91	0.309
	Water	
0.0280	1.83	0.350
0.0520	1.41	0.392
0.0160	3.25	0.375
0.0230	2.50	0.431

Mean values : $\overline{K}_\delta / b^{3/2}\delta$	
Air	0.267
Water	0.387
Dry N_2	0.460

The relationship between creep rate and specimen dimensions as predicted by the critical plastic zone size hypothesis agrees with the experimental results.

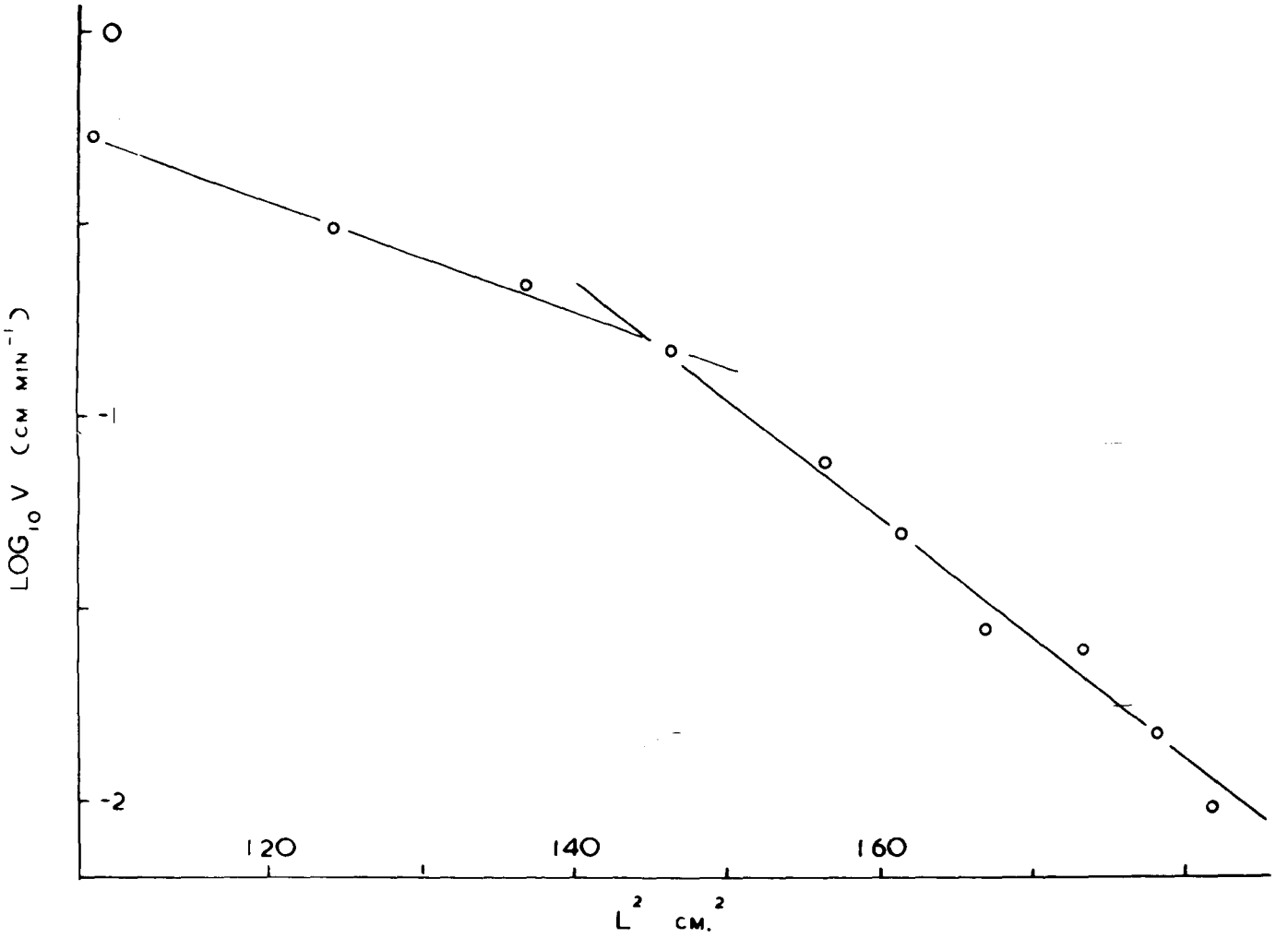

Fig. 50

Creep for 'Float' glass cleaved in dry nitrogen at constant deflection (0 - 25 hours)

The constant $\overline{K}_\delta$ in Table 11 above is $\frac{\sqrt{2}A^{\frac{1}{n}}R_c^{\frac{1}{2}}}{3kEw_2^{\frac{1}{n}}}$, and since A, E and w_2 are constants, by comparing values of $\overline{K}_\delta$ in the different environments we can compare $\frac{R_c}{k^2}$ ratios. Further, if we assume that k, which is related to the rate at which the flow stress falls in time, is the same for the three environments, air, water and dry nitrogen, then

$$\overline{K}_\delta(\text{water}) : \overline{K}_\delta(\text{air}) : \overline{K}_\delta(N_2) = R_c(\text{water}) : R_c(\text{air}) : R_c(N_2)$$

$$= 2 : 1 : 3$$

It is possible to obtain absolute values of R_c from the intercepts of these creep rate curves and also from the values of γ_o.

The fracture energy is related to the flow stress and the plastic extension as

$$\alpha' = \frac{2\gamma_o}{\sigma_y} \qquad 6.4.12$$

Assuming that σ_y is the same for air, water and dry nitrogen at the short times involved in the calculation of γ_o, we can evaluate α'. Taking σ_y as $\sim 3.5 \times 10^{10}$ dynes cm^{-2} (Marsh 1964), α' for air and dry nitrogen is $\sim 25\text{Å}$ and for water $\sim 16\text{Å}$. The corresponding critical plastic zone sizes R_c from equation 6.4.10 are $\sim 80\text{Å}$ and 55Å respectively. From these figures we would expect the ratios of R_c Air : Dry Nitrogen : Water to be 4: 4 : 3.

Finally the intercept on the ordinate (Figs. 48 - 50) from creep curve plots is log BR_c and B is simply $e^{c/k}$ (equation 6.4.23), where c and k are the empirical constants derived from Marsh's data (Fig. 47). The values of R_c obtained this way must be subject to large errors

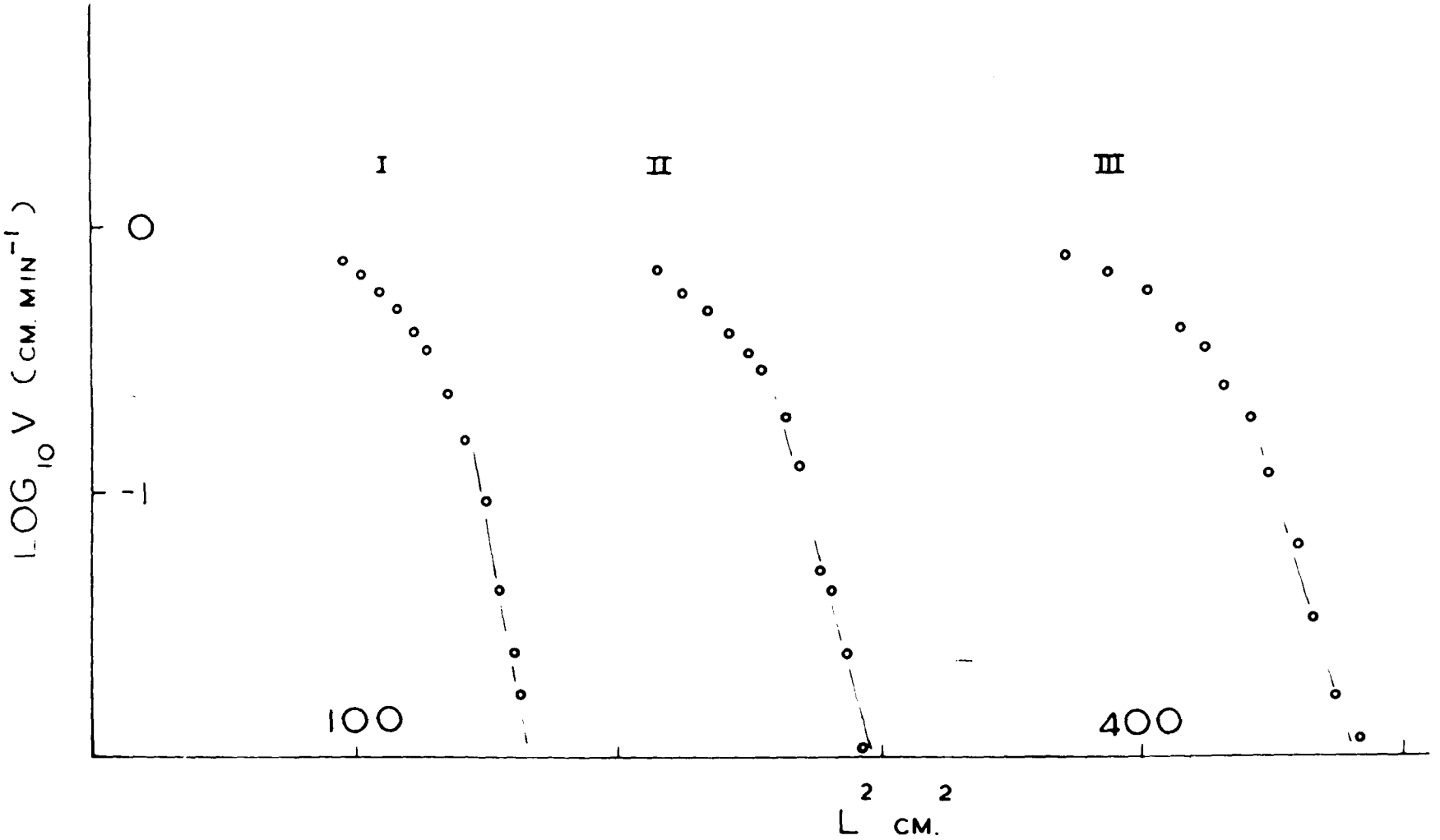

Fig. 51

Creep in air, at three points along the same 'Float' glass specimen

because of the small ranges in crack length involved in the plots and the extent of the extrapolation necessary as well as the uncertainty in the value of B. For air the calculated values ranged between 600Å and 2,700Å with a mean of ~1,400Å. These were calculated from the straight line section of the graphs obtained for lower crack velocities. The average values for dry nitrogen and water were ~6,000Å and 4,000Å respectively and again a large scatter was recorded. The values of R_c calculated from the creep velocity relationships observed at higher velocities in air and dry nitrogen (Figs. 48, 50) were ~1Å.

The values of the critical plastic zone size calculated in three different ways from the experimental data exhibit a certain inconsistency. Calculated from γ_o values, R_c is of the order of 100Å. On the other hand, when it is calculated from the intercepts of the creep curves the value of R_c approaches 10,000Å. The discrepancy is most likely to lie in the intercept calculation, for as we noted earlier, $B = e^{c/k}$ and obviously the quantity is highly sensitive to changes in the empirically observed constants c and k. Perhaps because of the extensive extrapolations required for the not very well defined lines, it is observed that R_c calculated from the intercept varies even for creep observations at different points along the same specimen, often by 25%.

In calculating R_c values from the slopes of the appropriate plots and comparing them for different environments, it was assumed that the constant k did not vary. In view of the experiments of Westbrook and Jorgensen (1965), which suggested that σ_y was dependent on the environment

we must conclude that there is no justification for this assumption. A small change in the rate at which σ_y falls with time might reverse the calculated values of R_c in water and air and remove the discrepancy between these and the ratio of the values of R_c calculated from γ_o.

Figs. 48 and 50 indicate that two stages of creep are evident in air and dry nitrogen: one corresponding to a fast crack movement and the other to a more extensive but slower crack growth. The primary creep observed earlier might be identified with the faster region observed in air (Fig. 48). It is possible that in both air and dry nitrogen, the change in slope reflects a change in the rate determining step in the fracture process. As it is absent in water, we surmise that this may be associated with a corrosion effect due to water. Fig. 51 illustrates that this initial section of the curve is not in fact linear and could perhaps be interpreted as a stage in which the critical plastic zone size is changing.

The straight line plots obtained at the lower velocities are associated with the secondary stage of creep and it is observed that this relationship extends over long periods of time in all environments as is illustrated in Fig. 50. This more extensive stage of creep is thought to be one in which the critical plastic zone size can be regarded as a constant, but the yield stress falls gradually in time.

In summary it is suggested that cleavage creep is explicable in terms of the critical plastic zone size criterion for cleavage fracture. Two stages of creep may be identified; one associated with water and the other with a time dependent yield stress. It is encouraging to note that

not withstanding the assumptions forced upon the hypothesis because of a lack of knowledge of the stress distribution at the crack tip, it is possible to predict a critical plastic zone size which is physically feasible.

6.6 Re-examination of cleavage fracture energies

By postulating a fracture process involving the propagation of a plastic zone ahead of the crack tip, and by adopting a critical plastic zone size as a fracture criterion, it has been possible to relate the phenomenon of creep to the high fracture energies observed. The interpretation of γ as a material constant cannot be strictly correct for a material which undergoes plastic flow in fracturing. To propagate a crack or a notch, it is necessary to satisfy two general conditions: firstly, the free energy released by the fracture must be sufficient to make the fracture propagate; secondly, there must be a mechanism for fracture. Although thermodynamically it may be possible for a blunt crack to extend, unless the conditions at the tip are appropriate to cause fracture of the material the crack will not propagate. If a critical plastic zone size hypothesis is applicable then we should expect γ to be a work of fracture and the Griffith condition as a micro-condition for fracture would not be appropriate: γ would vary with the stress configuration. The difference in γ calculated from tensile and cleavage experiments may be attributable to this distinction.

We have shown that the high work of fracture can be accounted for by a very small plastic distortion which would produce a layer of deformed material on the fracture surface between 10^2 and 10^4 Å thick., assuming an approximately spherical plastic zone. An attempt was made to see if any evidence existed which might verify the presence of such a layer. To this end a number of experiments were attempted in conjunction with other members of the department; these included diamond pyramid indentation experiments and an examination of the e.s.r. iron line for samples taken from fracture and other surfaces; no significant differences have been detected in the experiments carried out to date.

The high fracture energy values (work of fracture) imply that in glass fracture does not proceed by the propagation of an elastic crack. It is an essential characteristic of a true elastic crack that it is stable only under an applied stress of the correct magnitude. If the applied stress is reduced the crack will close up progressively under the then unbalanced attractive forces between the atoms in the opposite faces of the crack near the tip. It was generally observed that when the strain on a partially cleaved specimen was released the crack appeared optically to close up, but on reloading the crack length attained its previous value before the specimen would bear any load. On two occasions, however, one in dry ammonia and the other in dry nitrogen, the crack re-propagated down the specimen only under the application of a finite load. The effective fracture energy for this re-propagation process was approximately 500 ergs cm^{-2} and the reduced plot for both the original cleavage and the

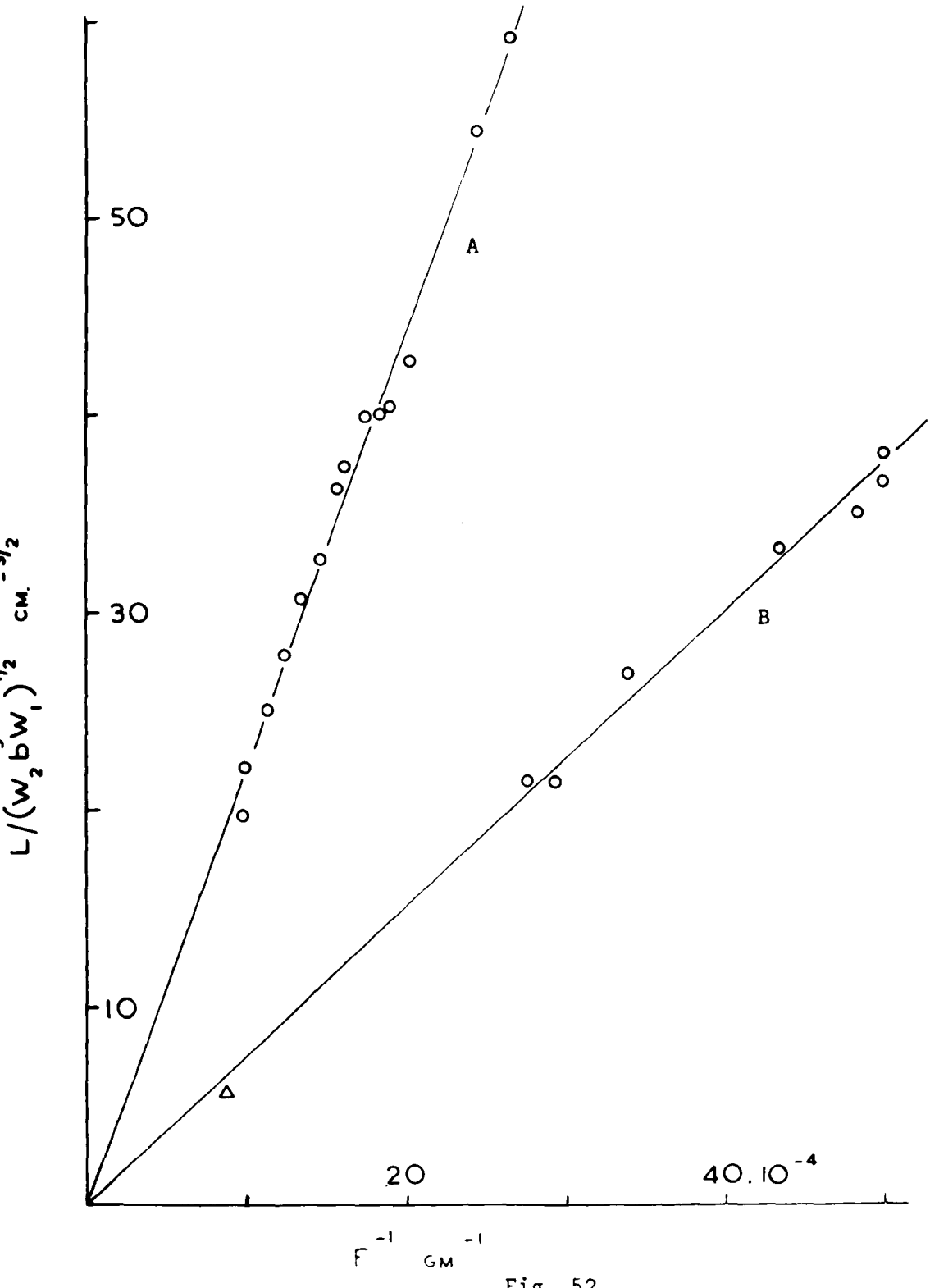

Fig. 52

(A) Cleavage of 'Float' glass and (B) 're-cleavage' of 'Float' glass, in dry nitrogen

re-cleavage is shown in Fig. 52. The single point obtained in ammonia is shown as a triangle. Obreimov (1930) and Bailey (1957) observed a similar effect in cleavage of mica, and Obreimov also recorded a greatly increased fracture energy for mica cleaved in vacuum. Derjaguin et al. (1957) explain the difference in γ values for mica entirely in terms of an electrical effect: when mica is split along a cleavage plane the newly formed surfaces are covered with a mosaic of areas with opposite signs of electrification. It is unlikely that a similar electrical effect could account for the high fracture energies of glass or the closing of the crack in view of the relatively small changes observed between the gaseous or liquid environments and vacuum. It is more likely that this re-propagation phenomenon can be explained in terms of a surface tension or capillary condensation effect.

The variation of γ_o with environment might, according to our fracture hypothesis, be associated with changes either in the flow stress or in the critical plastic zone size. It is unfortunate that effects due to changes in R_c and those due to σ_y cannot be separated by an examination of the cleavage data alone. This is because all the creep relationships involved terms in σ_y and R_c and in order to compare R_c values for two different environments it was necessary to assume that σ_y was independent of environment.

Nevertheless, from our model we may draw a few semi-qualitative conclusions which allow us to distinguish between the two effects in particular circumstances. We have expressed the fracture energy as:

$$\gamma = \tfrac{1}{2}\sigma_y \alpha' \simeq \frac{4R_c\sigma_y^2}{E} \qquad \text{(equations 6.4.10 and 6.4.12)}$$

and the limiting values of the yield stress σ_y at very short and very long times were recorded by Marsh to be in the ratio 16 : 5 ($\sim$ 4 : 1). Experimentally we have observed that for creep in air the ratio $\gamma_{t=o} : \gamma_{t=\infty} \simeq 16$; this suggests that during this process α' decreases by a factor of four, but that to a first approximation creep corresponds to a constant value of the critical plastic zone size R_c when the limits of σ_y are in the ratio of 4 : 1.

The calculation above has indicated that the creep process in air may be attributed solely to a fall in yield stress, the critical plastic zone remaining constant. The variation of γ_o with environment may be associated with either a reduction of R_c or σ_y. Westbrook and Jorgensen (1965) have suggested that for many materials water reduces the instantaneous value of σ_y and also produces a creep process. Until measurements of the indentation creep as a function of environment have been carried out we cannot say with any certainty that R_c varies with environment.

Nothing is known of the structural factors which determine the two fracture parameters R_c and σ_y except that both are expected to be intimately linked to the microstructure. We can, however, make a few general observations as to the important environmental factors which determine the instantaneous changes in R_c (or σ_y) from an examination of the γ_o values. It is interesting to note that water has a striking effect, reducing γ_o to almost half its dry value, and that water seems to be the dominant species even in very dilute HF solutions which would tend

to confirm our conclusions that creep is not an activation limited stress corrosion process; if it were the HF, which is known to be highly corrosive, would be expected to have an increased effect over water.

The reduction of γ_o by ammonia (dry) provides us with some information on the mechanisms of flow and fracture in glass. It is highly significant that water and ammonia, very similar species, have similar effects on γ_o. Water has an atomic weight of 18 and ammonia, 17, and although water is slightly smaller than ammonia, which might account for its greater reactivity, the two molecules have similar steric geometries and dipole moments. It is suggested that if flow and fracture in glass are related to the microscructure, then it is not surprising that the effect of water and ammonia seems to be steric: due to their size and structural geometry.

Finally we note that environments such as silicone oil simply serve to keep the moisture away from the fracture, although it is well known that glass contains a certain amount of intrinsic water.

6.7 Summary and suggestions for further work

The work described in this thesis has been principally an examination of cleavage fracture in 'Float' glass. Measurements were also made on polymethylmethacrylate and Pyrex plate glass which served as comparisons.

The cleavage technique was shown to be preferable to other methods of measuring the fracture energy of a material. It was observed that the instantaneous value of the fracture energy was independent of specimen

size but varied with environment. The fracture energy was highest in vacuum and lowest in water, but was reduced in any environment containing water. Although it was possible to discern a difference in γ due to the composition of the glass, the temperature seemed to have little effect.

In order to interpret more fully the high values of fracture energy and the variation with environment, an examination of the extended crack growth was carried out. Phenomenologically this creep appeared to exist in two stages; a primary stage which was environment dependent and a secondary stage essentially independent of environment. It was suggested that creep could only be explained as a reduction of the energy necessary to propagate the crack and following some observations of diamond pyramid hardness by Marsh (1964) and Westbrook and Jorgensen (1965) a plastic flow theory of fracture was developed. A critical plastic zone size criterion for fracture was not inconsistent with experiment, but in developing this hypothesis quantitatively, it was necessary to adopt a self-consistency argument to determine the stresses at the cleavage crack. The experimentally determined variation of yield stress with time (Marsh 1964) was incorporated into the development of our hypothesis and the predictions were observed to agree tolerably well with experiment. The interpretations of the results utilising our hypothesis suggested that two stages of creep in 'Float' glass are possible. In general terms it would appear that the idea of stress corrosion as an explanation of the primary creep is not unacceptable; the apparent lack of thermal activation may be explicable in terms of a transport limited process. The secondary creep which is observed in all

environments is extensive and is accounted for as a slow reduction of the yield stress in time. It is this process which may be correlated with the delayed fracture of glass which is observed even in liquid nitrogen. The more detailed predictions of this theory suggested that a plastic zone size of 10^{4}Å might exist and that we might expect an appreciable plastically deformed layer to cover the fracture surface, although the author failed to detect such a layer.

The subsidiary problems associated with this fracture hypothesis form the areas in which further work is most urgently required. It is felt that the hypothesis itself is basically sound. Few indications of the flow mechanisms can be drawn from the hypothesis and its predictions. To understand the form of the flow and the nature of the limiting processes which determine the critical value of the zone size requires a knowledge of the micro-structure particularly in the 20 - 100Å range. It is exciting to record that it is at this level that the present microscopists are working and within a few years it may be possible to formulate a structure for glass.

A solution of the stress distribution around a cleavage crack would eliminate a major ambiguity which surrounds the equations for the velocity of the creeping crack derived above. A detailed examination of cleavage in birefringent materials might provide a solution for the maximum stress at the tip of the cleavage crack. Until this theoretical problem has been solved a critical test of our hypothesis is impossible and the proposed model must ultimately be regarded as empirical and tentative.

One final problem associated with the hypothesis is the microscopic measurement of flow and the conversion of the diamond pyramid indentation figures to flow stresses. It is felt that the study of the time and environment dependence of glass would prove most informative, and the examination of the possibility of work hardening in glass essential!

REFERENCES

Ainsworth, L., 1954, J. Soc. Glass Tech., 38, 479.

Auerbach, F., 1902, H. Horestadt "Jena Glass".

Bailey, A.I., 1957, Proc. IInd Int. Congr. of Surface Activity, p.406, III Electrical phenomena of Solid/Liquid Interfaces.

Balodis, V., 1963, Aust. J. Appl. Sci., 14, 284.

Barrenblatt, G.I., 1962, Adv. Appl. Mech., 7, 109.

Benbow, J.J., 1961, Proc. Phys. Soc. (Lond.), 78, 970.

Benbow, J.J. and Roesler, F.C., 1956, Proc. Phys. Soc. (Lond.), 70, 201.

Berry, J.P., 1960, Nature, 185, 91.

Berry, J.P., 1961, J. Poly. Sci., 50, 107.

Berry, J.P., 1962, J. Appl. Phys., 33, 1741.

Berry, J.P., 1963, J. Appl. Phys., 34, 62.

Berry, J.P., 1964, J. Poly. Sci., Vol. 2.

Biggs, W.D. and Pratt, P.L., 1958, Acta. Met., 6, 694.

Bilby, B.A., Cottrell, A.M., and Swindon, K.H., 1963, Proc. Roy. Soc. A 272, 304.

Brearley, W., Hastilow, P.A.P. and Holloway, D.G., 1962, Phys. Chem. of Glasses, 3, 181.

Broutman, L.J. and McGarry, F.J., 1965, J. Appl. Polymer Sci., 9, 589.

Bruche, E. and Poppa, H., 1956, Proc. of the Stockholm Conf. on Electron Microscopy.

Bruche, E. and Schimmel, G., 1954, Proc. of IIIrd Intern. Conf. on Electron Microscopy (London).

Burgers, J.M., 1939, Proc. Kon. Ned. Akad. Wet., 42, 293, 378.

Charles, R.J., 1958, J. Appl, Phys., 29, 224.

Charles, R.J., 1961, Proc. in Ceram. Science, Vol. I, Pergamon Press (New York) p. 1-38.

Charles, R.J. and Hillig, W.B., 1961, Symposium on the Mechanical Strength of Glass and Ways of Improving It, Union Scientifique Continentale du Verre.

Clarke, F.J.P., Tattersall, H.G. and Tappin, G., 1966, Proc. Brit. Ceram. Soc., No. 6, 163.

Cottrell, A.H., 1964, Proc. Roy. Soc. A. 282, 2.

Culf, C.J., 1957, Trans. Soc. Glass Tech., 41, 157.

Dalladay, A.J. and Twyman, F., 1921, Trans. Opt. Soc., 23, 165.

Derjaguin, B.V. et al., 1957, Proc. of IInd Intern. Congr. of Surface Activity, III Electrical phenomena of Solid/Liquid Interface.

Dimmick, H.M., 1951, J. Soc. Glass Tech., 35, 318.

Douglas, R.W., 1958, J. Soc. Glass Tech., 42, 145.

Elliot, H.A., 1958, J. Appl. Phys., 29, 224.

Galileo Galilei, 1638, 'Two New Sciences' (English Translation, McMillan, New York 1933).

Gehloff, G. and Thomas, M., 1926, Z. Tech. Phys., 7, 105.

Gillis, P.P. and Gilman, J.J., 1964, J. Appl. Phys., 35, 647.

Gilman, J.J., 1959, Proc. Intern. Conf. on Mechanisms of Fracture, Swampscott, Mass. U.S.A. (Eds. B.L. Averbach et al.) p. 193, Wiley, New York.

Gilman, J.J., 1960, J. Appl. Phys., 31, 2208.

Gilman, J.J., Knudsen, C. and Walsh, W.P., 1958, J. Appl. Phys., 29, 601.

Griffith, A.A., 1920, Phil. Trans. Roy. Soc., A 221, 163.

Griffith, A.A., 1924, Proc. of Ist Intern. Congr. of Appl. Mech., Delft., (Ed. by C.B. Biezeno and J.M. Burgers; pub. by J. Waltman Jr., Delft. p.55 (1925)).

Griffith, R., 1967, Private Communication.

Gurney, C. and Pearson, J., 1949, Proc. Phys. Soc., 62, 469.

Guernsey, R. and Gilman, J.J., (see Gilman, J.J., 1959).

Hargreaves, F., 1928, J. Inst. Metals, 39, 301.

Hedges, J.M. and Mitchell, J.W., 1953, Phil. Mag., 44, 223.

Hill, R., 1950, 'The Mathematical Theory of Plasticity', Oxford: Clarendon Press.

Hillig, W.B., 1962, 'Modern Aspects of the Vitreous State', Vol. 2., Butterworth & Co. (London) p. 152.

Holland, A.J. and Turner, W.E.S., 1937, J. Soc. Glass. Tech., 21, 283.

Inglis, C.E., 1913, Trans. Inst. Naval Architects (Lond.), 55, 219.

Irwin, G.R., 1948, Trans. Amer. Soc. Metals., 40, 147.

Irwin, G.R., 1957, J. Appl. Mech., 24, 361.

Irwin, G.R., 1958, 'Fracture', Handbuch der Physik, Vol. 6, Springer-Verlach, Berlin, p. 551.

Irwin, G.R., 1964, Appl. Mat. Res., Vol. 3, No. 2, 65.

Irwin, G.R. and Kies, J.A., 1952, Welding J. Res. Suppl., 31, 95.

Irwin, G.R. and Wells, A.A., 1965, Metall. Rev., 10, 223.

Jackson, K.A., 1962, Phil. Mag., 7, 117.

Kambour, R.P., 1964, Polymer, 5, 143.

Kambour, R.P., 1965, J. Poly. Sci., A. 3, 1713.

Kerkof, F., 1958, Publication by Dept. of Appl. Phys. at University of Freiburg i Br., (7/58).

Keshishyan, T.N. and Epel'baum, M.B., 1959, Steklo Keram., 16 (8), 9.

Kies, J.A., 1953, U.S. Naval Res. Lab. Report. No. 237.

Kies, J.A. and Smith, H.L. (see Irwin, G.R., 1958).

Koehler, J.S., 1952, 'Imperfections in Nearly Perfect Crystals', Wiley, New York.

Kochendoerfer, A. et al., 1934, Arch. Eisenhuttenw, 25, 351.

Marsh, D.M., 1963, T.I.R.L. Report No. 1.6.1.

Marsh, D.M., 1964, Proc. Roy. Soc. A. 279, 420.

Milligan, W.O., Levy, H.A. and Peterson, J.W., 1951, Phys. Rev., 83, 226.

McLintock, F.A., 1958, J. Appl. Mech., 25, 581.

Mott, N.F., 1948, Engineering 165, 16, 53.

Mott, N.F., 1953, Phil. Mag., 44, 742.

Mould, R.E., 1960, J. Amer. Ceram. Soc., 43, 160.

Mulhearn, T.O., 1959, J. Mech. Phys. Solids, 7, 85.

Murgatroyd, J.B., 1942, J. Soc. Glass Tech., 26, 155.

Nakayama, J., 1964, Jap. J. Appl. Phys., 3, 422.

Neuber, H., 1937, 'Theory of Notch Stresses', Springer-Verlach, Berlin.

Newman, F.H. and Searle, V.H., 1957, 'The General Properties of Matter', Arnold (Lond.).

Obreimov, J.W., 1930, Proc. Roy. Soc. A. 127, 290.

Orowan, E., 1948-9, Rep. Progr. Phys., 12, 214.

Orowan, E., 1949, Lond. Phys. Soc., 12, 185.

Pearson, G.I., Read, W.T. and Feldmann, W.L., 1957, Acta. Met., 5, 181.

Petch, W.J., 1953, Iron Steel Inst., 173, 25.

Poncelet, E.F., 1948, Verres et Réfractaires, 2, 203.

Preston, E., 1926, J. Soc. Glass Tech., 10, 234.

Preston, E., 1942, J. Soc. Glass Tech., 26, 82.

Proctor, B.A. et al., 1967, Proc. Roy. Soc. A. 297, 534.

Rivlin, R.S. and Thomas, A.G., 1953, J. Poly. Sci., Vol. X, No. 3, 291.

Roberts, D.K. and Wells, A.A., 1954, Engineering, 178, 820.

Roberts, J.I., 1937, Proc. Roy. Soc., 161, 141.

Roesler, F.C., 1956, Proc. Phys. Soc., 69, 981.

Samuels, L.E. and Mulhearn, T.O., 1957, J. Mech. Phys. Solids., 5, 125.

Schardin, H., 1959, Proc. Intern. Conf. on Mechanisms of Fracture, Swampscott, Mass., U.S.A. (Ed. by B.L. Averbach et al.), Wiley : New York, p. 297.

Schardin, H. and Struth, W., 1937, Z. Tech. Physik, 18, 474.

Schlapp, D.M., 1965, Phys. Chem. Glasses, Vol. 6, No. 5, 168.

Shand, E.B., 1961, J. Amer. Ceram. Soc., 44, 451.

Shand, E.B., 1965, J. Amer. Ceram. Soc., 48, 43.

Spurr, O.K. and Niegisch, W.D., 1962, J. Appl. Polym. Sci., 6, 585.

Stroh, A.N., 1954, Proc. Roy. Soc. A. 223, 404.

Stroh, A.N., 1955, Phil. Mag., 46, 968.

Stuart, D.A. and Anderson, D.L., 1953, J. Amer. Ceram. Soc., 36, 416.

Svennsson, N.L., 1960, Proc. Phys. Soc., 77, 876.

Tabor, D., 1948, Proc. Roy. Soc. A., 192, 247.

Tabor, D., 1951, 'The Hardness of Metals', Oxford : Clarendon Press.

Taylor, G.I., 1934, Proc. Roy. Soc. A. 145, 362.

Taylor, E.W., 1950, J. Soc. Glass Tech., 34, 69.

Tilton, L.W., 1957, J. Res. of Nat. Bureau of Standards, 59, 139, Res. Paper 2782.

Tilton, L.W., 1960, J. Amer. Ceram. Soc., 43, 9.

Timoshenko, S., 1957, 'Strength of Materials', Parts I & II, D. van Nostrand Comp. Inc. (New Jersey).

Thomas, W.F., 1960, Phys. Chem. Glasses, 1, 4.

Van den Boogart, A., 1966, Proc. Conf. on the Physical Basis of Yield and Fracture (Inst. Phys. & Phys. Soc., Oxford).

Warshaw, I., 1960, J. Amer. Ceram. Soc., 43, 1, 4.

Wells, A.A., 1963, B.W.R.A., Report M13/63.

Westbrook, J.H., 1960, Phys. Chem. Glasses, 1, 32.

Westbrook, J.H. and Jorgensen, P.J., 1965, Trans. Met. Soc. AIME, 233, 425.

Westwood, A.R.C., 1961, Phil. Mag., 6, 195.

Westwood, A.R.C. and Hitch, T.T., 1963, J. Appl. Phys., 34, 3085.

Wiederhorn, S.M., 1966, Mat. Sci. Res., 3, 503 (Plenum Press).

Zarzycki, J. and Mezard, R., 1962, Phys. Chem. Glasses, 3, 5, 163.

APPENDIX

AN EXAMINATION OF THE ENERGY BALANCE EQUATIONS USED BY SVENNSSON (1960)

The fracture energy expression is derived by considering the changes in the energy of the system consequent on the growth of the crack.

Svennsson starts with a statement of the energy balance:

Initial Strain Energy + Work Done to Increase δ = Final Strain Energy + Work Done in Fracture

viz. $$U + F\Delta\delta = U + 2\gamma w\Delta L \qquad (1)$$

where U is the strain energy in the arms of the cantilever corresponding to δ and L, γ is the specific fracture energy and w is the thickness of the beam. The limit to this equation is given by Svennsson as:

$$\gamma = \frac{Fw}{2}\frac{d\delta}{dL} - \frac{1}{2w}\left(\frac{\partial U}{\partial L}\right) \qquad (2)$$

The stored strain energy, U, is evaluated from beam theory taking into account shearing stresses and also the effect of the axial compressive forces which stabilize the crack direction. The expression for U is given as:

$$U = \frac{48EI\delta^2}{L^3\lambda} \qquad (3)$$

where λ is introduced to account for the shearing and compressive stresses, and is a function of the crack length L.

In evaluating equation (2) Svennsson differentiates U and obtains:

$$\frac{\partial U}{\partial L} = \frac{3Eb^3\delta^2}{4L^4} + \frac{Eb^3\delta^2}{4L^3\lambda}\frac{d\lambda}{dL} \qquad (4)$$

Substituting this expression into equation (2) gives an expression for the fracture energy

$$\gamma = \frac{1}{4} \frac{Eb^3\delta^2}{L^4}\left(\frac{1}{\lambda}\left\{\frac{2Ld\delta}{\delta dL} + \frac{Ld\lambda}{\lambda dL} + 3\right\}\right) \qquad (5)$$

where ( ) = S

γ is evaluated from curves of $L^2/\sqrt{S}$ versus L.

The expression for $\frac{\partial U}{\partial L}$ used by Svennsson (equation (4)) was $\left(\frac{\partial U}{\partial L}\right)_\delta$, which does not give the correct limit to equation (1). In equation (1), ΔU is the difference between the initial and final strain energies of the system and this depends on both δ and L.

The correct limit to equation (1) should be

$$2\gamma w\Delta L = F\Delta\delta - \Delta U \qquad (6)$$

where

$$\Delta U = \left(\frac{\partial U}{\partial L}\right)_\delta \Delta.L + \left(\frac{\partial U}{\partial \delta}\right)_L \Delta\delta \qquad (7)$$

so that

$$2\gamma wL = F\Delta\delta - \left(\frac{\partial U}{\partial L}\right)_\delta \Delta L - \left(\frac{\partial U}{\partial \delta}\right)_L \Delta\delta \qquad (8)$$

However, since the work done in increasing δ is the change in strain energy if the crack does not move we may write

$$F\Delta\delta = \left(\frac{\partial U}{\partial \delta}\right)_L \Delta\delta \qquad (9)$$

Thence

$$\gamma = -\frac{1}{2w}\left(\frac{\partial U}{\partial L}\right)_\delta$$

This is the same basic equation as that used in Chapter IV of this thesis to calculate cleavage fracture energies. We note that the term representing the work done in increasing δ does not appear explicitly. In calculating γ from equation (2) Svennsson has overestimated the true value to the extent of the term $\frac{Fw}{2}\frac{d\delta}{dL}$. By comparing the magnitude of the two terms in the R.H.S. of equation (2), and using the published data, it can be shown that $\gamma_{corrected} \simeq \frac{\gamma}{2}_{Svennsson}$.